

**Targeting mutant p53 in spontaneous cancer  
by T cell receptor gene therapy**

Inaugural-Dissertation  
to obtain the academic degree  
Doctor rerum naturalium (Dr. rer. nat.)

submitted to the Department of Biology, Chemistry, Pharmacy  
of Freie Universität Berlin

by  
VASILIKI ANASTASOPOULOU

from Athens

2021



1. Gutachter: Prof. Dr. Thomas Blankenstein
2. Gutachter: Prof. Dr. Florian Heyd

Disputation am: 12/11/2021



“Το εὐδαιμον το ελεύθερον, το δ' ελεύθερον το εὐψυχον.”

Θουκυδίδης, 460-394 π.Χ.

“The secret of happiness is freedom. The secret of freedom is courage.”

Thucydides, 460-394 b.C.



## Acknowledgements

To begin with, I would like to thank Hans Schreiber for giving me the opportunity to follow my scientific dreams by pursuing this PhD. He has been particularly useful in providing advice and scientific support throughout the development of this project. I would also like to thank Thomas Blankenstein for all the critical discussions and his expert opinion on crucial topics. Most of all, I would like to thank Matthias Leisegang for his valuable supervision, guidance and scientific trust. His unlimited support has not only given the right direction to the project, but has also helped me to set the goals of my scientific career.

Special thanks to the MDC Graduate School for all the support and the training opportunities. Great thanks to all the people I have been working together since the beginning of my PhD. A warm thanks to Karin Schreiber and Kimberley Borutta for their excellent technical support. The greatest and loudest “thank you” goes to Christina Schulz for her support and patience. She might have joined the project at an advanced stage, but without her technical skills many essential experiments would not have been possible. Many thanks to all the people in the Leisegang, Schreiber, Blankenstein, Willimsky, Kammertöns and Uckert groups. Among all of them, special thanks to Leonie, Lena, Meng-Tung, Josi, George and Mete for sharing all the aspects of my PhD life. You have certainly made our lab life and offices better.

I should also thank all of my friends for their moral support. A huge thanks to my “Berlin” friends, the ones who are still here and the ones who are off to new adventures, for their joyful companion and for pulling through a pandemic together. Great thanks to my “Athens” friends for minimizing the physical distance through endless discussions and for our memorable meetings at home. Big thanks to my “Sifnos” friends for all the inspirational nights at “Che” and the most beautiful sunsets of my life. The most special thanks goes to Dimitris for managing to make me smile though the last and probably the most difficult bits of this journey.

Finally, the last part of all acknowledgements I have ever written is reserved for my parents, Maria and Thomas. “Thank you” seems too small to describe their support. They gave me the opportunity to study what I wanted and to follow my dreams. Dad, thank you for following me and standing by me everywhere I go. The fun part of my life would not have been the same without you. Mom, thank you for being the lighthouse of my life. You always show me the way when I am lost. I do not know what material you are made of to support my choices, decisions and the path I have taken, but I hope I have half of that to live up to you and to make you proud day by day. This work is dedicated to you.





---

## Table of Contents

<b>Acknowledgements</b>	<b>7</b>
<b>Summary</b>	<b>13</b>
<b>Zusammenfassung</b>	<b>15</b>
<b>1. Introduction</b>	<b>17</b>
<b>1.1 Cancer</b>	<b>17</b>
1.1.1 Cancer development	17
The role of p53	18
1.1.2 Tumor heterogeneity	19
1.1.3 Tumor stroma	20
<b>1.2 Tumor antigens</b>	<b>20</b>
1.2.1 Antigen presentation	20
1.2.2 Tumor-associated antigens	21
1.2.3 Tumor-specific antigens	22
<b>1.3 T cell biology</b>	<b>23</b>
1.3.1 Antigen recognition and effector mechanisms	23
1.3.2 Role of CD8 <sup>+</sup> and CD4 <sup>+</sup> T cells in anti-tumor immunity	25
<b>1.4 Cancer immunotherapy</b>	<b>26</b>
1.4.1 Cytokines	26
1.4.2 Checkpoint inhibitors	27
1.4.3 Cancer vaccines	28
1.4.4 Adoptive T cell therapy	29
“Unmodified” T cells	29
CAR-modified T cells	30
TCR-engineered T cells	31
Parameters that determine antigen quality	33
<b>1.5 Preclinical models</b>	<b>34</b>
1.5.1 Xenograft models	34
1.5.2 Syngeneic models	35
1.5.3 Ag104A as a model of spontaneous cancer	36
<b>Aim of the thesis</b>	<b>36</b>
<b>2. Materials and methods</b>	<b>37</b>
<b>2.1 Molecular biology</b>	<b>37</b>

---

---

2.1.1 Isolation of TCR sequences	37
2.1.2 Generation of MP71 vectors containing TCR transgene cassettes	39
2.1.3 Generation of MP71 vectors encoding MHCI sequences	39
2.1.4 Generation of pcDNA3.1 vectors	40
2.1.5 Generation of in vitro transcribed RNA	40
2.1.6 Isolation and detection of gene sequences by PCR	41
2.1.8 Genome engineering with the CRISPR/Cas9 system	43
<b>2.2 Cell culture</b>	<b>44</b>
2.2.1 Cell lines and primary cell cultures	44
2.2.2 Isolation and activation of mouse primary T cells	45
2.2.3 Retroviral gene transfer into cell lines and primary T cells	45
2.2.4 Electroporation of cell lines	46
2.2.5 IFN- $\gamma$ treatment	47
2.2.6 5-Azacytidine treatment	47
<b>2.3 Functional assays</b>	<b>47</b>
2.3.1 Flow cytometry	47
2.3.2 Cytokine release assay	48
<b>2.4 In vivo and ex vivo experiments</b>	<b>49</b>
2.4.1 Mice	49
2.4.2 Tumor challenge	49
2.4.3 Adoptive T cell transfer	49
2.4.4 Analysis of peripheral blood	49
2.4.5 Isolation and analysis of tumor samples	50
<b>2.5 Data and statistical analysis</b>	<b>50</b>
<b>3. Results</b>	<b>51</b>
<b>3.1 Immunization of immune-competent mice with Ag104A tumor cells generates tumor-specific T cell responses</b>	<b>51</b>
<b>3.2 Tandem minigene constructs serve as a reliable tool to determine TCR specificity</b>	<b>55</b>
<b>3.3 The Ag104A-specific TCR M2/3 recognizes a neoantigen that results from a point mutation in p53</b>	<b>58</b>
<b>3.4 TCR gene therapy targeting mp53 in established Ag104A tumors induces stable disease but cannot prevent relapse</b>	<b>62</b>
<b>3.5 Relapse of Ag104A tumors from T cell therapy is not due to insufficient expansion of M2/3-engineered T cells or their inability to infiltrate the tumor tissue</b>	<b>63</b>

---

---

<b>3.6 Ag104A tumors escape mp53-specific T cell therapy as variants that are no longer recognized by M2/3-engineered T cells</b>	<b>66</b>
<b>3.7 The level of mp53 gene copies in Ag104A variants that escaped T cell therapy is decreased</b>	<b>69</b>
<b>3.8 Genomic alterations affecting Trp53 cannot explain escape of Ag104A variants from T cell therapy</b>	<b>70</b>
<b>3.9 Clonotypes lacking the mp53 gene dominate the population of Ag104A variants that escaped mp53-specific T cell therapy</b>	<b>71</b>
<b>3.10 Ag104A tumors expressing high and homogeneous levels of mp53 are rejected by ATT using M2/3-engineered T cells</b>	<b>73</b>
<b>3.11 The mutation D253E in p53 provides a growth advantage and higher tumorigenicity to Ag104A cancer cells</b>	<b>74</b>
<b>4. Discussion</b>	<b>77</b>
<hr/>	
<b>4.1 Ag104A as a preclinical model for mutation-specific TCR gene therapy</b>	<b>78</b>
<b>4.2 Protocols to identify mutant neoantigens as T cell targets are essential for designing mutation-specific TCR gene therapy</b>	<b>79</b>
<b>4.3 Adoptive T cell therapy targeting mp53 in established Ag104A tumors leads to escape of antigen-negative variants</b>	<b>81</b>
<b>4.4 Nature of the p53<sup>D253E</sup> mutation in Ag104A</b>	<b>83</b>
<b>4.5 Combinatorial T cell therapy to overcome relapse caused by antigen-negative variants</b>	<b>86</b>
Simultaneous targeting of multiple neoantigens	86
The importance of CD4 <sup>+</sup> T cells and their combination with CD8 <sup>+</sup> T cells in tumor eradication	87
Combining TCR- and CAR-engineered T cells in vivo	88
<b>4.6 The prospect of patient-individualized mutation-specific T cell therapy as a powerful cancer treatment</b>	<b>90</b>
<b>5. References</b>	<b>93</b>
<hr/>	
<b>6. Abbreviations</b>	<b>117</b>
<hr/>	
<b>7. List of tables and figures</b>	<b>121</b>
<hr/>	
<b>7.1 Tables</b>	<b>121</b>
<b>7.2 Figures</b>	<b>121</b>
<b>Statement (Eidesstattliche Erklärung)</b>	<b>123</b>

---



## Summary

Somatic mutations in cancer can result in neoantigens that serve as attractive targets for cancer immunotherapy. Most human cancers develop “spontaneously” and harbor fewer mutations than murine cancers induced with carcinogens. The murine fibrosarcoma Ag104A arose spontaneously in an aging C3H mouse and serves here as a model to analyze adoptive T cell therapy under conditions that closely resemble the clinical situation. A tumor-specific TCR (M2/3) was isolated from T cells of mice immunized with Ag104A cancer cells. To identify the target of M2/3, mutations in Ag104A were determined by whole exome sequencing and their expression was verified by RNA sequencing. The resulting 77 potential neoantigens were expressed as tandem minigenes and pulsed into target cells engineered with H-2<sup>k</sup> restriction elements. Subsequent analysis revealed that the specific M2/3 response was directed against an H-2K<sup>k</sup>-presented peptide derived from mutant *Trp53*. The p53<sup>D253E</sup> mutation (mp53) was tested as target for neoantigen-specific TCR gene therapy. M2/3-engineered T cells were adoptively transferred into immunodeficient C3HxRag2<sup>-/-</sup> mice bearing established Ag104A tumors. The transferred T cells expanded in an antigen-specific manner and induced growth arrest of this otherwise aggressive and fast-progressing cancer followed by a phase of stable disease. However, all tumors relapsed 4-5 weeks after treatment. Analysis of the tumors that escaped mp53-specific TCR gene therapy showed that their populations were dominated by antigen-negative variants. Further analysis indicated that tumor escape was a result of low-frequency occurring mp53-negative variants due to intratumor heterogeneity. These findings suggest that neoantigen-specific TCR gene therapy is effective against a single target, since mp53-positive cancer cells were successfully eliminated *in vivo*. Interestingly, although the p53<sup>D253E</sup> mutation confers a growth advantage and higher tumorigenicity to Ag104A cancer cells and is supposed to be cancer-driving, it proved to be insufficient for eradication of established cancer when used alone as a target antigen of T cell therapy. Analysis of the Ag104A tumor model emphasizes intratumor heterogeneity as a critical parameter of neoantigen-specific TCR gene therapy that has to be addressed in clinical settings in order to make this form of immunotherapy successful for the treatment of human cancer.



## Zusammenfassung

Somatische Mutationen in Krebszellen können zu Neoantigenen führen, die sich als attraktive Ziele für die Krebsimmuntherapie nutzen lassen. Die meisten menschlichen Tumoren entwickeln sich "spontan" und weisen weniger Mutationen auf als murine Tumoren, die mit Karzinogenen induziert wurden. Das murine Fibrosarkom Ag104A entstand spontan in einer älteren C3H-Maus und dient hier als Modell, um die adoptive T-Zelltherapie unter Bedingungen zu analysieren, die der klinischen Situation sehr ähnlich sind. Ein tumorspezifischer TCR (M2/3) wurde aus T-Zellen von Mäusen isoliert, die mit Ag104A-Krebszellen immunisiert wurden. Um das Ziel von M2/3 zu identifizieren, wurden die Mutationen in Ag104A-Krebszellen durch Whole-Exome-Sequenzierung bestimmt und ihre Expression durch RNA-Sequenzierung verifiziert. Die resultierenden 77 potenziellen Neoantigene wurden als Tandem-Minigene exprimiert und in Zielzellen eingebracht, die mit H-2<sup>k</sup>-Restriktionselementen ausgestattet waren. Die anschließende Analyse ergab, dass die spezifische M2/3-T-Zellantwort in immunisierten Mäusen gegen ein H-2K<sup>k</sup>-präsentiertes Peptid gerichtet war, das von mutiertem Tp53 stammte. Die p53<sup>D253E</sup>-Mutation (mp53) wurde anschließend als Ziel für eine neoantigen-spezifische TCR-Gentherapie getestet. M2/3-exprimierende T-Zellen wurden adoptiv in immundefiziente C3HxRag2<sup>-/-</sup> Mäuse mit etablierten Ag104A-Tumoren transferiert. Die übertragenen T-Zellen expandierten antigenspezifisch und induzierten einen Wachstumsstopp dieses ansonsten aggressiven und schnell fortschreitenden Krebses, gefolgt von einer Phase in der die Tumoren sich in ihrer Größe nicht änderten. Allerdings kam es bei allen Tumoren 4-5 Wochen nach der Behandlung zu einem Rezidiv. Die Analyse der Tumoren, die der mp53-spezifischen TCR-Gentherapie entkommen waren, zeigte, dass sie von Antigen-negativen Klonotypen dominiert wurden. Weitere Analysen zeigten, dass der Tumor-Escape eine Folge von sehr seltenen mp53-negativen Krebszellvarianten war, die aufgrund intratumoraler Heterogenität in der ursprünglichen Ag104A-Tumorzellpopulation bereits vorhanden waren. Diese Ergebnisse deuten darauf hin, dass die neoantigen-spezifische TCR-Gentherapie gegen ein einzelnes Ziel prinzipiell effektiv sein kann, da mp53-positive Krebszellen erfolgreich *in vivo* eliminiert wurden. Interessanterweise erwies sich die p53<sup>D253E</sup>-Mutation allein jedoch als unzureichend für die Eliminierung eines etablierten Krebses, obwohl sie den Ag104A-Krebszellen einen Wachstumsvorteil und eine höhere Tumorigenität verleiht und daher als krebsfördernd angesehen werden kann. Die Analyse des Ag104A-Tumormodells hebt die Tumorerogenität als einen kritischen Parameter einer mutationsspezifischen TCR-Gentherapie hervor, der im klinischen Kontext adressiert werden muss, um diese Form der Immuntherapie für die Behandlung von menschlichem Krebs erfolgreich zu machen.





## **1. Introduction**

Cancer is the second leading cause of death worldwide (World Health Organization) and one of the most intensively studied health problems by scientists and clinicians. Cancer consists of cells that grow continuously, invade into neighboring normal tissues and / or spread (metastasize) to other organs or cavities, thereby ultimately killing the host. Cancer can be divided in two main categories, blood and solid cancers. Blood cancers refer to malignant cells of hematopoietic origin, while solid cancers form tumors and make up approximately 95% of human cancer. Despite the progress during the last decades, conventional cancer treatments like radiotherapy and chemotherapy have proven to be often insufficient particularly for solid malignancies. Cancer immunotherapy is an emerging field and refers to using the immune system or immunological agents to fight cancer. It includes options ranging from “off-the-shelf” ready-to-use reagents to highly individualized therapeutic approaches. Current efforts aim to transform cancer immunotherapy to a standard form of therapy in the future.

### **1.1 Cancer**

Independent from the tissue or organ it affects, cancer is a complex multi-parameter disease characterized by the progressive growth of transformed cells. Numerous cellular and molecular mechanisms are involved in tumor onset and growth. Therefore, cancer should not be considered as an independent entity but as part of the body, which at the same time affects several immune processes.

#### **1.1.1 Cancer development**

Human cancers undergo several stages of development until they are diagnosed. An early event termed tumor initiation, defined by experimental studies in mice, refers to the accumulation of essential somatic mutations in a cell population that persist for several years or an entire life without resulting in cancer. Somatic mutations are random and are caused by endogenous or exogenous factors such as environmental conditions or exposure to mutagens (e.g. UV light). The effect of chemical carcinogens on tumor initiation has been long studied and has facilitated the definition of cancer development stages [1, 2]. Mutations that affect oncogenes, tumor suppressor genes or genes of DNA repair pathways in particular can lead to the formation of premalignant lesions [3]. The occurrence of cancer in families is often a result of inherent germline mutations that in addition to accumulating somatic mutations can drive cancer development [4, 5]. As a result of mutations, cells can undergo transformation. Transformed cells exhibit unregulated proliferation due to the activation or inactivation of genes

that are affected. The accumulation of further sequential mutations can subsequently lead to the appearance of cancer cells during the next developmental stage called tumor promotion [6]. These cells transition from a precancerous to a cancerous state characterized by abnormal growth. The third stage, termed tumor progression, indicates an independent mass of cells in a tissue, organ or the blood stream, which proliferate uncontrollably [7, 8]. Tumor progression usually coincides with the time of diagnosis and the ability of cancer cells to metastasize [9, 10]. Studies in mouse models support the evidence that the induction of cancer is a complex multistep process [11, 12].

### **The role of p53**

*TP53* has been long classified as a tumor suppressor gene based on early studies that show its ability to repress oncogenic transformation *in vitro* and the high susceptibility of *TP53* knockout mice to tumor development *in vivo* [13, 14]. Therefore, the p53 protein has been characterized as the “guardian of the genome” due to its central role as a transcription regulator in numerous cellular processes that influence tumor initiation and progression [15]. In normal state, p53 is rapidly degraded through the proteasome due to its interaction with MDM2, which acts as an E3 ubiquitin ligase [16]. Stress signals, like acute DNA damage or hyperproliferative signals, induce p53 either by promoting its phosphorylation so that the aforementioned interaction is disrupted or by directly inhibiting MDM2 [17, 18]. Both processes result in p53 stabilization followed by the formation of tetramers, which bind to target genes in a sequence-specific manner and activate or inactivate their transcription [19]. Canonical p53 functions involve cell cycle arrest (e.g. *Cdkn1a* (p21<sup>Waf1/Cip1</sup>) activation), DNA repair (e.g. *Gadd45a* activation), apoptosis (e.g. *Puma* activation) and senescence (e.g. E2F inhibition) [20-23]. As a consequence, p53 is actively involved in maintaining genomic stability by preventing the accumulation of mutations that could drive tumor development and by counteracting the effects of oncogenic mutations. Therefore, p53 loss is directly correlated with malignant transformation and uncontrollable proliferation. In fact, p53 is mutated in approximately 50% of all human cancers [24, 25]. The DNA binding domain of p53 is considered a “hotspot” for mutations. More than 80% of observed mutations are located in this region, while 25% of them are recurrent. Furthermore, more than 70% of p53 mutations are missense, while the rest are nonsense (8%), silent (3,5%) or other mutations [26, 27]. Mutations lead to protein alterations that abrogate p53 interaction with other genes and proteins. The frequency of mutations in p53 underscores its important function as a tumor suppressor gene, as it is thought to drive tumorigenesis in many types of cancer. Although the functions of many p53 mutations have been well characterized, it has become evident that the p53 gene regulatory network highly depends on the cell type and its differentiation state as well as on the different stress signals.

The flexibility of the response to these factors is a result of the numerous pathways that p53 is involved along with the crosstalk between them. Therefore, each mutation can lead to different biochemical and phenotypic functions.

### 1.1.2 Tumor heterogeneity

The theory that advanced cancers consist of several branches that differ from each other has been long formulated [28]. Clonal evolution describes the process of acquiring new mutations during tumor cell division as a result of genomic instability. Most of the derived cells naturally die. However, some of them are selected because they have a growth advantage and give rise to subclones that phenotypically differ from their progenitors. Therefore, cancer is considered an adaptive system that follows the Darwinian rules of genetic drift and natural selection [29]. The distinct subclones are described as intratumor heterogeneity and they can be intermixed or spatially separated in several tumor sites [30]. Nowadays, advanced sequencing techniques can decipher both intratumor and intertumor heterogeneity. The latter refers to differences between tumor types and patients [31]. However, sequencing of bulk tumor specimens can only provide information about different mutations and their spatial distribution and not about clonal heterogeneity. Clonal evolution continues with cancer growth and eventually leads to a diverse tumor cell population at the time of diagnosis (Figure 1).

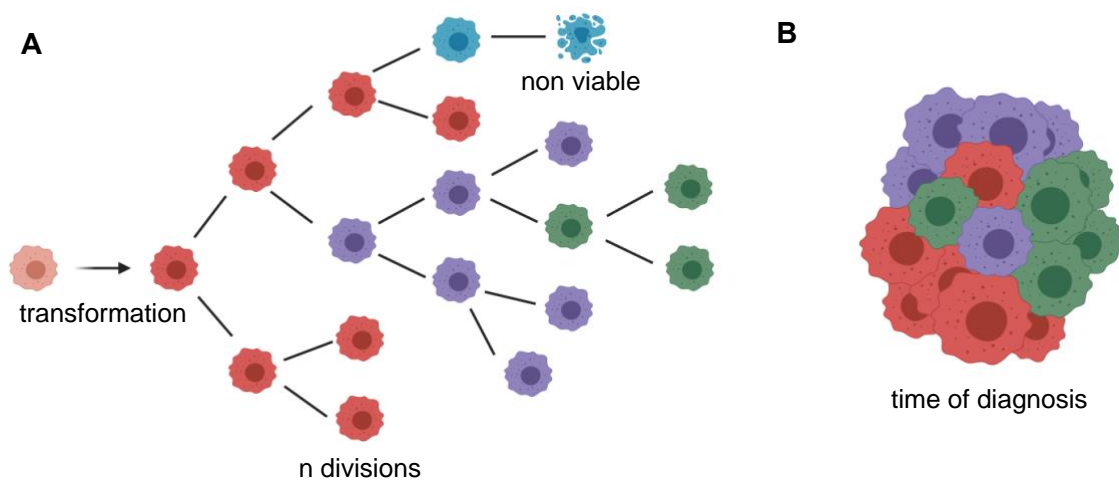


**Figure 1: Clonal evolution of cancer**

(A) Tumor initiation is defined by the appearance of mutations. Cells that undergo transformation can become malignant and proliferate uncontrollably during tumor promotion and progression (n number of divisions). Some of them acquire new mutations that are selected because they have a growth advantage, whereas some others are non viable. (B) Cancers at the time of diagnosis represent a diverse tumor cell population with distinct subclones mixed together or spatially separated.

### **1.1.3 Tumor stroma**

Tumor stroma is an essential part of every cancer and consists of nonmalignant cells and extracellular matrix that support tumor growth, thus forming the tumor microenvironment [32, 33]. Stromal cells include endothelial cells and fibroblasts as well as immune cells, like T cells and macrophages, and are recruited by tumor cells through the secretion of inflammatory chemokines [34, 35]. The presence of tumor-associated fibroblasts (TAFs) is of particular importance as they provide essential growth factors (e.g. vascular endothelial growth factor (VEGF), basic fibroblast growth factor (bFGF)) that activate endothelial cells to support angiogenesis [36]. The formation of new blood vessels is a fundamental part of a tumor's architecture, as it secures blood supply to the tumor. Moreover, TAFs produce extracellular matrix proteins, another key component of tumor stroma, necessary for mechanical support of the tumor. TAFs are overall considered to formulate a tumor-promoting environment [37]. Tumor-associated macrophages (TAMs) are also an essential part of any tumor stroma since they provide growth factors and nutrients, while they are also responsible for the removal of dead cells and waste, thus supporting tumor growth. They are often found to be polarized towards the M2 phenotype, which is correlated with angiogenesis and vascularization [38]. TAMs are also considered to hold a key role in metastasis as it has been shown that they promote the migration of tumor cells and establish the appropriate microenvironmental conditions at the metastatic sites [39]. Several other cell types, like adipocytes and pericytes, contribute to tumor stroma and support tumor cell invasion [40]. As a consequence, cancer cells remain in a dynamic constant communication with their microenvironment to receive and transmit signals needed for tumor growth.

## **1.2 Tumor antigens**

Tumor antigens differentiate cancer from normal cells and are derived from proteins that are presented as peptides by MHC (major histocompatibility complex) molecules at the cell surface. Tumor antigen processing and presentation follow the fundamental rules of these distinct processes of the immune system. Tumor antigens are divided in two major subgroups: tumor-associated and tumor-specific antigens.

### **1.2.1 Antigen presentation**

Tumor antigens are presented either by MHC class I or class II molecules at the cell surface. The two classes of MHC molecules differ in structure and expression patterns, but they both bear a cleft or groove where peptides are bound. On the one hand, endogenous antigens destined for presentation by MHC I molecules are processed by the cytosolic pathway, in a

similar fashion to the physiological turnover of intracellular proteins. Therefore, they are subjected to a ubiquitin-mediated proteosomal degradation in the cytosol. Proteasomes containing the LMP2, LMP7 and LMP10 subunits preferentially generate peptides that bind to MHC I molecules (immunoproteasome). The processed peptides are transported by the transporter protein TAP (transporter associated with antigen processing) to the rough endoplasmic reticulum and are picked up by MHC I molecules with the aid of the molecular chaperones calnexin, calreticulin and tapasin. MHC I molecules are present in all nucleated cells and consist of two noncovalently associated polypeptide chains, the  $\alpha$  chain that forms three distinct domains ( $\alpha_1$ ,  $\alpha_2$ ,  $\alpha_3$ ) and the  $\beta_2$ -microglobulin [41]. They are able to bind short peptides, which are usually 8 to 10 amino acids long. If the binding process is stable, it stabilizes the MHC I molecules at the cell surface. In most cases, the amino acids at the amino and carboxy termini of the peptides are crucial for the interaction with the peptide groove, thus they are characterized as anchor residues [42]. On the other hand, peptides presented by MHC II molecules are processed via the endocytic pathway. During this process, exogenous antigens are internalized by endocytosis or phagocytosis and while they move from early to late endosomes and finally lysosomes, they are cleaved in shorter peptides by hydrolytic enzymes. MHC II molecules are expressed only in antigen-presenting cells (APCs), namely dendritic cells, B cells and macrophages. A protein called invariant chain (CD74) interacts with the peptide groove of MHC II molecules and prevents the binding of peptides meant to be presented by MHC I molecules. As MHC II moves from the rough endoplasmic reticulum to the Golgi network, the invariant chain is degraded but a short fragment termed CLIP (class II-associated invariant chain peptide) remains bound to the peptide cleft. The non-polymorphic MHC molecule HLA-DM mediates the exchange of CLIP with processed antigenic peptides [43, 44]. MHC II molecules consist of two noncovalently associated  $\alpha$  and  $\beta$  polypeptide chains, each forming two distinct domains ( $\alpha_1$ ,  $\alpha_2$ ,  $\beta_1$ ,  $\beta_2$ ) and bind peptides which are at least 13 amino acids long, although they can be much longer. The anchor positions lie off the peptide termini at various distances [45, 46]. MHC molecules within the same species are highly diverse due to the polymorphism of the respective loci that leads to the presence of many different alleles. In humans and mice there are three main different class I genes (HLA-A, -B, -C and H2-K, -D, -L respectively) and three or two class II genes respectively (HLA-DR, -DP, DQ and H-2A, -E), resulting in a large number of possible haplotype combinations [47, 48]. Polymorphism also contributes to the range of antigens that can be presented.

### **1.2.2 Tumor-associated antigens**

Tumor-associated antigens (TAAs) constitute a broad category of antigens derived from normal proteins, which show aberrant expression levels in cancer cells [49]. They are further

subdivided in several categories usually indicating the tissue or the type of cells where they are expressed. As the list of TAAs is not exhaustive, a few representative examples are described below. Cancer-testis antigens, like the MAGE proteins or NY-ESO1, are expressed in spermatocytes in the testis, but are also often found in certain cancer types like melanoma [50, 51]. Embryonic antigens like the alpha-fetoprotein (AFP) and the carcinoembryonic antigen (CEA) are typically found in embryonic and fetal tissues and their expression in adult tissues is lower [52]. They are often re-activated in several cancer types, such as liver and gastrointestinal cancer [53, 54]. Another extensively studied category of TAAs is the so-called cluster of differentiation antigens, like CD19, CD20 or MART-1. Abundant expression of such antigens is associated with normal cells of a specific differentiation stage but also often found in malignant cells of several tumors, like leukemias and melanoma [55, 56]. Since TAAs are either overexpressed or re-activated normal proteins, their presence in healthy tissues is expected and certainly cannot be excluded. A detailed analysis of their individual expression pattern as well as of their isoforms is critical, as discussed below.

### **1.2.3 Tumor-specific antigens**

The term “tumor-specific antigens” (TSAs) is used to describe antigens that are exclusively expressed in cancer cells and are not found in healthy tissues, a substantial difference with TAAs. Early evidence in 1943 indicated that an immune response against tumors could be mounted, when mice inoculated with a methylcholanthrene-induced sarcoma, survived a second challenge with the same tumor [57]. Stronger evidence became apparent in 1957 in a series of experiments attempting to induce immunity against tumors. Mice were immunized with small tumor fragments excised from different hosts and were able to reject the tumors upon a second challenge, but failed to eradicate other tumors for which no previous immunization was performed [58]. These results suggested a tumor-specific immune response. The final confirmation of the presence of TSAs came about 40 years later, when it was shown that a single amino acid substitution resulted in a unique tumor antigen present only in cancer cells and not in healthy tissues of the same host [59]. It is nowadays known that TSAs arise from mutations in the cancer genome. Exposure to carcinogens, such as UV light and certain chemicals, or naturally occurring random mistakes during normal cell division result in DNA damage. Only a small fraction of those mistakes escape the endogenous repair mechanisms and give rise to somatic mutations [60]. Such mutations include single amino acid substitutions, inserts or deletions that lead to frameshift mutations or the generation of fusion genes, and copy number changes [61]. Somatic mutations are more common causes of cancer than germline mutations that are linked to familial types of malignancies [4, 62]. Mutations in the so-called cancer-driving genes allow cancer cells to proliferate uncontrollably. Driver

mutations may inactivate tumor suppressor genes, like p53, or activate oncogenes, like KRAS [63]. Mutations that affect the DNA repair machinery of a cell, like the family of BRCA genes, are also common and allow the tumor cells to acquire more mutations that offer further growth and metabolic advantages [64]. Other mutations perceived as not directly affecting tumor growth are often described as passenger mutations and might be acquired at the same time with driver mutations or during cancer development [60]. Another type of potential TSAs are spliced peptides which are the result of re-ligation of peptide fragments by proteosomal subunits and do not represent the linear sequence of the parental proteins [65]. TSAs are often called neoantigens, essentially meaning “new” antigens, as they derive from proteins, which were absent in the normal genome before mutations took place. Recurrent or shared TSAs are rare, however they do exist. Typical examples are the fusion proteins BCR-ABL and TEL-AML1 as a result of chromosomal translocations often found in chronic myelogenous leukemia (CML) and acute lymphoblastic leukemia (ALL) respectively [66-68]. Other representative examples are the shared hotspot mutations in the *TP53* gene among patients [69]. The recent and fast-developing technology of next-generation sequencing (NGS) allows the identification of all mutations in a given tumor by comparing cancer to normal cells of the same host. These techniques enable the study of not only genomic mutations (whole exome sequencing) but also the ones that are truly expressed (mRNA sequencing) [31, 70].

### **1.3 T cell biology**

Tumors are not isolated from the immune system. The adaptive arm and especially T cells can recognize tumor antigens via their T cell receptor (TCR) once they have been bound to MHC molecules on the cell surface. T cells also infiltrate the tumor environment. Although tumors originate from normal cells, they have certain characteristics that allow them to be recognized as non-self by the immune system.

#### **1.3.1 Antigen recognition and effector mechanisms**

T cells derive from a common lymphoid progenitor in the bone marrow and their development is completed in the thymus, where they migrate as so-called thymocytes [71]. During this process, TCR rearrangement takes place. TCRs in their final forms are heterodimers consisting of an  $\alpha$  and a  $\beta$  chain linked by a disulfide bond. Both chains bear a variable and a constant region and a short cytoplasmic tail. The constant domains are not diverse in contrast to the variable domains [72]. TCR $\alpha$  contains V (variable) and J (joining) gene segments, whereas TCR $\beta$  has an additional D (diversity) segment [73]. There is a variety of different gene segments in mice and humans leading to an enormous number of TCR combinations. The most crucial parameter for antigen recognition is the highly diverse CDR3 (complementarity

determining region 3) region of each chain, located in the junctions of the  $V_{\alpha}$  -  $J_{\alpha}$  and  $V_{\beta}$  -  $D_{\beta}$  -  $J_{\beta}$  segments respectively. The segments along with the addition of P- and N-nucleotides contribute to the high variability of the CDR3 region [74]. During thymic T cell development, TCR $\beta$  is rearranged first by somatic recombination [75, 76]. Only thymocytes with successful  $\beta$  chain rearrangements will proceed to the next developmental stages, which are marked by the sequential expression of all distinct T cell markers. The complete TCR complex further includes the CD3 complex ( $\gamma$ ,  $\delta$ ,  $\epsilon$  chains) and the  $\zeta$  chain, which is a disulfide-linked homodimer [77]. The proteins CD4 and CD8, which define the fate of T cells are also expressed during T cell development and are characterized as co-receptors. Finally, TCR $\alpha$  rearrangement is the last step of the process [78]. Mature naïve T cells leave the thymus and start circulating from the bloodstream into the peripheral lymphoid organs (lymph nodes, spleen, mucosa-associated lymphoid tissues), where they are sampling for antigens. CD4<sup>+</sup> T cells recognize antigens presented on MHCII molecules, whereas CD8<sup>+</sup> T cells recognize MHCI-bound peptides [79]. T cells that recognize self peptide:MHC complexes with low affinity are positively selected in the thymus and exit to the periphery as T cells with functional TCRs [80]. T cells that recognize self-antigens strongly are negatively selected and die in the thymus through apoptosis, thus setting the basis for self-tolerance [81]. Dendritic cells (DCs), a subset of APCs, are thought to be responsible for T cell priming, a process that describes the first contact of a T cell with its antigen and leads to T cell activation [82]. DCs circulate constantly throughout the body and ingest antigens via endocytosis, which they present on their MHCI and MHCII molecules, as they process peptides through both pathways previously described. These activated DCs migrate to the lymph nodes. The first signal for T cell activation derives from the engagement of the TCR with its antigen and the interaction of the co-receptors, CD4 or CD8, with the respective MHC molecules [83]. The second signal originates from co-stimulatory molecules. The most well-characterized co-stimulatory signal is the interaction of CD28 on the surface of T cells with B7 molecules on DCs [84]. Upon activation, T cells enter a phase of rapid proliferation driven by IL-2, a cytokine produced and used by them and acquire their effector functions. CD8<sup>+</sup> effector T cells differentiate to cytotoxic T cells (CTLs), which can directly kill their target cells via the production of cytotoxins. They also produce other effector molecules like perforin, granzymes and Fas ligand, which trigger apoptosis in the target cells, and further cytokines [85, 86]. CD4<sup>+</sup> effector T cells act as helper cells (T<sub>H</sub>) and they produce cytokines that act as growth factors, mediate a variety of effector and differentiation processes and help CD8<sup>+</sup> T cells to become fully activated [87, 88]. They also stimulate B cells to produce antibodies for cognate antigens [89].



### 1.3.2 Role of CD8<sup>+</sup> and CD4<sup>+</sup> T cells in anti-tumor immunity

Both T cell subsets hold a central role in anti-tumor immunity through the recognition of tumor antigens presented by MHC I and MHC II molecules followed by their subsequent activation. On the one hand, CD8<sup>+</sup> T cell priming takes place in draining lymph nodes, where dendritic cells have migrated upon antigen uptake from dying tumor cells in the tumor tissue. This process is long described as cross-presentation [90, 91] and it has been shown for a number of antigens [92, 93]. Upon activation, CTLs can directly recognize tumor cells and kill them via perforin-dependent cytotoxicity [94]. However, CD8<sup>+</sup> effector T cells produce a number of cytokines, especially IFN- $\gamma$  and TNF- $\alpha$  that act on the tumor stroma and are thought to be necessary for tumor rejection [95, 96]. Early evidence revealed that IFN- $\gamma$  is sufficient for tumor rejection [97]. It was later shown that it acts on endothelial cells in the tumor stroma and causes destruction of the tumor vasculature [97, 98]. IFN- $\gamma$  is also shown to inhibit angiogenesis [99]. TNF- $\alpha$  acts on endothelial cells as well and induces tumor necrosis, while it also leads to reduced angiogenesis [100, 101]. Moreover, CD8<sup>+</sup> T cells are thought to directly kill stromal cells that cross-present antigens probably by perforin [102]. On the other hand, CD4<sup>+</sup> T cells are essential for providing help to CD8<sup>+</sup> T cells, as shown by CD40/CD40L interactions upon the engagement of TCRs on antigens presented by MHC II molecules on dendritic cells [88]. Ligation of CD40 on dendritic cells with CD40L on the surface of CD4<sup>+</sup> T cells is thought to enhance antigen presentation and promote CD8<sup>+</sup> T cell activation via the production of several cytokines [103]. Furthermore, CD4<sup>+</sup> T cells produce cytokines that act on the tumor stroma. The T<sub>H</sub>1 subset is characterized by IFN- $\gamma$  production that has the aforementioned effects on tumor vasculature [104]. The T<sub>H</sub>2 subset expresses IL-4, which is thought to act on tumor-associated fibroblasts that support tumor growth. In this case, the function of IL-4 is to suppress angiogenesis [105, 106]. T cells can employ all described mechanisms synergistically, while the importance of tumor stroma modulation to achieve tumor rejection is underscored. However, the impact of naturally occurring interactions between a cancer and the immune system on cancer growth is often controversially discussed.

## 1.4 Cancer immunotherapy

Several forms of therapy fall under the category “cancer immunotherapy” ranging from immune modulatory agents to advanced cell therapies. The ultimate goal of all forms is to utilize a patient’s own immune system in the most effective way in order to fight against its own cancer cells or promote an anti-tumor immune response. Promising discoveries as well as fast-developing technology enable rapid progress in the field of cancer immunotherapy.

### 1.4.1 Cytokines

Cytokines are essential proteins of the immune system as they provide growth, differentiation and other regulatory signals in response to specific stimuli. Once they bind to their high-affinity receptors on the cell surface of immune cells, they activate intracellular signaling pathways that alter the transcription profile of a cell and also support cell-to-cell communication [107]. Therefore, cytokines are considered immunomodulatory agents and their use in cancer immunotherapy has for long been studied [108-110]. Interleukin-2 (IL-2) was the first approved agent in clinical cancer immunotherapy, a few years after the first melanoma patient showed a durable response upon administration of IL-2 in 1984, followed by further positive outcomes [111, 112]. It is known that IL-2 stimulates T cell growth and survival, thus enhancing potential antitumor effects of tumor-infiltrating lymphocytes (TILs) and natural killer cells (NK cells) [113]. Although IL-2 immunotherapy is approved for metastatic melanoma and renal cell carcinoma, only a minority of patients benefit from it, while severe toxicities are linked with its administration [114, 115]. Nowadays, IL-2 is mainly used in cell culture conditions to support T cell growth *ex vivo*. IL-15 is a cytokine with similar functions to IL-2, as it has been shown to enhance T cell survival and promote T cell differentiation to effector states [116]. As a consequence, its use has been extensively studied in preclinical models with encouraging results [117, 118]. However, these results could not be reproduced in human clinical trials, where only minimal and not durable responses were observed often accompanied with severe toxicity [119, 120]. IL-15 is now used in combination with other immune-modulating agents and to improve T cell culture conditions. Other cytokines that have been investigated for their efficiency in antitumor activity are IL-7, IL-12 and IL-21. Likewise, despite the promising results in experimental models, no significant success has been monitored in clinical trials when exploited as monotherapy [121-123]. Due to the findings about the importance of tumor vasculature destruction to achieve tumor rejection, the use of IFN- $\gamma$  and TNF- $\alpha$  is being explored. Initially, the use of recombinant proteins had induced severe toxicity, while no remarkable clinical benefit was observed for the maximum tolerated doses [124-126]. However, recent studies, where both cytokines were modified to have reduced biological

activity and to specifically target tumor stromal cells, may pave the way for new clinical trials [127, 128].

#### **1.4.2 Checkpoint inhibitors**

A well-studied mechanism accounting for the inability of the immune system to fight cancer is the dysregulation of immune cell activity through the activation of T cell inhibitory pathways, also described as checkpoint pathways [129]. CTLA-4 was the first immune checkpoint receptor extensively studied as a target for cancer immunotherapy. It has been shown that CTLA-4 shares the same ligands with the T cell co-stimulatory receptor CD28 required for T cell activation and survival, namely CD80 and CD86 (B7 molecules). As it outcompetes CD28 in ligand binding, it has been proposed that CTLA-4 decreases and inhibits T cell activation by not allowing the activation of CD28-dependent downstream pathways following antigen recognition by a T cell [130, 131]. CTLA-4 influences CD4<sup>+</sup> T cells more than CD8<sup>+</sup> T cells and plays physiologically a significant role in peripheral tolerance. It weakens responses to self-antigens and it prevents autoimmunity, as it is found abundant on a CD4<sup>+</sup> T cell subset, the T-regs, which hold a central role in these processes [132, 133]. However, due to these properties, it also dampens T cell responses in the tumor microenvironment and usually serves as a marker of T cell exhaustion [134]. Early research in preclinical models with antibodies inhibiting CTLA-4 had showed antitumor responses against immunogenic but not against non-immunogenic tumors, suggesting that blocking CTLA-4 can enhance pre-existing immune responses [135]. The monoclonal antibody ipilimumab is nowadays an FDA approved CTLA-4 inhibitor used in melanoma as it improves patient survival and clinical outcome although it usually induces severe toxicities [136-138]. PD-1 is another protein that plays a critical role in tolerance and prevention of autoimmunity. Its expression is induced upon T cell activation. Binding to its ligands, PD-L1 and PD-L2, provides inhibitory signals that decrease cytokine production, T cell activity, proliferation and survival [139-141]. PD-1 is often upregulated on TILs in several cancers, like melanoma, ovarian and lung cancers and PD-L1 is often found in high levels on the surface of solid tumor cells [142, 143]. Nowadays, PD-1 is considered one of the most typical exhaustion markers correlated with anergic T cells in the tumor microenvironment. Blocking PD-1 in preclinical models resulted in enhanced antitumor responses and initiated clinical trials [144, 145]. To date, the monoclonal antibodies nivolumab and pembrolizumab are two FDA approved PD-1 inhibitors that are used in standard care for the treatment of several cancers including melanoma, non-small cell lung cancer and renal cell carcinoma among others. However, administration of PD-1 inhibitors as monotherapy or in combination with anti-CTLA-4 improves survival and overall clinical outcome in a limited proportion of patients. The combination therapy further leads to the occurrence of more

adverse events, although most are well-tolerated [146, 147]. The biggest challenge of checkpoint inhibitors immunotherapies is the lack of predictive biomarkers that can support identification of patients likely to respond. It is generally believed that smaller tumors and tumors with higher mutational loads and thus more abundant presence of neoantigens correlate with better clinical outcomes after such immunotherapies [148, 149]. Certain limitations, like upregulation of other inhibitory markers or acquired resistance to therapy, are also often described [150]. Therefore, extensive research is still required to understand the mechanisms behind responses related to checkpoint inhibition in order to improve clinical efficacy.

### **1.4.3 Cancer vaccines**

The aim of every vaccine is to stimulate the immune system to mount a response against an antigen. Prophylactic vaccines have been notably useful in preventing the onset of virus-associated cancers, like the hepatitis B virus (HBV) vaccine developed in the late 1970s and the human papilloma virus (HPV) vaccine. Chronic infection by HBV is associated with hepatocellular carcinoma. The vaccine efficiently protects from the onset of cancer, as the production of virus-neutralizing antibodies prevents the development of both acute and chronic hepatitis [151, 152]. HPV is associated with cervical and head and neck cancers. The first HPV vaccine, approved by the FDA in 2006, contains virus-like particles able to stimulate the production of antibodies, thus preventing infections that may eventually lead to the development of HPV-associated cancers [153-155]. Vaccines against other viruses also associated with certain cancer types, like the Epstein-Barr virus (EBV), are currently being under investigation [156]. The prospect of therapeutic vaccines aiming to deliver targeted antigens into a cancer patient in order to elicit an antitumor response is also been explored. Targeting shared TAAs in the scope of making vaccines an eligible therapy for many patients has not delivered satisfying clinical results [157]. Clinical trials targeting common TAAs, such as MART-1 in melanoma or MUC1 in lung cancer, showed only limited objective responses probably due to established central tolerance against these antigens [158, 159]. To date, the only therapeutic vaccine approved by the FDA is Sipuleucel-T, which is used as a first-line treatment of metastatic prostate cancer despite discussions on its efficacy. It consists of autologous peripheral blood mononuclear cells activated with a prostate antigen (prostatic acid phosphatase, PA2024) fused to an immune-cell activator (granulocyte-macrophage colony stimulating factor, GM-CSF) [160]. Later, studies started focusing on TSAs. Early evidence in preclinical models showed that vaccination with CD4<sup>+</sup> neoantigens conferred anti-tumor activity and T cell responses were able to control tumor growth [161]. Neoantigen vaccination is a personalized approach and a significant challenge is the selection of the target antigen(s).

Several tools have been developed to predict epitopes able to elicit immune responses [162, 163]. Another requirement is the proper presentation of the selected antigens; therefore different antigen delivery methods have been studied. Monocytes from a patient's peripheral blood can be isolated and mature to DCs *ex vivo* with the use of specified cytokine cocktails. DC vaccines consist of a dendritic cell population pulsed with antigens of choice and are delivered to the patient to fulfill their role as antigen-presenting cells. Such vaccine was able to induce antigen-specific T cell responses and influence the TCR repertoire in melanoma patients [164]. Direct injection of RNA molecules or long peptides, which are ingested, processed and presented by APCs, is another delivery method. In respective clinical trials in melanoma and gastrointestinal cancer patients, such neoantigen vaccines were able to induce specific T cell responses [165-167]. This fast emerging field has led to a variety of currently ongoing clinical trials, while there are efforts to improve vaccine formulation and antigen selection.

#### **1.4.4 Adoptive T cell therapy**

The adoptive T cell therapy (ATT) of solid tumors was pioneered over half a century ago, but has gained a lot of interest during the last decades [168]. The rationale behind ATT is the *ex vivo* expansion of a T cell population of interest under appropriate conditions and the transfer of sufficient cell numbers back to the cancer patient. This allows overcoming obstacles that lead to tumor progression, such as lack or inadequacy of tumor-specific T cells, T cell inhibition, tolerance and infiltration. The origin of the T cells is usually autologous and they can be modified or unmodified.

##### **“Unmodified” T cells**

ATT with TILs in a wide range of clinical trials has led to durable and even complete responses in the clinic. TILs occur naturally and infiltrate tumors. They can be isolated from tumor material, e.g. surgical resections, and they are expanded *ex vivo* in the presence of IL-2 before they are reinfused to a patient. It has been shown that expanded TIL products consist mainly of T-effector-memory cells [169]. TIL presence in the tumor microenvironment has been long correlated with natural anti-tumor responses and improved clinical outcomes [170]. Several small-scale clinical studies led to the final proof that TIL therapy can induce anti-tumor immunity in melanoma patients, who were pre-conditioned with chemotherapy and received high doses of IL-2 along with TILs expanded *ex vivo* with a proven tumor specificity [169, 171, 172]. Lymphodepletion prior to therapy is thought to reduce the competition for nutritional factors and cytokines from endogenous populations and eliminate immunosuppressive population like T-regs [173]. The simultaneous administration of IL-2 boosts TIL expansion

[174]. Although TIL therapy is usually well-tolerated, its application has been limited to melanoma [175, 176]. Efforts against other types of cancers are constantly being made [177, 178]. A main limitation remains the recovery of TILs from a tumor tissue, where they are often found in insufficient numbers and with an already impaired function [179]. Even though it has been shown that TIL impairment may be reversible during *ex vivo* expansion, re-exposure to the antigens upon ATT may lead to an irreversible dysfunctional state through epigenetic changes [180]. The most interesting question that has been raised regarding TILs concerns their specificity. Initially, it was widely believed that TILs are directed against TAAs, like melanoma differentiation antigens or cancer-testis antigens. Later, it was shown that precursor frequency against these antigens is rather rare and often less than 1% [181, 182]. To date, it is known that in cases of effective TIL therapy, T cell responses were also mounted against neoantigens presented by both HLA (human leukocyte antigen) class I and class II molecules [183-185]. These findings partially explain the success of TIL therapy against melanoma, a cancer type with a usually high mutational load, which is thought to give rise to a variety of neoantigens that enable endogenous anti-tumor responses. The rise of the TIL field led to the evolution of T cell engineering in order to transfer antigen specificity and make the transferred T cell products highly tumor-specific.

### **CAR-modified T cells**

Chimeric antigen receptors (CARs) refer to hybrid receptors with distinct characteristics. They consist of a single chain variable fragment (scFv) of a monoclonal antibody able to bind an antigen on the cell surface, a CD3 $\zeta$  chain as an intracellular TCR signaling domain and a co-stimulatory signaling domain such as CD28 or 4-1BB [186, 187]. Therefore, CARs contain properties of both TCRs and antibodies. CAR recognition circumvents the need for antigen processing and presentation via MHC molecules as it is directed against surface-expressed antigens [188]. CARs can be directed against recurrent antigens shared among many patients and cancer types. The therapeutic approach is based on the genetic modification of autologous peripheral blood lymphocytes (PBL) with CARs. Isolated T cells are genetically engineered with a CAR of interest and expanded *ex vivo* before they are reinfused into the patient (CAR-T cell therapy). Since the first construction of CARs, the construct design of the receptors has undergone significant changes and improvements, resulting to four CAR generations with different properties. The first CAR generation contained only the scFv and a CD3 $\zeta$  signaling domain, which were able to mediate IL-2 production and cell lysis in a non-MHC-dependent manner [189]. Second and third generation CARs exploited the addition of the co-stimulatory domains CD28 and 4-1BB and relevant combinations of those, which resulted in enhanced T cell activation and proliferation [190-192]. Fourth generation CARs or alternatively called

TRUCKs (T cells redirected for universal cytokine killing) deliver transgenic products, like IL-12 or IL-18, to the tumor tissue upon CAR binding to the targeted antigen. Such inducible releases are able to mediate acute inflammation in the tumor stroma and attract other immune cells in order to augment improved anti-tumor responses [193-195]. In the clinic, CAR-T cell therapy has shown great success against certain hematological malignancies, when targeting CD19, which is overexpressed on the surface of leukemic cells. Nowadays, CD19 CAR-T cell therapy is FDA approved for patients with ALL and non-Hodgkin lymphoma [196]. However, a common escape mechanism that has been described is loss of CD19 [197, 198]. Other targets derived from the B cell lineage, like CD22 and BCMA, are also being investigated [199-201]. Targeting solid tumors with CARs has achieved limited clinical efficacy so far, assumingly due to the unavailability of suitable extracellular targets and the inaccessibility of the tumor microenvironment. Studies in preclinical models and in the clinic have involved CARs against the receptor tyrosine kinase HER2 in sarcomas, the epidermal growth factor (EGFR) in non-small cell lung cancer and the carbonic anhydrase IX (CAIX) in renal cell carcinoma [202-205]. However, the use of CARs against solid cancers remains a challenge.

### **TCR-engineered T cells**

T cells can be equipped with new antigen specificity through genetic engineering using genes encoding for a specific TCR. This process can be facilitated with lentiviral and retroviral vectors that carry TCR cassettes and allow for stable gene expression upon transduction [206, 207]. The design of the transgene cassettes has been extensively investigated, as it is important that both the  $\alpha$  and  $\beta$  chain of a TCR are translated into a functional pair. Initially, either two single vectors were used for transduction or the chains were linked via an internal ribosomal entry site (IRES), but both methods resulted in poor TCR expression [208]. To date, the most widely accepted strategy is a cassette linking the  $\alpha$  and the  $\beta$  chain via a picorna virus-derived peptide element (2A element). This peptide causes a ribosomal skip during translation that results in the production of two proteins from the same mRNA molecule, which efficiently form a functional TCR pair on the T cell surface [209-211]. TCR-gene encoding vectors are used to transduce PBLs, which acquire a new receptor specificity and can be further expanded *ex vivo* before ATT. Expectedly, the selection of antigen is one of the most critical parameters, as both TAAs and TSAs can be targeted with a TCR. Although the presence of TAAs in normal tissue cannot be excluded, as they are normal proteins overexpressed or aberrantly expressed in cancer cells, they are often selected as targets for ATT as they are shared between different patients. An early clinical trial that targeted the melanoma differentiation antigen MART-1 resulted in objective responses against metastatic melanoma lesions as well as serious toxicity [212]. An example of successfully targeting a self-antigen is NY-ESO1, a cancer-testis antigen

discovered using the SEREX technique by screening patient sera for antitumor responses [51]. Melanoma and synovial sarcoma patients treated with NY-ESO1-transduced T cells showed durable responses [213, 214]. However, toxicities associated with the targeting of TAAs in clinical trials remain a concern [215, 216]. As a consequence, there is an essential need to evaluate TAAs as targets prior to any therapeutic attempt [217]. There is overwhelming evidence that immune responses can be mounted against TSAs [218-220]. Recent findings suggest that successful clinical responses are mediated through T cells that recognize neoantigens [149, 184, 221]. Along with the rapid progress of sequencing techniques that allow the in-depth analysis of mutated genes in a tumor, neoantigens are explored as ideal T cell targets for ATT [222]. To date, such therapeutic strategies are evaluated in mouse models. Initial studies have shown that tumors overexpressing a mutant neoantigen can be successfully targeted by TCR gene therapy achieving tumor eradication [223, 224]. In these studies, treating tumors with natural and unmanipulated antigen expression levels led to tumor escape. Tumor heterogeneity indicating the presence of variants that do not contain the targeted antigen is one of the greatest challenges of neoantigen-specific TCR gene therapy. Another aspect is the source of TCRs that are going to be used to genetically modify T cells. As in neoantigen vaccines, it is common practice to rely on prediction algorithms to evaluate whether a mutated protein can be a good target or not. Based on the *in silico* outcome, mutated peptides are often used to prime T cells *ex vivo*. T cells that respond to the peptides are subsequent to TCR isolation [225]. However, such strategies do not take endogenous antigen processing and presentation into consideration, often leading to insufficient TCR recognition in an actual experimental setting [226]. Moreover, studies are focused mainly on the human HLA-A2 allele, which is expressed in many individuals of specific populations [227]. This focus creates a bias in both experimental efforts and prediction algorithms, which subsequently remain underdeveloped for the other MHC alleles. Efforts to isolate mutation-specific TCRs from the endogenous repertoire have brought encouraging results, as TCRs against driver mutations have been isolated from TIL products [228, 229]. Figure 2 describes the ideal clinical course upon cancer diagnosis till the adoptive transfer of tumor-reactive T cells back to the patient.



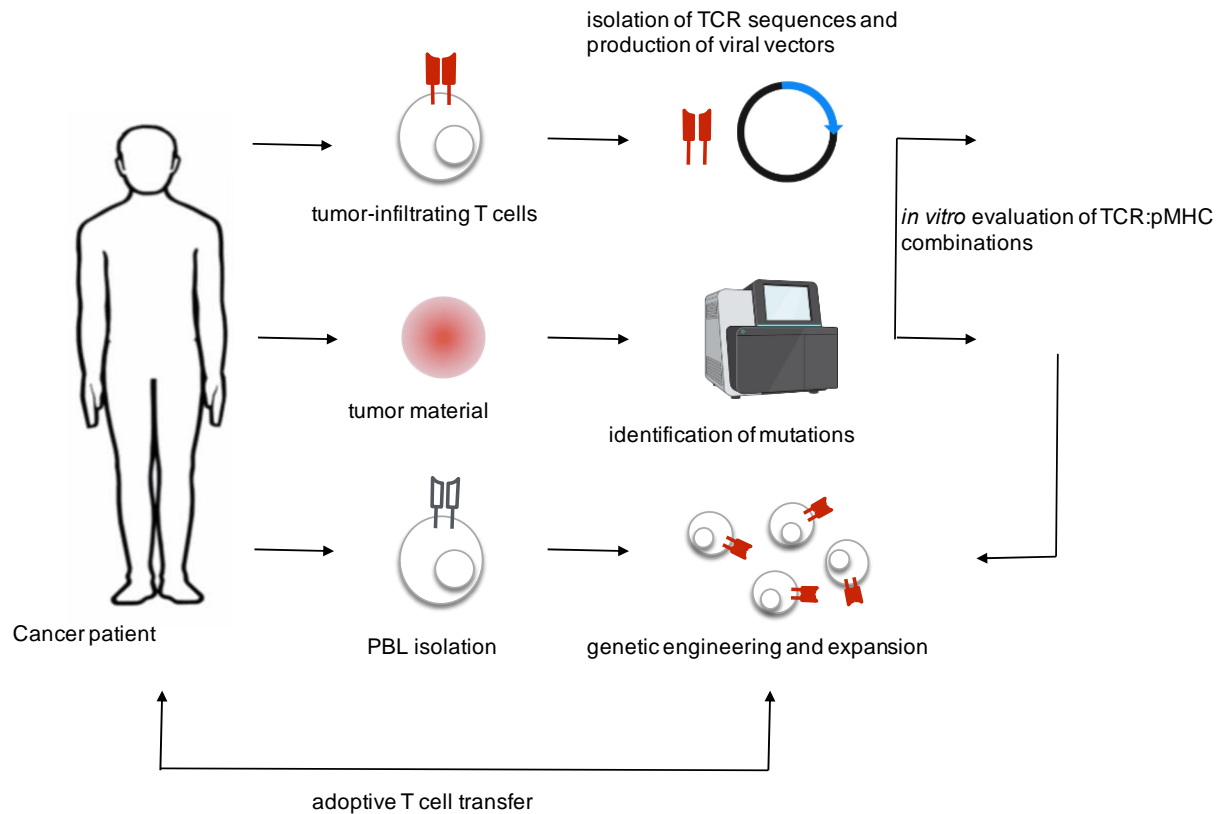


**Figure 2: Schematic representation of adoptive T cell transfer**

Tumor-infiltrating T cells can be used to isolate tumor-reactive TCR gene sequences, which can be encoded in viral vectors. Tumor material is used to identify all mutations of a cancer entity by whole exome and RNA sequencing. The nature of the T cell response can be evaluated *in vitro* and the viral vectors are used to genetically engineer healthy peripheral blood lymphocytes (PBL) from the cancer patient. Once the modified T cells are expanded *ex vivo* in sufficient numbers, they can be adoptively transferred back to the patient and find their target in the tumor environment. pMHC: peptide-MHC.

### Parameters that determine antigen quality

The recognized antigen of TCR-engineered T cells has to bear certain attributes in order to be effectively targeted. An important prerequisite is antigen processing and presentation. The binding of an epitope to MHC molecules depends on the peptide-MHC (pMHC) affinity, which is measured by the  $IC_{50}$  value. This value is determined in competition experiments and is defined as the peptide concentration needed to cause 50% inhibition of a standard peptide bound to a specific MHC molecule [230]. Tolerance mechanisms are usually established against TAAs as they are self-antigens [231]. On the contrary, TSAs have the potential to create high affinity epitopes due to the amino acid changes, which affect both direct binding to the MHC groove as well as TCR recognition of the cognate antigen. As already mentioned, algorithms can predict the pMHC affinity of a given peptide. However, the predicted values might differ significantly from the ones measured experimentally as algorithms are only trained

sufficiently well only for some MHC molecules [232, 233]. Therefore, algorithms for rarely studied MHC molecules do not exist or are less predictive. It has been shown that the pMHC affinity is a critical parameter for efficient ATT and usually affinities <200 nM are considered optimal [234, 235]. Another important parameter when selecting a target antigen is its abundance in cancer cells. One aspect is the expression level of an epitope, as it has to be sufficiently presented on the cancer cell surface. A second aspect is intratumor heterogeneity as any tumor consists of different subpopulations with distinct genotypes that have been acquired during tumor development. Therefore, an antigen present in the parental population might no longer be expressed in other branches and vice versa new antigens are acquired during proliferation or in metastatic populations. However, an antigen essential for tumor maintenance has higher chances to be present in all cancer cells even at later stages of cancer development. Advanced methods like NGS and single-cell sequencing are necessary to dissect intratumor heterogeneity, as it can lead to inevitable tumor escape. Last, the spatial expression of an antigen underscores the advantage of targeting TSAs. Since the presence of TAAs in normal tissue is often not excluded, targeting such antigens has led to severe adverse events, as mentioned above. Therefore, targeting TSAs exclusively found in the tumor tissue could lead to an optimal therapeutic efficacy and safety. As a consequence, several criteria have to be considered to determine a suitable target for ATT.

## **1.5 Preclinical models**

Preclinical models aim to resemble the clinical situation, in order to evaluate parameters for effective therapeutic approaches. In cancer research, there are distinct categories of mouse models each having different advantages and disadvantages, that need to be considered when designing a study.

### **1.5.1 Xenograft models**

Xenograft models refer to a distinct category of mouse models commonly used in cancer research. Nowadays, the most common strain used is abbreviated as NSG (NOD-SCID-IL2 $\gamma$ <sup>null</sup>), which was generated by crossing non-obese diabetic mice (NOD) that have impaired innate immunity with severe combined immunodeficiency mice (SCID) that lack the adaptive arm of the immune system. A mutation in the IL-2 receptor  $\gamma$  chain gene was also introduced, thus leading to severely immunodeficient mice that lack NK cells and T and B cell function combined with impairments in several cytokines [236]. These mice allow the engraftment of established human cancer cell lines to develop tumors that are subjected to immunotherapies, especially CAR-T cell therapies [237]. Patient-derived xenograft (PDX) models are a distinct subcategory. These mice are engrafted with primary human tumor material and are believed

to develop tumors identical to the originals [238, 239]. Such models are frequently used to evaluate the course of the disease and to test several therapies [240]. However, there are many challenges associated with PDX models concerning tumor engraftment, which is limited to a few tumor types and severe graft-versus-host disease due to the simultaneous transfer of human immune cells attacking the mouse tissues. Specifically in ATT, the presence of murine stroma and other species-specific factors, like cytokine receptors, may limit the function of transferred human T cells in mice [241].

### **1.5.2 Syngeneic models**

Syngeneic tumor models refer to inbred mouse strains, like C57BL/6, BALB/c and C3H mice, where tumors can grow in a reproducible manner and provide a native tumor microenvironment with rapid tumor growth kinetics. Cancer growth takes place upon transplantation of established murine tumor cell lines. These cell lines originate from hosts where tumors developed spontaneously or were induced after exposure to carcinogens, like methylcholanthrene (MCA) or UV light [242]. Several therapeutic approaches can be evaluated in these models. An advantage is that these lines can be easily manipulated to bear certain characteristics, such as high levels of antigen expression. However, these models do not address interpatient heterogeneity and cancer development, because cell lines from fully progressed and homogenous tumors are transplanted. Genetically engineered mouse models (GEMMs) provide insights regarding tumor onset and development because autochthonous tumors with physiological microenvironments arise [243]. These models include transgenic mouse strains that develop tumors in a spontaneous fashion, e.g. through the expression of mutated oncogenes and conditional models, which develop tumors in a regulated and spatiotemporal fashion, e.g. through tissue-specific expression of oncogenes [244-246]. Transgenic models can be particularly useful in the study of human cancer antigens. The basis of this field was set early with the generation of mice expressing the human HLA-A2 molecule [247]. To date, many strains carry transgenes that encode for a variety of HLA class I and II molecules, like HLA-B\*0702 or HLA-DR4 as a few characteristic examples [248, 249]. The generation of a transgenic mouse strain that also co-expresses a human TCR repertoire along with HLA-A2 led to the development of a therapeutic TCR against MAGE-A1 [250]. The selection of a suitable preclinical model depends on the question(s) that each study attempts to answer. The advantages of employing syngeneic mouse models in cancer research, such as representative tumors of the original cancers, reproducibility and native responses can compensate for potential drawbacks, like the absence of physiological cancer development.

### 1.5.3 Ag104A as a model of spontaneous cancer

Most syngeneic mouse models that are used in cancer research involve transplantable tumors that were induced by carcinogens like MCA or after exposure to UV light. Such tumors harbor an unnaturally high number of somatic mutations and thus the chances of finding relevant immunological targets for immunotherapy are also high. Moreover, tumors that are frequently described as spontaneous, like the B16 melanoma, have been serially passaged and transplanted for many years, raising often questions about their value as preclinical models [251]. The Ag104A tumor is a fibrosarcoma and arose spontaneously in an aging female mouse of the C3H/HeN strain [252]. The tumor cell line has been established from the original tumor, which has never been passaged in mice. Ag104A, results in aggressive fast-growing tumors, when inoculated in immune-competent hosts and it also metastasizes spontaneously [252]. Like many human cancers, Ag104A is considered poorly immunogenic. Repeated immunizations of immune-competent hosts with lethally irradiated Ag104A tumor cells were able to elicit specific CTL responses. In detail, spleens of immunized mice were cultured with Ag104A tumor cells *ex vivo*, which resulted in the expansion of T cells able to specifically recognize and kill Ag10A4 *in vitro* in a <sup>51</sup>Cr release assay. The same T cells were not reactive against other tumors even when derived from the same mouse strain. Whole exome sequencing of Ag104A revealed a number of mutations comparable to some human cancers. The aforementioned characteristics point Ag104A as a suitable preclinical model to evaluate parameters of ATT under conditions that are often met in the clinical situation.

#### Aim of the thesis

The aim of this doctoral thesis was to investigate critical parameters of neoantigen-specific TCR gene therapy in the native mouse model of spontaneous cancer, Ag104A. The non-manipulated and minimally passaged tumor cell line along with the CTL cultures were obtained as a result of lab exchange with the laboratory of Hans Schreiber at the University of Chicago. Native antigen expression and intratumor heterogeneity in Ag104A resemble human cancers. As a result, this syngeneic mouse model was employed to determine whether poorly immunogenic tumors harboring a low mutational burden can elicit antigen-specific T cell responses and whether targeting a neoantigen with TCR-engineered T cells can impact tumor growth. The steps from TCR isolation to ATT aimed to follow relevant clinical procedures that should be performed when neoantigen-specific TCR gene therapy is the selected therapeutic approach.

## 2. Materials and methods

### 2.1 Molecular biology

#### 2.1.1 Isolation of TCR sequences

Total RNA was isolated from T cell pellets (RNeasy Micro Kit, Qiagen) and subjected to 5' rapid amplification of cDNA ends (RACE) Polymerase Chain Reaction (PCR) using the SMARTer RACE cDNA Amplification kit according to the manufacturer's protocol (Clontech, Takara). Reverse transcription and cDNA synthesis were performed in one reaction. The SMARTScribe Reverse Transcriptase (RT) generates a first cDNA strand with an extended 3' tail due to its terminal transferase activity. The addition of the SMARTer II A oligonucleotide, which anneals to the cDNA tail and carries an additional SMARTer sequence, allows RT to switch templates and generate a complete cDNA copy of the original RNA. A 5'-CDS primer is added to prime the first-strand cDNA synthesis (protocol summarized in Table 1). The 5' RACE PCR reaction was performed in 50  $\mu$ l according to the following protocol (Tables 2 and 3). The SMARTer II A oligonucleotide and the Universal Primer Mix are not gene-specific and allow for the amplification of all TCR diverse sequences (V(D)J regions) at the 5' end which are unknown. The sequence of at least 23-28 nucleotides at the 3' end of the gene to be amplified needs to be known in order to design gene-specific antisense primers. Therefore, 3' primers were designed to anneal to the  $\alpha$  or the  $\beta$  chain mouse constant region (Table 4) and used in separate reactions (Eurofins Genomics).

5' cDNA synthesis (per sample)	
2,75 $\mu$ l	RNA
1 $\mu$ l	5'-CDS Primer
3 min	72°C
2 min	42°C
1 $\mu$ l	SMARTer RACE IIA oligo
2 $\mu$ l	5x First strand buffer
1 $\mu$ l	DTT (20 mM)
1 $\mu$ l	dNTP Mix (10 nM)
0,25 $\mu$ l	RNAse inhibitor (40 U/ $\mu$ l)
1 $\mu$ l	SMARTScribe Reverse Transcriptase
90 min	42°C
10 min	70°C
20 or 100 $\mu$ l	Tricine - EDTA

**Table 1: Reaction mix and protocol of cDNA synthesis**

5' RACE Mix (per sample)	
29 $\mu$ l	H <sub>2</sub> O
10 $\mu$ l	5x GC PCR buffer (Thermo Scientific)
1 $\mu$ l	Primer mCa-RACE or mCb-RACE (10 $\mu$ M)
5 $\mu$ l	Universal Primer Mix (Clontech)
1 $\mu$ l	dNTPs (10 nM)
1 $\mu$ l	Phusion polymerase (Thermo Scientific)
3 $\mu$ l	cDNA (previously diluted according to Clontech)

**Table 2: Reaction mix of 5' RACE PCR**

Touch-down PCR			
denaturation	98°C	2 min	5x
denaturation	98°C	30 sec	
annealing/elongation	72°C	2 min	
denaturation	98°C	30 sec	5x
annealing	70°C	30 sec	
elongation	72°C	2 min	
denaturation	98°C	30 sec	25x
annealing	68°C	30 sec	
elongation	72°C	2 min	
final elongation	72°C	5 min	
hold	4°C	-	

**Table 3: Reaction protocol of 5' RACE PCR**

Gene-specific primers (mouse)	
mCa-RACE	5'-CAGGCAGAGGGTGCTGTCCTGAGA-3'
mCb-RACE	5'-GGAGACCTTGGGTGGAGTCACATTTCT-3'

**Table 4: List of primers used in 5' RACE PCR**

RACE PCR products were analyzed in an ethidium bromide-containing agarose gel and DNA was isolated (Invisorb Fragment CleanUp, Invitex Molecular). Amplified DNA fragments were bluntly cloned into the pcR4 TOPO vector (Zero Blunt TOPO PCR cloning kit, Invitrogen by Life Technologies) according to the manufacturer's instructions. MACH1 chemically competent *E. coli* bacteria (Thermo Fisher) were transformed. Plasmid DNA was isolated from clones (24-30 clones per sample, Invisorb Spin Plasmid Mini Two, Invitex Molecular) and sequenced

(Eurofins Genomics). Identification of TCR sequences was done with the IMGT V-QUEST software available online ([http://www.imgt.org/IMGT\\_vquest/vquest](http://www.imgt.org/IMGT_vquest/vquest)) [253, 254].

### 2.1.2 Generation of MP71 vectors containing TCR transgene cassettes

TCR $\alpha$  and TCR $\beta$  chain sequences were combined to identify functional pairs. Transgene cassettes were created *in silico* (Serial Cloner 2.6.1) in a TCR $\beta$ -P2A-TCR $\alpha$  configuration as previously described and synthesized by GeneArt (Thermo Fisher) [210]. The sequences were optimized for most frequent mouse codon usage. To enable cloning, transgene cassettes were designed to contain NotI and EcoRI restriction sites at the 5' and 3' end respectively. The synthesized products were digested and ligated into the digested and dephosphorylated (alkaline phosphatase, Roche) pMP71-PRE (pMP71) vector (Rapid DNA ligation, Roche). MACH1 bacterial cells were transformed and plasmid DNA was sequenced as indicated above. Verified sequences were used to generate high yields of transfection-grade plasmid DNA (Plasmid Maxi Kit, Qiagen).

### 2.1.3 Generation of MP71 vectors encoding MHCI sequences

To generate vectors encoding H-2<sup>k</sup> MHCI sequences, the following primers were designed (Table 5, Eurofins Genomics). Total RNA was extracted from spleen cells of C3H mice and used for cDNA synthesis (SuperScript II, Invitrogen) using a random primers mix (Promega). PCR was performed on cDNA to isolate H-2K<sup>k</sup> or H-2D<sup>k</sup> sequences. The primers contained NotI and EcoRI restriction sites as listed below to enable cloning into pMP71. Cloning and subsequent procedures were performed as indicated above.

H-2k specific primers (mouse)		Protein ID (Uniprot)
H2Kk_F	5'-CAG <u>CGGCCGCCACCATG</u> GCACCCTGCATGCT-3'	P04223
H2Kk_R	5'-TCGAATTCTCACGCTAGAGAATGAGGGTCA-3'	
H2Dk_F	5'-CAG <u>CGGCCGCCACCATG</u> GGGGCGATGGTACC-3'	P01899
H2Dk_R	5'-TCGAATTCTCACGCTTTACAATCTGGGAGA-3'	

**Table 5: List of primers specific for H-2<sup>k</sup> MHCI sequences**

Restriction sites are underlined and the Kozak sequence is shown in italic. Start and stop codons are highlighted in red.

### 2.1.4 Generation of pcDNA3.1 vectors

pcDNA3.1 vectors containing cassettes of interest were generated to allow *in vitro* transcription of RNA. Tandem minigenes cassettes were designed *in silico* (see Results) and synthesized by GeneArt. Mouse codon optimization was performed. The synthesized products were cloned into the pcDNA3.1 vector by using NheI and XhoI restriction sites at the 5' and 3' end respectively. DNA for subsequent procedures was generated as indicated above.

### 2.1.5 Generation of *in vitro* transcribed RNA

pcDNA3.1 vectors allow for *in vitro* transcription of RNA under the control of the T7 primer. 10 µg of vectors containing sequences of tandem minigenes were linearized by the XbaI restriction enzyme. Digested products were analyzed on an agarose gel and linearized DNA was purified as previously described. 1 µg of linearized plasmid DNA was used to generate *in vitro* transcribed RNA (mMESSAGE mMACHINE T7 transcription kit, Thermo Fisher) according to the manufacturer's protocol in a 20 µl reaction (Table 6). Immediately after this reaction, generated RNA was tailed by polyadenylation (poly(A) tailing kit, Thermo Fisher) according to the manufacturer's protocol in a 100 µl reaction (Table 7). The reactions were stopped in nuclease-free H<sub>2</sub>O solutions containing 5 M ammonium acetate and 50 mM EDTA. Tailing was confirmed by gel electrophoresis by comparing the size of non-tailed (smaller size) and tailed RNA (larger size by approximately 150 bp). Prior to gel analysis, 1 µl of tailed or non-tailed RNA was denatured for 10 min at 75°C and diluted with 9 µl nuclease-free H<sub>2</sub>O.

<i>in vitro</i> RNA transcription (per sample)	
x µl (1 µg)	linearized DNA
10 µl	2x NTP/CAP
2 µl	10x reaction buffer
2 µl	enzyme mix
up to 20 µl	H <sub>2</sub> O
1 h	37°C
1 µl	TURBO DNase
15 min	37°C

**Table 6: Reaction mix and protocol of *in vitro* RNA transcription**



RNA tailing (per sample)	
20 µl	reaction mix from <i>in vitro</i> transcription
36 µl	nuclease-free H <sub>2</sub> O
20 µl	5x E-PAP buffer
10 µl	25 mM MnCl <sub>2</sub>
10 µl	10 mM ATP
4 µl	E-PAP enzyme (2 U/ml)
1 h	37°C

**Table 7: Reaction mix and protocol of RNA tailing**

Tailed *in vitro* transcribed RNA was extracted by phenol/chloroform purification. In details, 575 µl nuclease-free H<sub>2</sub>O were added along with the aforementioned stop solution. Next, 750 µl of 1:1 phenol/chloroform mixture were added and the mix was centrifuged for 4 min at 11.000 x g and 4°C. The aqueous phase was transferred to a new tube and 750 µl of chloroform were added followed by another centrifugation step (same as before). The new aqueous phase was incubated with 750 µl of isopropanol at -20°C for 15 min. RNA was precipitated by another centrifugation step and pellets were washed once with 200 µl of 100% ethanol. Pellets were resuspended in nuclease-free H<sub>2</sub>O for subsequent procedures.

### 2.1.6 Isolation and detection of gene sequences by PCR

PCR reactions were performed to detect or isolate gene sequences of interest. The following primers were designed to amplify a p53 region of 1.130 bp and 327 bp on genomic DNA and cDNA level respectively (Table 8, Eurofins Genomics). Primers designed for copy number analysis of the p53 gene are also listed with their respective probes (Eurofins Genomics). Genomic DNA (Invisorb Spin Tissue Mini kit, Invitex Molecular) or RNA (RNeasy Micro Kit, Qiagen) was isolated from 5-10x10<sup>6</sup> Ag104A tumor cells. 1 µg of isolated RNA was used for cDNA synthesis (SuperScript II, Invitrogen) using a random primers mix (Promega). 50 ng of genomic DNA or 100 ng of cDNA were used as templates to amplify the aforementioned p53 region in a 50 µl reaction according to the following protocol (Tables 9 and 10). PCR products were analyzed by gel electrophoresis and isolated DNA was sequenced.

p53 specific primers (mouse)	
p53_FWD	5'-gaagacaggcagacttttcg-3'
p53_REV	5'-agaggcgcttgtgcaggt-3'
Trp53-F	5'-gccgacctatcctaccatcatc-3'
Trp53-R	5'-cctaccacgcgccttcta-3'
Trp53-C-FAM	5'-cactggaagactcc-3'
Trp53-F-FAM	5'-cactggaagagtcc-3'
Trp53-F-FAM	5'-cactggaagagtcc-3'

**Table 8: List of mouse p53 specific primers**

PCR protocol		
98°C	2 min	
98°C	30 sec	35x
65°C	30 sec	
72°C	30 min	
72°C	5 min	
4°C	-	

**Table 9: Standard PCR protocol**

PCR Mix (per sample)	
x µl	H <sub>2</sub> O
10 µl	5x GC PCR buffer
1 µl	Forward primer (10 µM)
1 µl	Reverse primer (10 µM)
1 µl	dNTPs (10 nM)
1 µl	Phusion polymerase
y µl	gDNA or cDNA

**Table 10: Standard PCR mix**

When necessary, fragments of tandem minigene constructs were obtained by PCR in order to analyze specific sequences (see Results). pcDNA3.1 vectors containing tandem minigene sequences were used as templates to amplify regions of interest. The following primers were designed (Table 11, Eurofins Genomics). Amplified PCR products were analyzed by gel electrophoresis and DNA was isolated. To enable *in vitro* RNA transcription of purified fragments when necessary, the sequence of the T7 primer was added to the forward primers.

PCR reactions and protocol were the same as indicated above. The sequences of isolated fragments were confirmed by Sanger sequencing.

p53 specific primers (mouse)	
M7_P1F	5'-GAAATTAATACGACTCACTATAGGGAGACC-3'
M7_P1R	5'-GCTCACAGCACGCAGCTCTCGTGCAGAT-3'
M7_P2F	5'-GAAATTAATACGACTCACTATAGGGGCCACCATGCTGCTGACCATCTACATGGC-3'
M7_P2R	5'-GCTCACTGGAAGTTCCTCTGAAGGTGTAC-3'
M7_P3F	5'-GAAATTAATACGACTCACTATAGGGGCCACCATGCCACCCCTAGCGTGCCACA-3'
M7_P3R	5'-GCTCATTCCACGAACTGCTTCCGTTCCAGG-3'
Trim8_REV	5'-GCTCAGCCAGGCTGCTGAGAGGCATCCAGC-3'
Trp53_FWD	5'-GAAATTAATACGACTCACTATAGGGGCCACCATGAACAGAAGGCCCATCCTGAC-3'
Trp53_REV	5'-GCTCACTCGAAGCTGTCTCTGCCAGCAGG-3'
Ttc21b_FWD	5'-GAAATTAATACGACTCACTATAGGGGCCACCATGCTGGTGGCCAGCGAGGGCAT-3'
Ttc21b_REV	5'-GCTCACAGGGTGCCGTAGGCGTGGTAGAAT-3'
Ttf2_FWD	5'-GAAATTAATACGACTCACTATAGGGGCCACCATGCCTAGCCAGCCAGAAACCC-3'

**Table 11: List of TMG-specific primers**

The T7 promoter sequence needed for *in vitro* transcription of RNA is underlined and the Kozak sequence necessary for translation is shown in *italic*. Start and stop codons are highlighted in red.

### 2.1.8 Genome engineering with the CRISPR/Cas9 system

The CRISPR/Cas9 system was employed to target the p53 gene via homology-directed-repair (Fig. 3). A customized protocol was determined according to previously published guides [255, 256]. A desired guide-RNA (gRNA) was designed by analyzing the target sequence (NCBI gene ID: NM\_011640) with the GPP sgRNA Designer tool provided by the Broad institute (<https://portals.broadinstitute.org/gpp/public/analysis-tools/sgrna-design>). This tool identifies a protospacer adjacent motif (PAM) sequence in the desired area, which enables a cut by Cas9 3 bp upstream the 5' end of PAM. A 20-nucleotides long (cut between nucleotide 17 and 18) gRNA was chosen based on predicted maximum efficiency and the least off-target events. In details, forward and reverse single-stranded oligonucleotides (Eurofins Genomics) were annealed and phosphorylated according to the published protocol and by using the T4 polynucleotide kinase (Thermo Fisher). The PX458 vector encoding the Cas9 endonuclease linked to GFP via a 2A element was digested with the restriction enzyme BbSI to enable blunt ligation of the generated double-stranded oligonucleotide. After dephosphorylation, ligation followed as previously described. MACH1 bacterial cells were transformed and successfully ligated products were verified by sequence analysis of isolated plasmid DNA. The repair template was designed to harbor 40-nucleotides long homology arms on either side of the

target nucleotide. It also contained a silent blocking mutation at the PAM sequence to avoid repeated re-cutting by Cas9 once the desired edit had been introduced and promote efficient homology-directed-repair. One repair template was designed for each of the sense or the antisense strands of p53 and they were purchased as single-stranded oligonucleotides from Eurofins Genomics. The PX458 vector and the repair template were electroporated into target cells as described below.

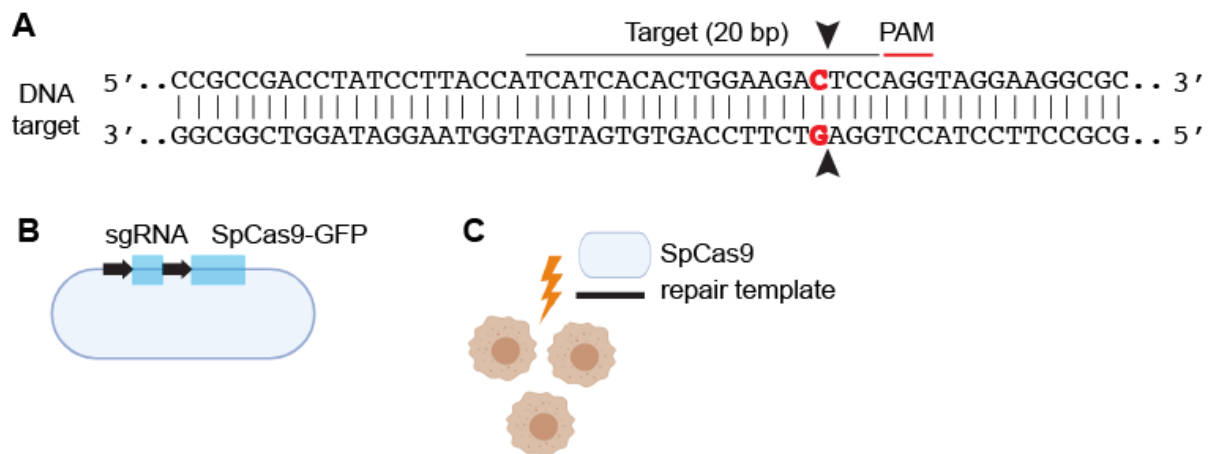


**Figure 3: CRISPR/Cas9 to target p53**

(A) Illustration of p53 target sites by the Cas9 endonuclease. The 20-nt guide RNA sequence pairs with the DNA target upstream of a PAM motif. Cas9 mediates double strand breaks 3 bp upstream of the PAM, indicated by arrows. The mutation to be corrected is shown in red. (B) The gRNA was cloned into the PX458 vector containing the Cas9 endonuclease coupled to GFP. (C) The gRNA-Cas9 vector and the repair template were pulsed into Ag104A tumor cells. One repair template against the sense or the antisense chain was used in 2 independent reactions.

## 2.2 Cell culture

### 2.2.1 Cell lines and primary cell cultures

All cell lines and primary cells were cultured in RPMI 1640 GlutaMAX medium (Gibco, Thermo Fisher) supplemented with 10% heat-inactivated fetal calf serum (FCS, PAN Biotech), 100 U/ml penicillin/streptomycin, 1mM sodium pyruvate, 100  $\mu$ M non-essential amino acids and 50  $\mu$ M 2-mercaptoethanol (complete medium). The Ag104A tumor cell line was established in the laboratory of Hans Schreiber at the University of Chicago [252]. EL4 cells were kindly provided by Wolfgang Uckert, Max-Delbrück-Center for Molecular Medicine, Humboldt University. The mouse packaging cell line Platinum E (Plate-E, Cell Biolabs) was used to generate retroviral supernatants. The cell line is derived from the Human Embryonic Kidney 293T cells (HEK 293T) and expresses the *gag-pol* and *env* genes of the Murine Leukemia Virus (MLV). Plat-E cells were cultured in Dulbecco's modified Eagles medium (Gibco, Thermo Fisher)

supplemented with 10% heat-inactivated FCS and 100 U/ml penicillin/streptomycin. The medium contained 10 µg/ml blasticidin and 1 µg/ml puromycin (Sigma-Aldrich) as selection markers. All cell culture supplements were purchased from Thermo Fisher unless otherwise stated. When necessary, cells were frozen in FCS containing 10% DMSO and stored at -80°C or liquid nitrogen.

### **2.2.2 Isolation and activation of mouse primary T cells**

Spleen cells were isolated from 12-16 weeks old mice and washed with complete RPMI medium. Erythrocytes were removed in ammonium chloride lysis buffer (150 mM NH<sub>4</sub>Cl, 1 mM KHCO<sub>3</sub>, 100 mM Na<sub>2</sub>EDTA, pH 7.2-7.4) during a 5-minute incubation. Cells were washed again in complete RPMI medium and a single cell suspension was generated through a 40 µm cell strainer. The cell concentration was adjusted to 2x10<sup>6</sup> cells/ml. Cells were activated for 24 h with 1 µg/ml anti-CD3 monoclonal antibody, 0.1 µg/ml anti-CD28 monoclonal antibody (both BD Biosciences) and 10 IU/ml recombinant IL-2 (Proleukin, Novartis). All washing steps were performed by centrifugation at 350 x g and room temperature for 5 min.

### **2.2.3 Retroviral gene transfer into cell lines and primary T cells**

To produce ecotropic virus supernatants, Plat-E cells were transfected by calcium phosphate precipitation. Prior to the day of transfection, 8.5x10<sup>5</sup> Plat-E cells were seeded in 6-well cell culture plates. On the day of transfection, a 150 µl solution containing 18 µg plasmid DNA of interest and 250 mM calcium chloride was prepared and another 150 µl of transfection buffer (1.6 g NaCl, 74 mg KCl, 50 mg Na<sub>2</sub>HPO<sub>4</sub>, 1 g HEPES in 100 ml H<sub>2</sub>O, all Sigma Aldrich) were added dropwise. The precipitate-containing solution was incubated at room temperature for 15 minutes and added to the Plat-E cells. After a 6 h incubation, Plat-E medium was exchanged with complete medium and transfected cells were further incubated for 42-48 h. Viral supernatants were harvested and filtered (0.45 µm pore size). Plat-E cells were provided with fresh complete medium and incubated for another 24 h, before harvesting supernatants for the second time. Transduction was performed in 24-well cell culture plates coated with 12.5 µg/ml RetroNectin (Takara) for 2 h at room temperature or at 4°C overnight. Coated plates were blocked with 2% BSA for 30 minutes at 37°C and washed with 2 ml PBS/well. For transduction of suspension cell lines, 1 ml of medium containing 2x10<sup>5</sup> cells was mixed with 1 ml of harvested virus supernatant provided into the coated plates. 8 µg/ml of protamine sulfate (Sigma Aldrich) were additionally provided and plates were centrifuged for 90 minutes at 800 x g and 32°C. The second transduction followed 24 h later, when 1 ml was carefully removed from each well and supplied with 1 ml of freshly harvested viral supernatant containing 4 µg/ml protamine sulfate. For transduction of primary spleen cells, RetroNectin-coated 24-well plates

were provided with 1 ml of harvested viral supernatants and centrifuged for 90 minutes, at 3.000 x g and 4°C. After this step, 1 ml of complete medium containing  $1.5 \times 10^6$  activated spleen cells supplemented with  $4 \times 10^5$  mouse T-activator CD3/CD28 beads (Invitrogen), 10 IU/ml recombinant IL-2 and 8 µg/ml protamine sulfate was added to each virus-coated well and centrifuged again for 30 minutes, at 800 x g and 32°C. For the second transduction, 1 ml was carefully removed from each well and supplied with 1 ml of freshly harvested viral supernatant containing 10 IU/ml recombinant IL-2 and 4 µg/ml protamine sulfate. The plates were then centrifuged for 90 minutes, at 800 x g and 4°C. For transduction of adherent cell lines, 24-well tissue-treated cell culture plates were used without the need for RetroNectin coating. One day prior to transduction,  $2 \times 10^4$  cells/well were seeded to the plates. On the day of transduction, 1 ml of freshly harvested viral supernatant containing 8 µg/ml protamine sulfate was provided to each well and plates were centrifuged for 90 minutes at 800 x g and 32°C. The second transduction was performed as for suspension cell lines. Transduced cell lines and primary cells were incubated for further 6 h after the second transduction and transferred to appropriate cell culture vessels. Transduced primary cells were washed with complete medium and supplemented with 50 ng/ml recombinant IL-15 (Miltenyi). Cell concentration was adjusted to  $1 \times 10^6$  cells/ml. Transduction efficiency was evaluated by flow cytometry after 72 h. Genetically engineered spleen cells were either used immediately for adoptive T cell transfer or incubated for an additional week before subsequent *in vitro* procedures and freezing. Every 2-3 days fresh medium containing 50 ng/ml IL-15 was provided to the cells. Where indicated, specific T cell subpopulations were isolated for further analysis with the Easysep Mouse CD8α Positive Selection Kit II or the Easysep Mouse CD4 Positive Selection Kit II (both STEMCELL Technologies) according to the manufacturer's protocol.

#### **2.2.4 Electroporation of cell lines**

Cell lines were electroporated with a MicroPulser Electroporator instrument in 0.4 cm wide cuvettes suitable for mammalian cells (both Bio-Rad Laboratories). Pulsing conditions were determined at 350 V and 250-500 µFD. Cultured cells were washed and resuspended in pre-chilled Opti-MEM medium (Gibco, Thermo Fisher) without any supplements. For the electroporation, 200 µl containing  $2 \times 10^6$  cells were mixed with 10 µg of *in vitro* transcribed RNA in a cuvette and the mix was pulsed according to the instrument's specifications. Control cells were pulsed by adding comparative volumes of H<sub>2</sub>O. Immediately after pulsing, cells were washed with pre-warmed cell culture medium (complete RPMI medium), transferred in an appropriate vessel and incubated for 16-24 h at 37°C and 5% CO<sub>2</sub> before further analysis.

### 2.2.5 IFN- $\gamma$ treatment

To upregulate antigen presentation, cells were treated with recombinant IFN- $\gamma$  (BD Biosciences) where indicated. Cells were seeded in 6-well plates with a cell concentration of  $1 \times 10^6$  cells/ml and 100 ng of IFN- $\gamma$  were added to each well. After a 24-h incubation, the medium was renewed and additional 100 of IFN- $\gamma$  were added for another 24 h (37°C, 5% CO<sub>2</sub>). Treatments were performed in triplicates. Cells were immediately used for subsequent procedures.

### 2.2.6 5-Azacytidine treatment

To inhibit methylation processes, cells were treated with 5-Azacytidine (Sigma-Aldrich) where indicated. Cells were seeded in 6-well plates with a cell concentration of  $1 \times 10^6$  cells/ml and indicated amounts (1 - 25  $\mu$ M, see Results) of 5-Azacytidine were added every 24 h for 4 consecutive days after medium renewal [257]. Treatments were performed in triplicates. After 96 h (37°C, 5% CO<sub>2</sub>), cells were immediately used for subsequent procedures.

## 2.3 Functional assays

### 2.3.1 Flow cytometry

Expression of surface antigens was detected by flow cytometry by staining  $5 \times 10^5$  to  $1 \times 10^6$  cells with 0,2-1  $\mu$ g of specific monoclonal antibodies conjugated with allophycocyanine (APC), phycoerythrin (PE), fluorescing isothiocyanate (FITC) or brilliant violet (BV421) in 50  $\mu$ l PBS solutions for 20 min at 4°C or room temperature when necessary. Cells were washed twice with PBS and analyzed by FACS (FACSCanto, BD Biosciences or MacsQuant, Miltenyi). Discrimination between living and dead cells was achieved by adding Sytox-Blue (Biolegend) to the stained solution immediately before FACS analysis without any additional wash step at a 1:1.000 dilution. For proliferation assays, the CellTrace Far Red Cell proliferation kit (Invitrogen, Thermo Fisher) was used according to the manufacturer's instructions. FACS sorting of desired cells was performed in a FACS Aria instrument to acquire living cells for further analysis. Data were analyzed with FlowJo (BD Biosciences).

Specificity	Conjugate	Clone	Source
v $\beta$ 5.1, 5.2 T-Cell Receptor	PE	MR9-4	Biolegend
v $\beta$ 6 T-Cell Receptor	PE	RR4-7	Biolegend
v $\beta$ 7 T-Cell Receptor	PE	TR310	Biolegend
v $\beta$ 8.3 T-Cell Receptor	PE	1B3.3	BD Biosciences

vβ8.1, 8.2 T-Cell Receptor	PE	MR5.2	Biolegend
vβ9 T-Cell Receptor	PE	MR10-2	Biolegend
CD3ε	PE/FITC/APC/BV421™	145-2C11	Biolegend
CD4	PE	RM4-5	Biolegend
CD8α	PE/APC/BV421™	53-6.7	Biolegend
CD90 (Thy1.1)	APC	OX-7	Biolegend
H-2Kb	APC	AF6-88.5	Biolegend
H-2Db	APC	KH95	Biolegend
H-2Kk	APC	36-7-5	Biolegend
H-2Dk	PE	15-5-5	Biolegend
PD-1 (CD79)	PE	J43	Biolegend
2B4	PE	m2B4 (B6) 458.1	Biolegend
Tim-3	PE	B8.2C12	Biolegend
<b>Isotype controls</b>	<b>Conjugate</b>	<b>Clone</b>	<b>Source</b>
Rat IgG1, k	PE	MOPC-21	Biolegend
Rat IgG2a, k	PE/APC	MOPC-173	Biolegend
Rat IgG2b, k	PE/APC	MPC-11	Biolegend

**Table 12: List of antibodies used for flow cytometry**

### 2.3.2 Cytokine release assay

To determine antigen-specific stimulation of T cells, co-cultures were performed. In details,  $5 \times 10^4$  effector cells (gene-engineered T cells) were incubated together with  $5 \times 10^4$  target cells in round-bottom 96-well plates for 16-24 h at 37°C and 5% CO<sub>2</sub>. Non-engineered effector cells were used as control. Effector cells were treated with 1 μM ionomycin (Calbiochem) and 5 ng/ml phorbol-12-myristate-13 acetate (PMA) (Promega) for TCR-independent stimulation. Supernatants were harvested and 50 μl were analyzed for IFN-γ concentration by enzyme-linked-immunosorbent assay (ELISA, BD Biosciences) according to the manufacturer's protocol. Effector T cells incubated only with medium are indicated as "none" values and PMA/Ionomycin stimulated T cells are indicated as "max" values. For peptide stimulation and titration, effector T cells were co-cultured with peptide-loaded freshly isolated and irradiated (63 Gy) spleen cells of C3H mice. Peptides were purchased from Biosyntan and resuspended in DMSO at 1 mM stock concentrations. Serial dilutions were performed from a starting concentration of  $10^{-6}$  M (1 μM). All co-cultures were performed in triplicates.



## **2.4 *In vivo* and *ex vivo* experiments**

### **2.4.1 Mice**

C3H Rag<sup>+/+</sup>, C3HxRag2<sup>-/-</sup> and B6 mice were bred in a specific pathogen-free environment at the animal facility of the Max-Delbrück-Center for Molecular Medicine. Mice were used for *in vivo* experiments between 8 and 16 weeks of age. All animal experiments were conducted under the institutional and national guidelines and approved by LAGeSo Berlin.

### **2.4.2 Tumor challenge**

C3HxRag2<sup>-/-</sup> mice were challenged with 5x10<sup>6</sup> living Ag104A tumor cells per mouse resuspended in 100 µl PBS. Cells were subcutaneously injected into the left flank of the mice with a 27G needle. Mice were anesthetized by continuous flow administration of an isoflurane-O<sub>2</sub> mixture. Tumor growth was assessed every 2-3 days by using a caliper. Tumor volume was determined according to the following formula:  $\pi/6 \times (a \times b \times c)$ , where a, b and c refer to all three tumor dimensions.

### **2.4.3 Adoptive T cell transfer**

Adoptive T cell transfer (ATT) took place 14 days after tumor cell inoculation. On day 3 after retroviral transduction, 1x10<sup>6</sup> genetically engineered antigen-specific T cells were resuspended in 100 µl PBS per mouse. Cell suspensions were injected intravenously to the mice. Transduction efficiency was determined by flow cytometry. Mice were sacrificed when tumor volume reached the permitted limit, when overall health condition of the mouse imposed it or when 100 days survival post ATT was achieved.

### **2.4.4 Analysis of peripheral blood**

Peripheral blood was obtained from vena facialis on days 4, 7, 14, 21 and 28 post ATT. In cases of 100 days survival post ATT, peripheral blood was again analyzed before sacrifice. Blood analysis was performed by flow cytometry. In details, 50 µl of blood were blocked with Fc Block (BD Biosciences) for 10 min and stained with antibodies of interest (50 µl antibody mixture in PBS per sample) for 20 min at room temperature. Erythrocytes were removed in ammonium chloride lysis buffer as previously described. Samples were washed twice with PBS and whole sample measurements were analyzed. All washing steps were performed by centrifugation at 350 x g for 5 min and 4°C.

#### **2.4.5 Isolation and analysis of tumor samples**

Tumors of sacrificed mice were excised and disrupted with a gentleMACS Dissociator in gentleMACS tubes (Miltenyi). Digestion of tumor pieces took place for 1 h at 37°C in RPMI medium supplemented with 5% FCS, 2 mg/ml collagenase D (Roche) and 10 IU/ml DNase I (Sigma). Another 30-min incubation at 37°C followed by adding 1 ml trypsin-EDTA solution (Gibco, Life Technologies). Tumor digests were washed in complete RPMI medium and used for subsequent procedures. To analyze TILs, aliquots of tumor digests were stained with markers of interest and analyzed by flow cytometry. Where indicated, CD3<sup>+</sup> T cells were isolated by negative selection (Easypep negative selection Mouse T-Cell Isolation Kit, STEMCELL Technologies) according to the manufacturer's protocol. To establish cell lines from reisolated tumors, 5x10<sup>6</sup> cells of digests were seeded in an appropriate culture vessel in complete RPMI medium and observed for cell growth for 3 days. Before subsequent procedures, they were passaged for 3 times unless otherwise indicated.

#### **2.5 Data and statistical analysis**

All data were analyzed in GraphPad Prism 6 (GraphPad, La Jolla, CA, USA) and displayed as mean and the standard deviation where applicable. Statistical analysis was performed in the same software. Statistical significance between two groups was determined by unpaired Student's *t* tests with Welch's correction. *P* values > 0,05 were considered significant and are indicated where applicable. Illustrations were made with the BioRender online software (<https://biorender.com/>).

### 3. Results

Ag104A is a tumor that arose spontaneously in an aged C3H/HeN (C3H) mouse, as previously described. First, the specific cytotoxic responses of T cell cultures originating from immunized immune-competent hosts were subjected to isolation of TCR sequences. Second, it was investigated whether these responses were directed against a neoantigen by establishing an antigen-identification protocol that allows for the simultaneous evaluation of the target. Third, it was examined whether neoantigen-specific TCR gene therapy is effective against large established Ag104A tumors with natural levels of antigen expression.

#### 3.1 Immunization of immune-competent mice with Ag104A tumor cells generates tumor-specific T cell responses

Immunocompetent C3H mice were immunized with irradiated Ag104A tumor cells two to four times at 2-weeks intervals. Spleens from these mice were isolated 10 days after the last immunization and incubated *ex vivo* with living Ag104A cancer cells. Cytotoxic CD8<sup>+</sup> T cell cultures were obtained by limiting dilution cloning [252]. These CTLs were used as starting material and provided by Hans Schreiber. Based on previously observed CTL cytotoxicity, several Ag104A-specific cultures, named L1, A2, A3 and P7, were analyzed to obtain TCR $\alpha$  and TCR $\beta$  chain sequences. RNA was isolated from all cultures, and cDNA was synthesized and subjected to 5' RACE PCR. Respective DNA bands were cloned bluntly into a TOPO vector (Figure 4).

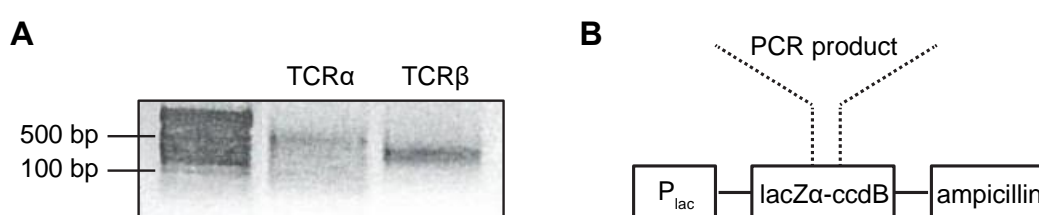


**Figure 4: 5' RACE PCR on CTL cultures**

(A) cDNA from Ag014A-specific cytotoxic T cell cultures was subjected to 5' RACE PCR. A representative example for culture A3 is shown. Expected band sizes are 500 and 350 bp for TCR $\alpha$  and TCR $\beta$  chains respectively. (B) Graphic illustration of the TOPO vector indicating the site of blunt insertion of isolated DNA fragments from the 5' RACE PCR. Successful insertion disrupts the lethal *E. coli* gene *ccdB*, thus allowing growth of transformed bacterial cells. P<sub>lac</sub>: lac promoter, ampicillin: resistance and selection marker.

Plasmid DNA from bacterial colonies was isolated and sequenced. All sequences were analyzed in the IMGT/V-Quest software, which compares input T cell receptor sequences with reference sequences for similarity and successful rearrangement. Several TCR $\alpha$  and TCR $\beta$  chains were isolated in varying frequencies. Culture P7 represents an early stage of an anti-Ag104A culture, whereas L1, A2 and A3 refer to late stages of spleen cell cultures incubated together with Ag104A cells. As expected many chains were isolated at a very low frequency from culture P7. However, all chains that were isolated from cultures L1, A2 and A3 were also detected in P7 (Table 13).

		V region	CDR3	J region	Frequency
L1	$\alpha$ chain	TRAV9D-3*01	CAVSGGGSNYKLTF	TRAJ53*01	50%
		TRAV12-1*03	CAFSGNYKYVF	TRAJ40*01	25%
		TRAV3-4*01	CAVSNTDKVVF	TRAJ34*01	25%
	$\beta$ chain	TRBV13-1*02	CASSGRDRNAEQFF	TRBJ2-1*01	93%
		TRBV13-3*01	CASSDWGSYEQYF	TRBJ2-7*01	7%
A2	$\alpha$ chain	TRAV9D-3*01	CAVSGGGSNYKLTF	TRAJ53*01	100%
	$\beta$ chain	TRBV13-1*02	CASSGRDRNAEQFF	TRBJ2-1*01	100%
A3	$\alpha$ chain	TRAV9D-3*01	CAVSGGGSNYKLTF	TRAJ53*01	100%
	$\beta$ chain	TRBV13-1*02	CASSGRDRNAEQFF	TRBJ2-1*01	100%
P7	$\alpha$ chain	TRAV3D-3*01	CAVSNDSGYNKLTF	TRAJ11*01	24%
		TRAV7D-2*01	CAASMDSNYQLIW	TRAJ33*01	16%
		TRAV11*01	CVVGDRGSALRRLHF	TRAJ18*01	16%
	$\beta$ chain	TRBV13-1*02	CASSERQNDTQYF	TRBJ2-5*01	52%
		TRBV13-2*01	CASGDWGDYQYF	TRBJ2-5*01	5%
		TRBV13-2*01	CASGDRGQDTQYF	TRBJ2-5*01	5%

**Table 13: TCR $\alpha$  and TCR $\beta$  chain frequencies isolated from Ag104A-specific CTLs**

Plasmid DNA from 24-30 colonies for each CTL culture was isolated and analyzed for successful TCR rearrangement. Chains with a frequency lower than 5% are not shown.

The most prominent clonotypes were chosen for further analysis and combined to construct different TCR cassettes according to the previously described configuration, which links the  $\beta$  chain at the 5' end with the  $\alpha$  chain at the 3' end via a 2A element [210]. Notably, cultures A2 and A3 were clonal, as the same TCR $\alpha$  and TCR $\beta$  chain was isolated from both. Their sequences were used to design a TCR pair. Since this pair was also found in the L1 culture, the remaining chains detected in L1 were combined in two TCRs. Three  $\alpha$  chains detected in P7 were combined only with the most abundant  $\beta$  chain to construct three further TCRs (Table 14). *In silico* designed pairs were ordered as genes (ThermoFisher, GeneArt gene synthesis)

and subcloned into the vector pMP71 to enable retroviral transduction of mouse primary cells (Figure 5).

TCR	V region	CDR3	J region
M2/3	TRAV9D-3*01	CAVSGGGSNYKLTF	TRAJ53*01
	TRBV13-1*02	CASSGRDRNAEQFF	TRBJ2-1*01
L8	TRAV12-1*03	CAFSGNYKYVF	TRAJ40*01
	TRBV13-3*01	CASSDWGSYEQYF	TRBJ2-7*01
P1	TRAV7D-2*01	CAASMDSNYQLIW	TRAJ33*01
	TRBV13-1*02	CASSERQNQDTQYF	TRBJ2-5*01
P5	TRAV3D-3*01	CAVSNDSGYNKLTF	TRAJ11*01
	TRBV13-1*02	CASSERQNQDTQYF	TRBJ2-5*01
P8	TRAV11*01	CVVGDRGSALRRLHF	TRAJ18*01
	TRBV13-1*02	CASSERQNQDTQYF	TRBJ2-5*01
L3	TRAV3-4*01	CAVSNTDKVVF	TRAJ34*01
	TRBV13-3*01	CASSDWGSYEQYF	TRBJ2-7*01

**Table 14: TCR $\alpha$  and TCR $\beta$  chain combinations**

The most prominent clonotypes were combined into TCR pairs in order to be tested for Ag104A specificity.

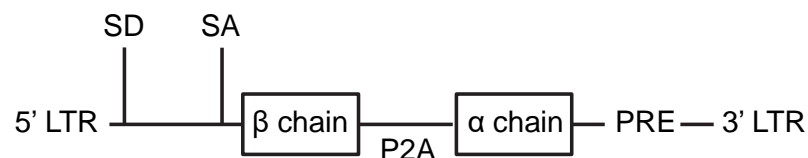


**Figure 5: TCR transgene cassettes**

Transgene cassettes were cloned into the pMP71 vector shown at the illustrated configuration. LTR: long terminal repeats of the myeloproliferative sarcoma virus (MPSV), SD: splice donor, SA: splice acceptor, PRE: post-transcriptional regulatory element, P2A: picorna virus-derived peptide element used as linker.

TCR $\alpha$  and TCR $\beta$  chain pairs were transduced in freshly isolated and polyclonally stimulated spleen cells of immunocompetent C3HxRag<sup>+/-</sup> mice. Expression was monitored by analyzing the presence of the  $\beta$  chain of each pair with flow cytometry. All combinations could be expressed (Figure 6A). To test whether the TCRs recognize Ag104A, genetically engineered T cells were co-cultured at 1:1 ratio with Ag104A tumor cells *in vitro*. Recognition was assessed by IFN- $\gamma$  secretion in an ELISA assay. Two of the TCRs, M2/3 and L8, recognized Ag104A tumor cells and were therefore selected for further analysis (Figure 6B). The tumor cell lines

6132A and 6139B served as specificity control. Both established cancer cell lines originate from tumors that were UV-induced in immunocompetent C3H/HeN mice [252].

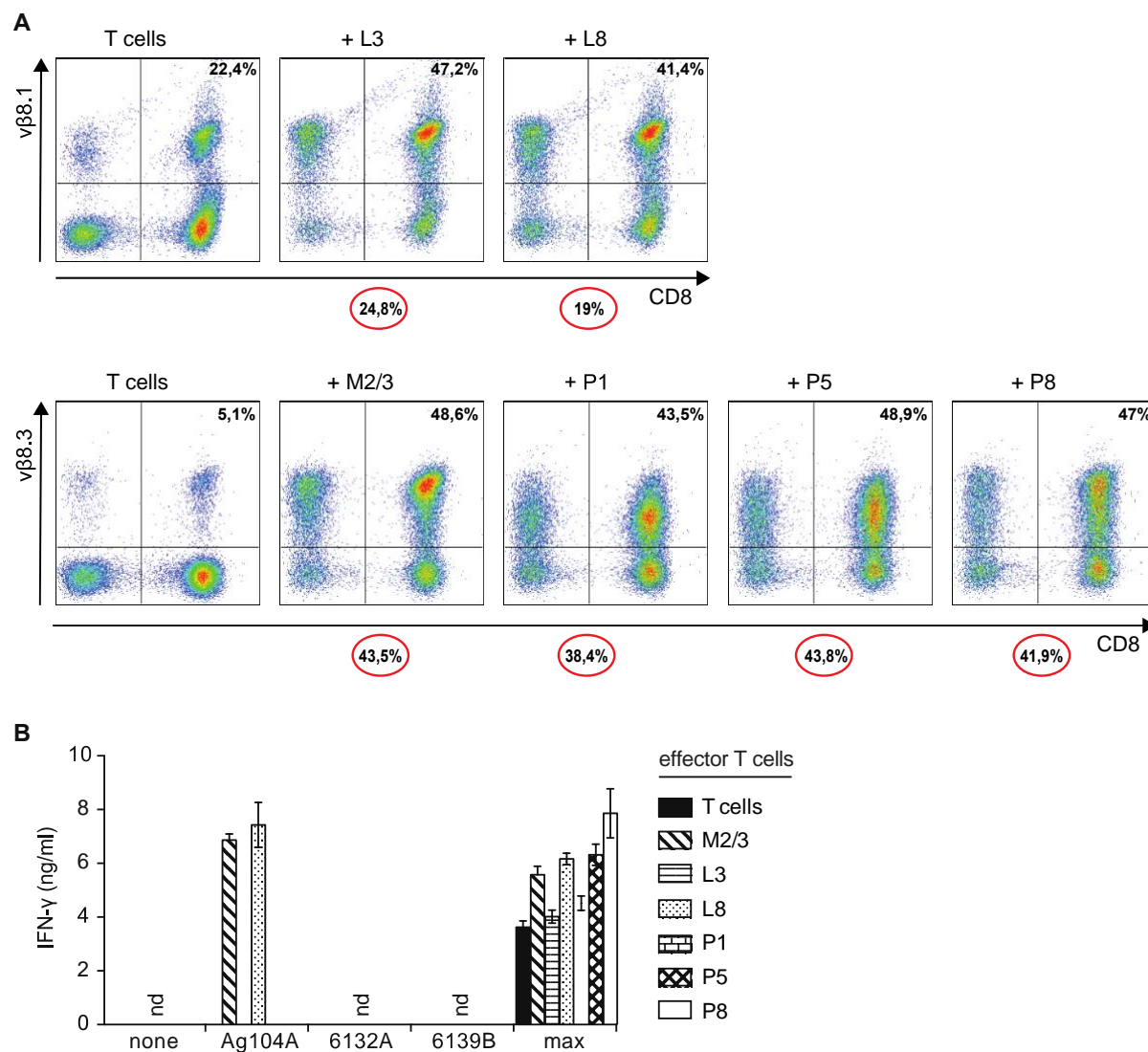


**Figure 6: Expression of TCR transgene cassettes and recognition of Ag104A**

(A) TRC transgene cassettes were transduced in primary T cells. Surface expression and transduction rates (indicated in red circles by subtracting the percentage of the endogenous population from the gate percentage of  $CD8^+TCR\beta^+$  cells) were assessed by flow cytometry by staining for the  $\beta$  chain of each pair. Numbers within the gates indicate percentage of cells in each gate. Gates were set according to the endogenous populations of non-engineered spleen T cells. (B) Non-engineered and engineered T cells were incubated with Ag104A tumor cells ( $5 \times 10^4$  cells, 1:1 ratio), medium (none) or PMA and ionomycin (max) for TCR-independent stimulation. Recognition was determined by IFN- $\gamma$  secretion with an ELISA assay. A representative example of three independent experiments is shown. nd: not detected.

### 3.2 Tandem minigene constructs serve as a reliable tool to determine TCR specificity

Computational algorithms can be used as a tool to predict neoepitopes as suitable targets for TCR gene therapy based on pMHC affinities. However, it has been shown that they are not always accurate for all MHC or HLA alleles mainly due to the lack of sufficient experimental data that are needed to train these algorithms. For some alleles (e.g. for H-2D<sup>k</sup>), they are not even available. As a result, an alternative and reliable method is needed. To prove that a given TCR isolated from a tumor-bearing or an immunized host is mutation-specific and therefore recognizes a neoepitope, a method that allows for rapid antigen identification and covers the entire tumor mutanome was developed. Important criteria for method design were the applicability to different tumor types and the independency from primary material, which is often a limiting factor.

To address this challenge, a strategy based on tandem minigenes (TMGs) encoding for potential neoantigens was followed. The recent development of TMGs has facilitated the analysis of the nature of T cell responses [258, 259]. However, the published methodologies have certain caveats. First, it is not ensured that every peptide in a TMG construct is properly cleaved by the proteasome to generate an epitope. Second, since TMGs encode consecutive sequences of several peptides, it has not been examined whether each position can serve equally well for antigen expression and presentation. Here, the 75bp long sequences (minigene) of 10 different potential neoepitopes were concatenated in each TMG, thus resulting in the expression of 10 different 25-mers with the mutation of the respective gene in the center. An AAY proteasomal cleavage site separates the minigenes from each other [260]. Both characteristics, the length of minigenes and the addition of AAY, ensure processing and presentation of the potential neoepitopes. The construct is linked to GFP via a 2A element to allow monitoring of gene expression in subsequent experiments (Figure 7A). The constructs were cloned into the pcDNA3.1 vector, which allows for *in vitro* RNA transcription (Figure 7B).

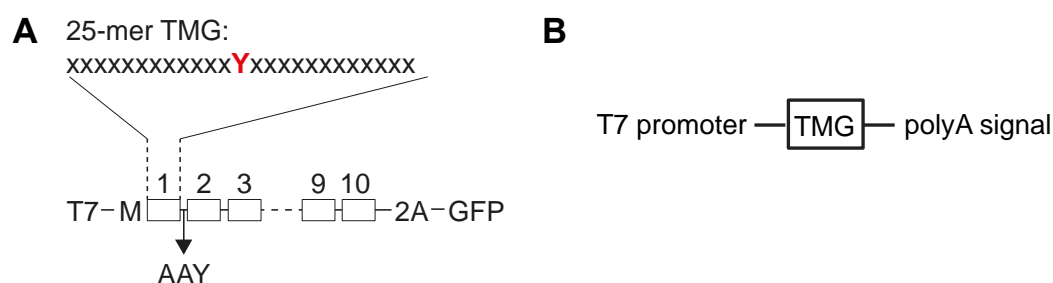


**Figure 7: Design of tandem minigenes**

(A) Schematic illustration of a tandem minigene construct. Each TMG consists of sequences of 10 different potential neoepitopes and results in the expression of 25-mers with the mutation in the center. Each sequence is separated from the next by an AAY proteosomal cleavage site. To monitor gene expression, GFP is linked to the construct via a 2A element. A methionine (M) and a Kozak sequence

were added at the 5' end of each TMG to ensure translation. (B) TMGs were cloned into the pcDNA3.1, which allows for *in vitro* RNA transcription enabled by the T7 promoter. A polyA signal at the 3' end of the construct included in the vector ensures proper RNA polyadenylation for mRNA translation.

To confirm that all 10 positions in such construct can be processed and presented, four control minigenes were created by employing five previously described antigens for which respective TCRs were available (Table 15).

Antigen	Epitope	Restriction	TCR	Reference
mp68	SNFVFAGI	H-2K <sup>b</sup>	1D9	[223]
SV40 pI	SAINNYAQKL	H-2D <sup>b</sup>	TCRI	[261]
SV40 pIV	VVYDFLKC	H-2K <sup>b</sup>	TCRIV	[261]
LCMV (gp33 <sub>33-41</sub> )	KAVYNFATC	H-2D <sup>b</sup>	P14	[262]
OVA	SIINFEKL	H-2K <sup>b</sup>	OT-1	[263]

**Table 15: List of epitopes used to construct control TMGs**

Four control minigenes were designed to assess efficiency of the antigen identification method. All positions of control TMGs were exchanged against five described antigens for which the respective TCRs were available. The table shows the epitope sequences, which were flanked by the adjacent sequences of each protein to a total of 25 amino acids. The epitopes were in the center of each minigene. MHC I restriction and TCRs that recognize the epitopes are also listed.

In each control TMG, five positions were exchanged according to the scheme shown in Figure 8A. To complete the desired 25-mer, the flanking wild-type sequences of each protein were added. Empty positions encoded for 25-mer sequences irrelevant to the experimental setup. EL4 cells, which are of H-2<sup>b</sup> background, were used as antigen-presenting cells (target cells) [264]. Expression of MHC I molecules was confirmed by flow cytometry (Figure 8B). All five antigens are H-2<sup>b</sup>-restricted, therefore T cells of B6 mice were transduced with the respective TCRs (Figure 8C). *In vitro* transcribed RNA (ivtRNA) encoding for the control TMGs was electroporated into target cells and GFP expression was assessed by flow cytometry after 24 hours (Figure 8D). The cells were then co-cultured with genetically engineered B6 T cells. Antigen recognition was determined by IFN- $\gamma$  secretion in an ELISA assay. All antigens independent of their position were recognized in all control TMGs (Figure 8E).



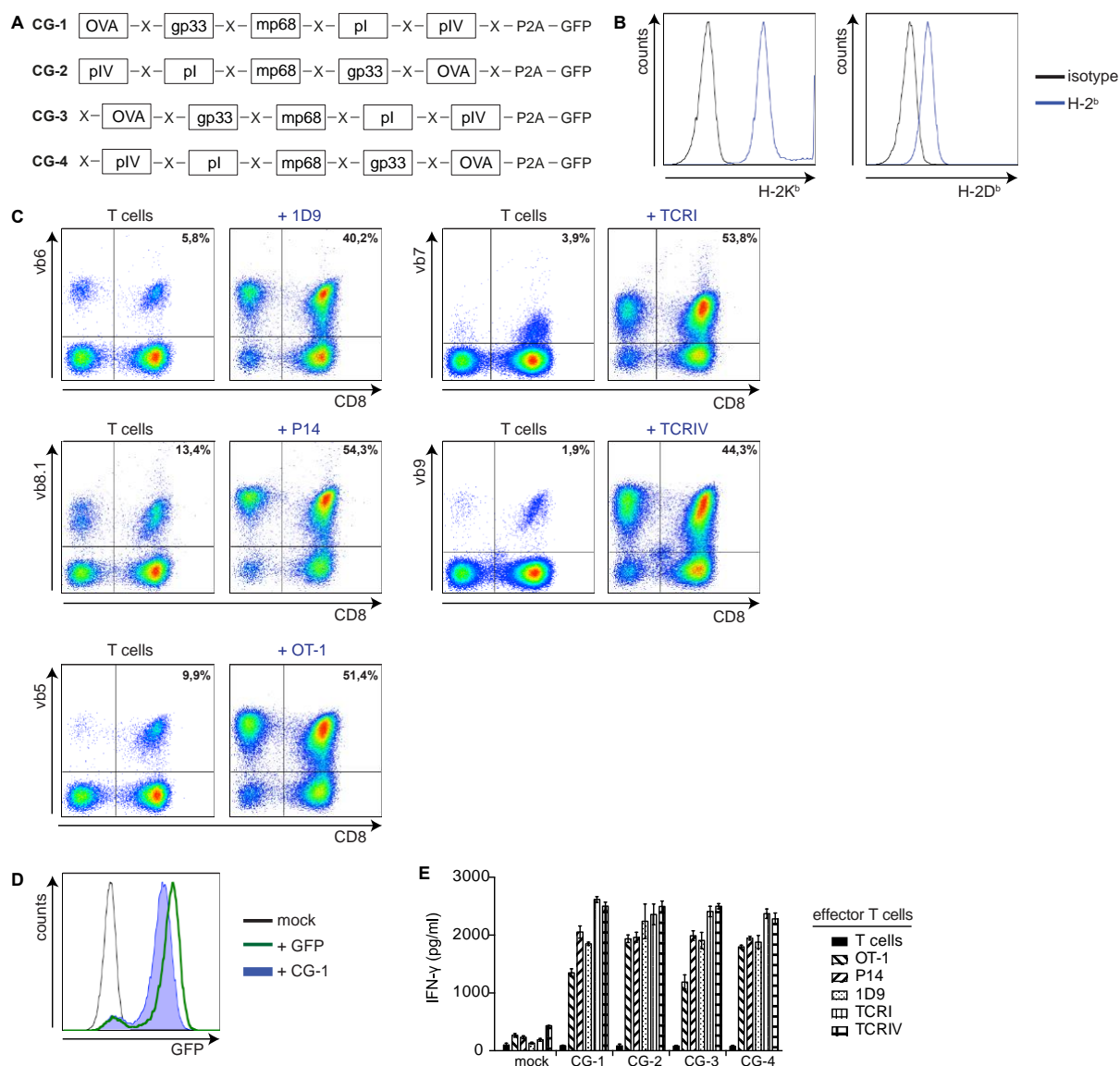


**Figure 8: Each position of a TMG construct supports antigen expression and presentation**

(A) Schematic illustration of the four designed control minigenes (CG = control TMG). X: 25-mer peptide sequences irrelevant to this experimental setup. (B) H-2<sup>b</sup> expression in EL4 cells was assessed by flow cytometry. An isotype control was included. (C) TCRs that recognize epitopes of control minigenes were expressed in B6 T cells after retroviral transduction. Transduction rates were determined by flow cytometry by staining for the  $\beta$  chain of each TCR. Non-engineered T cells were also stained as controls and for gating. Numbers indicate percentage of cells in each gate. (D) *In vitro* transcribed RNA of control minigenes was electroporated into EL4 cells. GFP expression was assessed 24 hours later by flow cytometry. GFP RNA was electroporated into EL4 cells as control. Mock control EL4 cells were electroporated with H<sub>2</sub>O. CG-1 is shown as a representative example. (E) Genetically engineered B6 T cells were incubated with electroporated EL4 cells expressing control minigenes ( $5 \times 10^4$  cells, 1:1 ratio), medium (none) or PMA and ionomycin (max). Mock refers to irrelevant TMG RNA. Recognition was determined by IFN- $\gamma$  secretion in an ELISA assay. A representative example of two independent experiments is shown.

### 3.3 The Ag104A-specific TCR M2/3 recognizes a neoantigen that results from a point mutation in p53

The aforementioned experiments served as an internal control of the assay and proved that the use of TMGs for antigen identification is reliable. Ag104A harbors 172 mutations on genomic DNA level, 77 of which are expressed as revealed by whole exome and RNA sequencing (Table 16). The sequencing was performed at the University of Chicago by Kazuma Kiyotani. Mutations were assessed by comparison of Ag104A cancer cells with autologous nonmalignant heart-and-lung fibroblasts (HLF) isolated from the original Ag104A-bearing host as “germline control”. All expressed mutations were analyzed by the NetMHC 4.0 Server to predict pMHC affinity [232, 233]. C3H mice bear MHCI molecules of the H-2<sup>k</sup> haplotype. No prediction algorithm is available for H-2D<sup>k</sup>, therefore predicted affinities could only be shown for H-2K<sup>k</sup>. The analysis showed that 14 out of 77 expressed mutant peptides are predicted to be strong binders to H-2K<sup>k</sup> (pMHC < 200 nM). Some of them are also highly expressed (Figure 9).

Gene	AA change	Copies (wt)	Copies (mut)	Gene	AA change	Copies (wt)	Copies (mut)
Adam19	H585R	23	24	Mvp	L715R	103	131
Ado	T20S	52	37	Nuak1	P277S	9	5
Aff4	K920T	134	86	Nup98	G366D	135	20
Aspm	A1480G	28	29	Pdxk	V254G	42	16
Atf7	A222P	20	21	Pgm2	Q533E	72	90
Ath1	W662C	36	8	Pip5k1c	I83V	41	10
AU040320	T609P	50	6	Plekhg5	V611L	4	6
Bmper	G477R	32	35	Pnkd	A313T	1	1
Caprin1	Q444H	718	10	Prrt4	C464W	3	2
Ccdc102a	Q430R	26	31	Rhobtb2	R277H	3	3
Ccdc71l	L88V	23	9	Rpl7	R44L	4975	2
Cpsf2	A533G	140	150	Rpn2	T394A	506	502
Ctdspl2	E64D	79	19	Rpsa	N110D	6228	2
Dhx15	A268P	354	157	Sbsn	G128R	7	9
Dhx15	T22A	209	161	Smad3	E149A	8	3
Dimt1	P65A	94	22	Smarca4	R885P	117	79
Dpp9	F55V	90	6	Smarca5	K298N	466	265
Dst	A3023P	175	33	Snx24	I154L	113	38
Eef1e1	V52G	96	136	Srgap2	K248N	65	7
Emp2	S15P	0	69	Stt3b	V518M	261	190
Fam57a	V121I	40	42	Syne2	A5815P	34	4
Fbxo30	C524Y	26	45	Tecta	D2103G	0	2
Gpcpd1	K184Q	26	29	Tes	F324V	0	283
Gpt2	K132T	42	43	Tle1	D616Y	54	24
Gtpbbp10	K294N	63	12	Tmem135	T136A	26	31
Hist1h1e	A47P	2426	1338	Tmem189	A127G	68	4
Hivep3	P2165A	1	3	Trim7	D271G	3	4
Irak1bp1	G171A	55	56	Trim8	A520P	193	36
Jak1	P959R	98	103	<b>Trp53</b>	<b>D253E</b>	<b>131</b>	<b>100</b>
Kank1	G1170A	0	12	Ttc21b	D36A	0	22
Kras	Q61H	0	155	Ttf2	K132T	48	56

Krtcap3	L119V	4	2	Ugp2	D430E	80	122
Lrrk2	K2399N	106	47	Uhrf1	H757R	78	84
Macf1	A4547T	213	175	Vgll4	R170H	33	23
Magi1	V1109A	0	2	Zbtb11	E151G	20	1
Man2a1	T1057A	125	118	Zfhx3	A3496P	6	5
Mcm6	R143H	197	142	Zfp456	R368C	19	4
Meox2	R199S	2	7	Zfp786	G712S	0	3
Mtfmt	T50S	27	17				

**Table 16: Expressed mutations in Ag104A**

All expressed mutations (77) determined by RNA sequencing are listed. Mutations (mut) were assessed by comparison of Ag104A tumor cells with HLF (wt) generated as an autologous tissue germline control. Gene names and amino acid changes are listed based on gene and mRNA sequences of the NCBI Nucleotide database (<https://www.ncbi.nlm.nih.gov/nucleotide/>). Copies represent sequencing reads. AA: amino acid.

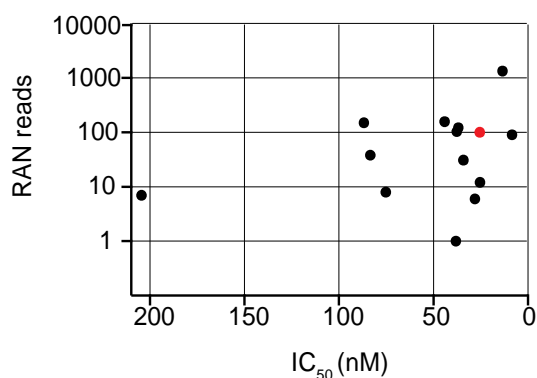


**Figure 9: Varying pMHC affinity and gene expression of potential Ag104A neoepitopes**

Predicted pMHC binding affinities < 200 nM (IC<sub>50</sub> values, NetMHC 4.0) are shown as strong binders to H-2K<sup>k</sup> and plotted against their respective RNA expression levels (RNA reads, logarithmic scale). Mutant p53 is shown as a red dot.

For Ag104A, eight minigenes were designed that incorporated all 77 expressed mutations in the alphabetical order of gene names. To generate suitable target cells without the need of primary Ag104A cancer cells, EL4 cells were stably transduced with H-2<sup>k</sup> constructs (Figure 10A). H-2<sup>k</sup> sequences were isolated from spleens of C3HxRag<sup>+/-</sup> mice. As a result, two target populations were generated, thus allowing for identifying the MHC I restriction of a potential neoantigen. Each population was electroporated with the ivtRNA of TMGs in separate reactions and upon confirmation of GFP expression in the vast majority of cells (Figure 10B), the antigen-presenting populations were co-cultured with M2/3- and L8-genetically engineered T cells. M2/3-engineered T cells specifically recognized TMG-7 presented on H-2K<sup>k</sup>. On the contrary, L8-engineered T cells secreted IFN- $\gamma$  upon stimulation by every TMG expressed on H-2D<sup>k</sup> background (Figure 10C). As a consequence, the L8 TCR was excluded from further analysis as unspecific and all experiments were carried on with the M2/3 TCR.

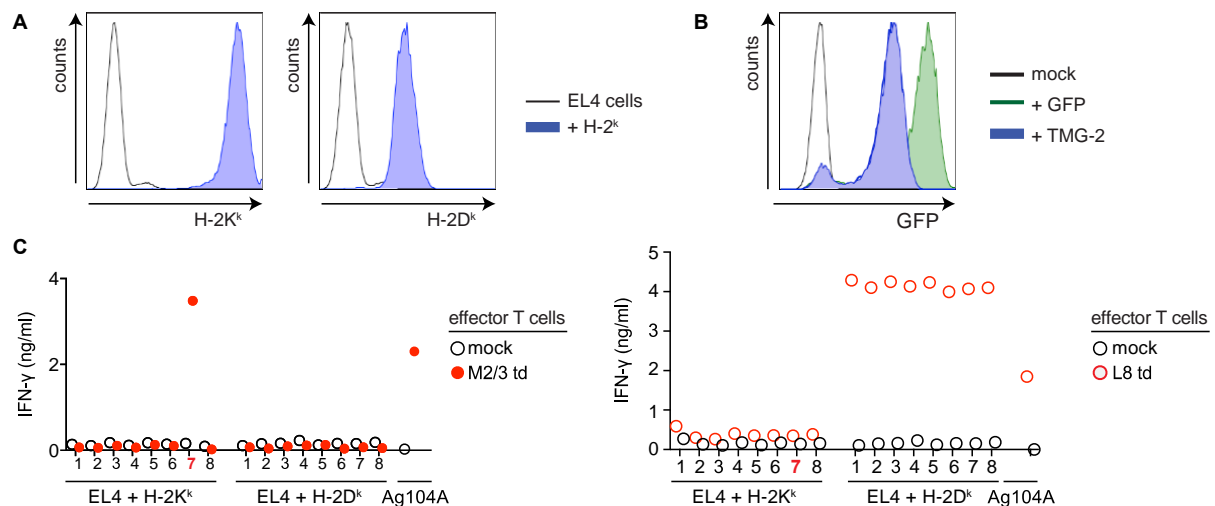


**Figure 10: The antigen recognized by TCR M2/3 is presented by H-2K<sup>k</sup>**

(A) EL4 cells were retrovirally transduced with H-2<sup>k</sup> constructs, resulting in H-2K<sup>k</sup> and H-2D<sup>k</sup> target populations. Expression of H-2<sup>k</sup> was assessed by flow cytometry. Isotype controls were included. (B) H-2<sup>k</sup> transduced EL4 cells were electroporated with each one of the 8 TMGs encoding for potential neoantigens in Ag104A. GFP expression was assessed 24 hours later by flow cytometry. GFP RNA was electroporated into EL4 cells as control. Mock control EL4 cells were electroporated with H<sub>2</sub>O. TMG-2 is shown as a representative example. (C) M2/3- and L8-genetically engineered T cells were incubated with electroporated antigen-presenting EL4 cells expressing all mutations of Ag104A ( $5 \times 10^4$  cells, 1:1 ratio). Recognition was determined by IFN- $\gamma$  secretion in an ELISA assay. Ag104A tumor cells were included as control. A representative example of two independent experiments is shown. td: transduced.

Next, it had to be determined which of the 10 potential neoepitopes included in TMG-7 is the actual target of the M2/3 TCR. Therefore, truncated versions of TMG-7 were generated by PCR. *In vitro* RNA transcription was possible by incorporating the T7 promoter in each fragment (Figure 11A). lvtRNA from each fragment was electroporated into EL4-H-2K<sup>k</sup> cells and co-cultured with M2/3-transduced T cells. In the first screening, TMG-7 was split in three fragments and M2/3 specifically recognized fragment M7-3 (Figure 11B), out of which further truncated versions were generated. During the second screening, it was shown that M2/3 recognizes a mutation in *Trp53* (*TP53* in humans) resulting from a single amino acid substitution of aspartic acid to glutamic acid in position 253 (p53<sup>D253E</sup>) (Figure 11B). RNA sequencing showed that there are 131 copies of wild-type p53 and 100 copies of mutant p53 in Ag104A tumor cells, indicating an equal expression of both variants. Mouse and human p53 proteins are highly similar. According to the COSMIC database (Catalogue of Somatic Mutations in Cancer), the same mutation has been detected in three human tumors, but has not yet been described in murine cancer [265-267]. Recognition of the p53<sup>D253E</sup> mutation (mp53) was confirmed by peptide recognition. A 9-mer peptide (LEESSGNLL) with the mutation in position +3 is predicted to have a slightly stronger pMHC affinity to H-2K<sup>k</sup>

( $IC_{50}$ =25,39 nM) in comparison to the wt peptide (LEDSSGNLL) ( $IC_{50}$ =64,33 nM). Irradiated C3H spleen cells from immunocompetent mice were loaded with either the wt or the mutant peptide. The M2/3 TCR recognized only the mutant peptide. A peptide titration to show TCR avidity was also performed (Figure 11C).

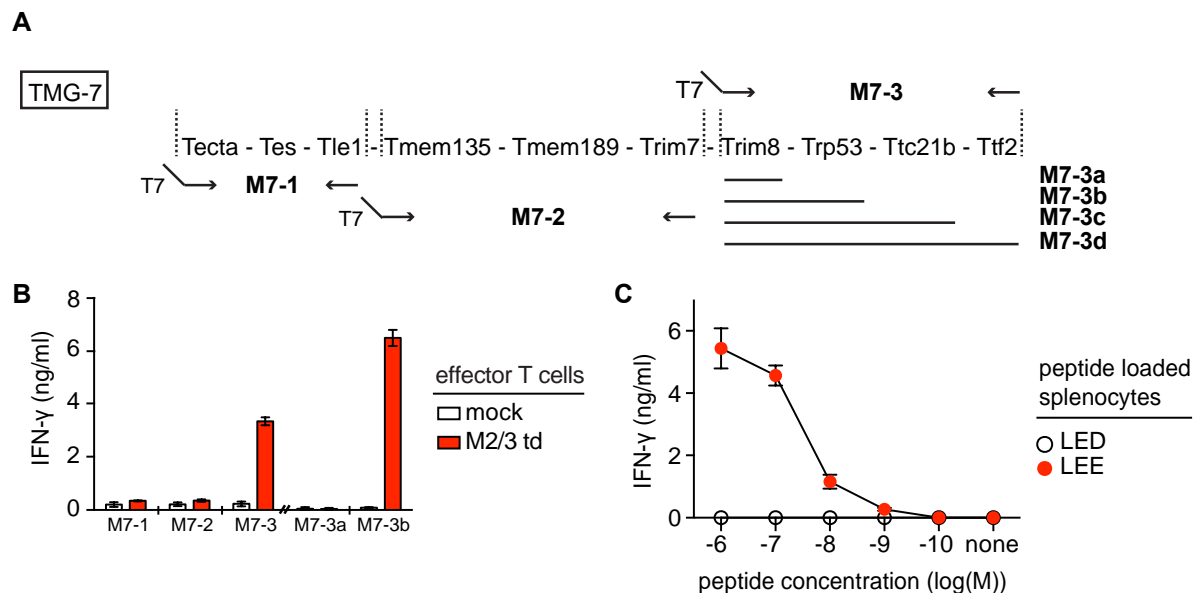


**Figure 11: TCR M2/3 recognizes a neoepitope resulting from a mutation in *Trp53***

(A) Truncated versions of TMG-7 were generated by PCR. The T7 promoter was added in each fragment to allow *in vitro* RNA transcription. All 10 potential neoepitopes of TMG-7 are depicted. (B) EL4-H-2K<sup>k</sup> cells were electroporated with TMG-7 fragments and incubated with M2/3-transduced T cells ( $5 \times 10^4$  cells, 1:1 ratio). Recognition was assessed by IFN- $\gamma$  secretion with an ELISA assay. The figure shows a combination of 2 screenings performed to reveal the M2/3 target. (C) A peptide titration curve was generated by loading wt and mp53 peptides in irradiated spleen cells incubated with M2/3-transduced T cells. Recognition was assessed by IFN- $\gamma$  secretion in an ELISA assay. LED: wtp53, LEE: mp53. A representative example of two independent experiments is shown. td: transduced.

Primary mouse and human tumors are heterogeneous. Therefore, it was necessary to detect potential antigen-negative variants *in vitro*. Ag104A bulk tumor cells derived from the autochthonous primary tumor were single-cell cloned and 133 clones were obtained. All clones were co-cultured with M2/3-engineered T cells and were recognized, indicating that mp53 shows a uniform expression pattern in all tumor branches (Figure 12) and it is therefore a suitable target for neoantigen-specific TCR gene therapy.

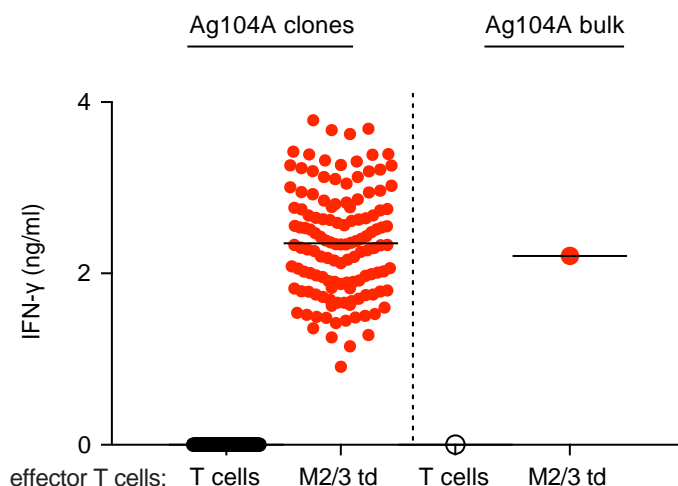


**Figure 12: M2/3-engineered T cells recognized all Ag104A single-cell clones**

Ag104A bulk tumor cells derived from the autochthonous primary tumor were single-cell cloned and 133 clones were obtained. All clones were incubated with M2/3-engineered T cells ( $5 \times 10^4$  cells, 1:1 ratio). Recognition was assessed by IFN $\gamma$  secretion in an ELISA assay. Ag104A bulk, representing the parental uncloned cell line, was included as control. A representative example of two independent experiments is shown. td: transduced.

### 3.4 TCR gene therapy targeting mp53 in established Ag104A tumors induces stable disease but cannot prevent relapse

Next, the potential of the M2/3 TCR to induce cancer destruction *in vivo* was examined. M2/3-engineered T cells were adoptively transferred to C3HxRag2<sup>-/-</sup> mice bearing established Ag104A tumors. Mice older than 8 weeks were subcutaneously injected with  $5 \times 10^6$  living Ag104A cancer cells and ATT with M2/3-engineered T cells followed 14 days later, when the size of the tumors was approximately  $100 \text{ mm}^3$  on average. After determining the T cell transduction rate,  $1 \times 10^6$  CD8<sup>+</sup>TCR $\beta$ <sup>+</sup> T cells were injected into the mice. Activated but non-engineered T cells were transferred to a group of mice as control (mock). Tumor growth was observed and peripheral blood was analyzed in indicated time points (see Methods, Figure 13A). Mice were sacrificed when tumors exceeded  $2.000 \text{ mm}^3$  or when the overall health of the animals appeared compromised. Mice that received the mock treatment were sacrificed 23 days post treatment on average ( $\pm 3$  days, 8 mice). Tumor growth of M2/3-treated mice was initially arrested and was followed by tumor regression. These observations lasted for an average of 30 days after ATT. Past this time point, tumors relapsed and mice were sacrificed according to the specified guidelines (Figure 13B). The average survival of M2/3-treated mice was 42 days after T cell transfer ( $\pm 4$  days, 16 mice). In summary, the mp53-specific M2/3 TCR

induced stable disease in mice bearing established Ag104A tumors and resulted in a significantly better survival outcome compared to the mock-treated group (Figure 13C).

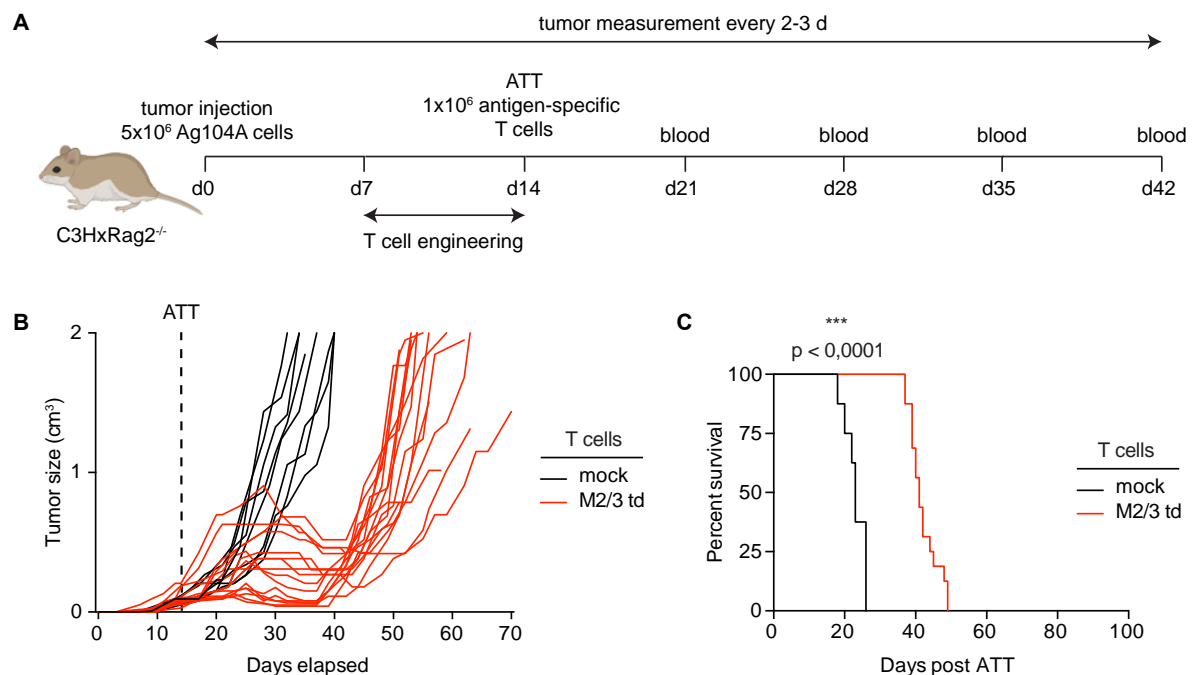


**Figure 13: Targeting mp53 in Ag104A tumors prolongs survival**

(A) Schematic overview of the therapeutic protocol. C3HxRag2<sup>-/-</sup> mice were injected with 5x10<sup>6</sup> Ag104A tumor cells. After 14 days, 1x10<sup>6</sup> M2/3-engineered T cells were adoptively transferred to the mice. Tumor growth was observed every 2-3 days and peripheral blood was analyzed at the indicated time points. (B) Growth of Ag104A tumors after treatment with M2/3-engineered T cells. In total, 16 mice were treated with the M2/3 TCR in 4 independent experiments (red lines). Eight mock-treated animals that received non-engineered T cells are shown as control (black lines). The dashed line indicates the day of ATT. (C) Kaplan-Meier survival plot of treated Ag104A tumor-bearing mice post ATT. The calculated p value is indicated. ATT: Adoptive T cell transfer, td: transduced.

### 3.5 Relapse of Ag104A tumors from T cell therapy is not due to insufficient expansion of M2/3-engineered T cells or their inability to infiltrate the tumor tissue

To determine whether insufficient T cell function is responsible for the relapse of Ag104A tumors, T cells in blood and tumor tissue were analyzed. Peripheral blood was drawn at indicated time points for a total duration of one-month post ATT to examine presence and expansion of T cells. Rag-deficient mice lack endogenous T cells, therefore only the transferred T cells were detected. Antigen-specific CD8<sup>+</sup> T cells (CD8<sup>+</sup>TCRβ<sup>+</sup>) were found to be the majority of the CD8<sup>+</sup> T cell compartment at all time points. On days 7 and 14 post ATT, they were approximately 60% of total CD8<sup>+</sup> T cells, which indicated proliferation of this subpopulation in comparison to the transferred T cells on the day of ATT (Figure 14A). The

ratio of CD8<sup>+</sup>TCRβ<sup>+</sup>/CD4<sup>+</sup>TCRβ<sup>+</sup> (CD4<sup>+</sup>) T cells remained similar at all time points, suggesting that these cells showed no antigen-specific expansion (Figure 14B). Absolute numbers of T cells in peripheral blood revealed that M2/3-engineered CD8<sup>+</sup> T cells expanded and proliferation reached its peak between days 7 and 14 after ATT. In detail, a 13-fold and 47-fold expansion on average for days 7 and 14 respectively was observed in comparison to peripheral blood analyzed on day 4 (Figure 14C). Non-engineered T cells transferred to mock-treated mice were detected in peripheral blood at all time points but showed no expansion (Figure 14C). The observed proliferation of CD8<sup>+</sup> T cells was similar for both mock- and M2/3-treated mice and therefore not antigen-specific (Figure 14D). In summary, only CD8<sup>+</sup>TCRβ<sup>+</sup> T cells proliferated after ATT, indicating antigen-specific expansion. However, the analysis also indicated presence of M2/3-engineered T cells in treated mice at the time point when relapse of Ag104A tumors became first apparent (day 28).

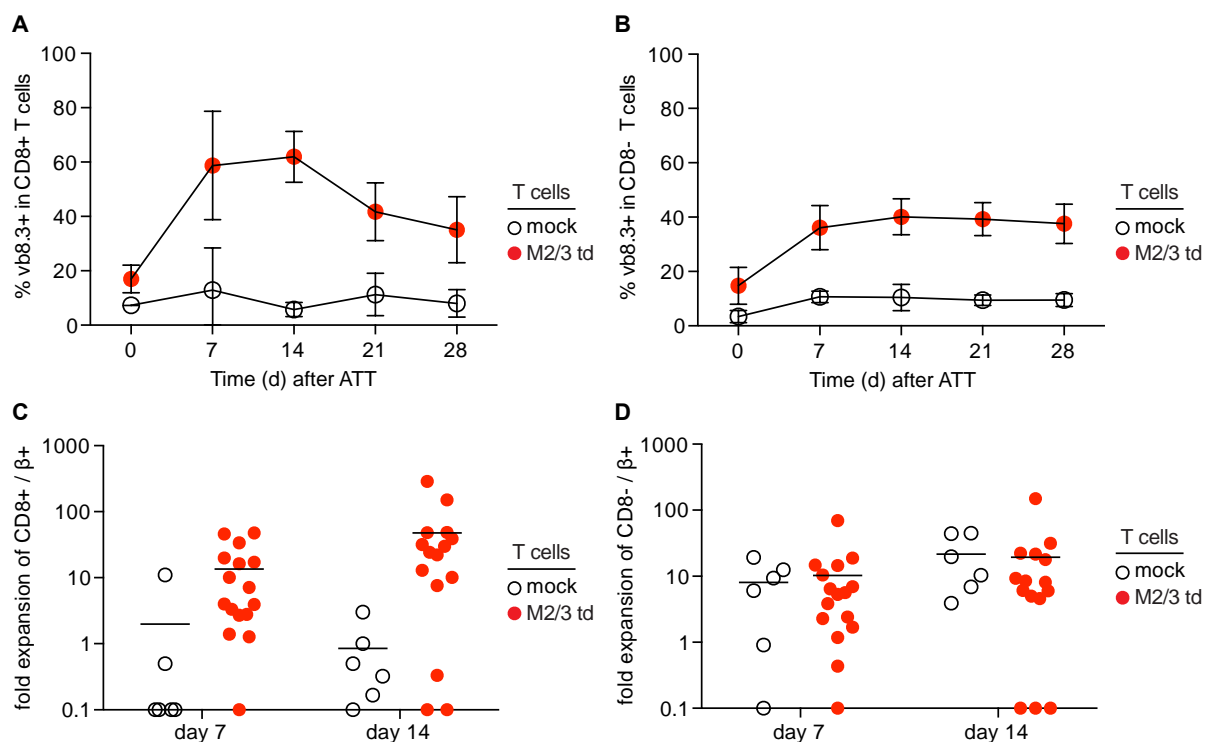


**Figure 14: Proliferation of CD8<sup>+</sup> M2/3-engineered T cells peaks 7 – 14 days after ATT and T cells persist over time**

Peripheral blood was analyzed on days 4, 7, 14, 21 and 28 after ATT. The staining was performed with 50  $\mu$ l of blood and analysis was done by flow cytometry. (A) Percentage of TCRβ<sup>+</sup> cells in the CD8<sup>+</sup> T cell compartment. All values from mock (N=6) and M2/3 treated mice (N=16) from 4 independent experiments were pooled. Day 0 represents analysis of T cells on day of transfer. (B) Percentage of TCRβ<sup>+</sup> cells in the CD8<sup>-</sup> T cell compartment. All values from mock and M2/3 treated mice from 4 independent experiments were pooled. (C) Fold expansion of CD8<sup>+</sup>TCRβ<sup>+</sup> T cells on day 7 and day 14 after ATT. The average expansion was 13-fold and 47-fold for days 7 and 14 respectively. (D) Fold



expansion of CD8<sup>+</sup>TCR $\beta$ <sup>+</sup> T cells on day 7 and day 14 after ATT. All values in (C) and (D) are normalized to the cell counts found on day 4. ATT: Adoptive T cell transfer, td: transduced.

Blood analysis indicated that relapse was not due to the lack of T cells. To determine whether M2/3-engineered T cells that infiltrated Ag104A tumors were still functional, relapsed tumors were resected approximately 50 days after ATT. Relapsed tumors were reisolated for further analysis. Reisolates were first examined for presence of TILs by digesting the tumor material to obtain a single cell suspension. Digested material was sorted for CD3<sup>+</sup> T cells by negative selection. Sorted TILs (derived from 4 M2/3-treated and 2 mock-treated mice) were stained and analyzed by flow cytometry. M2/3-engineered T cells could be found back in the tumor microenvironment, as shown by the staining of TILs for the  $\beta$  chain of the M2/3 TCR. Antigen-specific CD8<sup>+</sup> T cells were found enriched in all four tumors in comparison to the transferred population (Figure 15A). Non-engineered T cells transferred to mock-treated mice were also found in the tumor microenvironment. Moreover, isolated TILs from M2/3-treated mice were still able to recognize Ag104A tumor cells *in vitro* (Figure 15B). As expected, TILs from mock-treated mice did not recognize Ag104A tumor cells (Figure 15B).

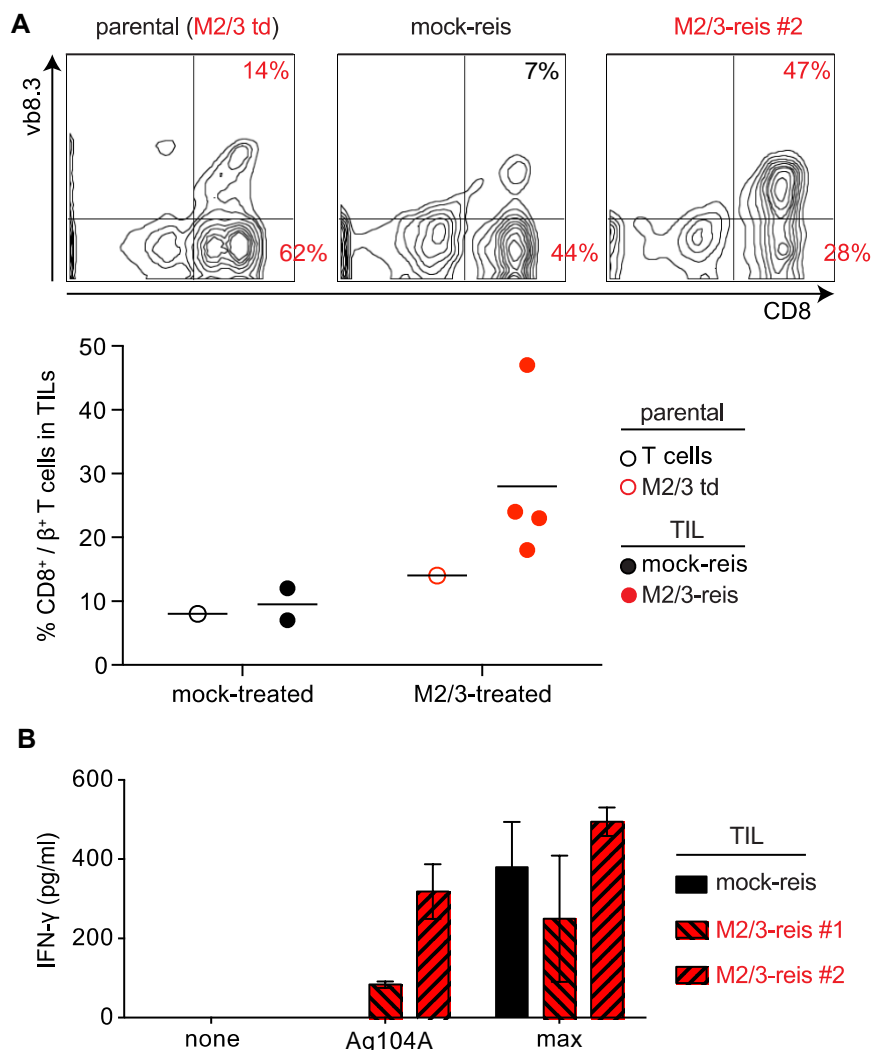


### Figure 15: M2/3-engineered T cells infiltrate the tumor microenvironment and are functional

Relapsed Ag104A tumors (4 from M2/3-treated and 2 from mock-treated mice) were reisolated and digested to obtain single cell suspensions. (A) Digested material was stained against CD8 and the  $\beta$  chain of the M2/3 TCR to detect antigen-specific T cells. Analysis was done by flow cytometry. Parental M2/3-transduced spleen cells were stained as control for gate setting. The upper panels show representative examples of stained TILs from mock- or M2/3-treated mice. Quadrants represent gates of CD3<sup>+</sup> T cells. Numbers in the lower graph represent cell percentages of the indicated population (CD8<sup>+</sup>TCR $\beta$ <sup>+</sup>). (B) TILs were incubated with Ag104A tumor cells *in vitro* (5x10<sup>4</sup> cells, 1:1 ratio), medium (none) and PMA/Ionomycin (max). Representative examples of TILs from mock- and M2/3-treated mice are shown. Recognition was assessed by IFN- $\gamma$  secretion in an ELISA assay. A representative example of two independent experiments is shown. td: transduced, reis: reisolate.

TILs of reisolates were also analyzed for expression of exhaustion markers, thus stained for PD-1, Tim-3 and 2B4. TILs from both mock- and M2/3-treated mice showed PD-1 expression. Only in one (M2/3-reis #3) out of the four reisolated tumors, PD-1 expression was higher (Figure 16). Tim-3 and 2B4 expression was not detected in none of the TILs (Figure 16). These findings together suggested that antigen-specific exhaustion or T cell inhibition may not be the reasons for tumor escape.

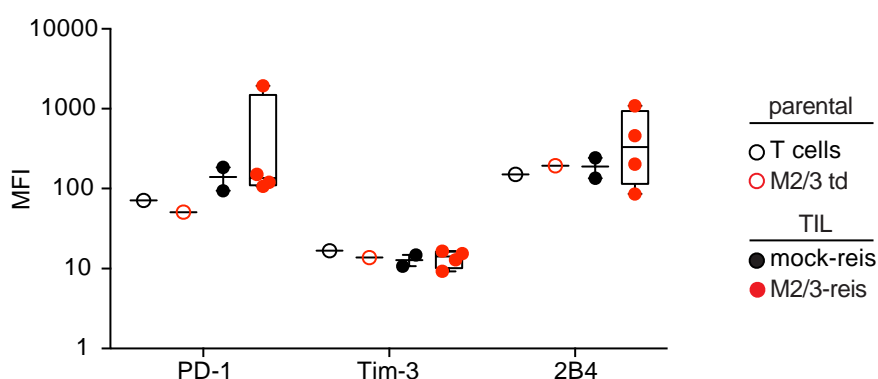


### Figure 16: Expression of exhaustion markers in TILs isolated from M2/3- and mock-treated mice is similar

TILs of reisolated tumors were stained for expression of exhaustion markers (PD-1, Tim-3 and 2B4) and analyzed by flow cytometry. Values are shown for all reisolated tumors analyzed and stem from gates of CD3<sup>+</sup>CD8<sup>+</sup> T cells. MFI: Mean Fluorescence Intensity, td: transduced, reis: reisolate.

### 3.6 Ag104A tumors escape mp53-specific T cell therapy as variants that are no longer recognized by M2/3-engineered T cells

As M2/3-engineered T cells seemed to be still functional when Ag104A tumors relapsed, Ag104A tumor variants that escaped therapy were analyzed. Reisolated tumor cells were co-

cultured with M2/3-engineered T cells. Interestingly, they were no longer recognized by the M2/3 TCR (Figure 17). The only exception was the reisolate originating from the M2/3-treated mouse, in which TILs were found to be exhausted (M2/3-reis #3). This finding indicated that tumor escape was associated with absence of the mp53 antigen.

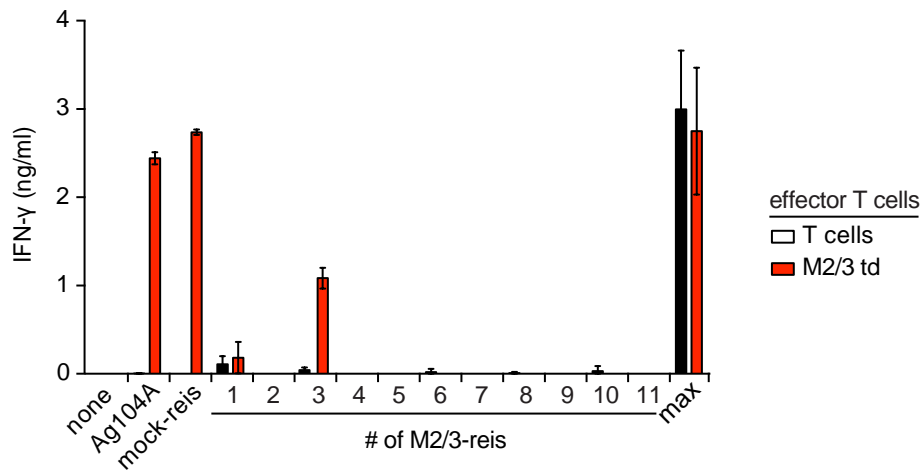


**Figure 17: Ag104A tumor cell variants that escaped mp53-specific TCR gene therapy are no longer recognized by M2/3-engineered T cells *in vitro***

Ag104A tumor cell variants generated from reisolated tumor material were incubated with M2/3-transduced T cells *in vitro* ( $5 \times 10^4$  cells, 1:1 ratio). Recognition was assessed by IFN- $\gamma$  secretion in an ELISA assay. Ag104A bulk was used as control. A representative example of three independent experiments is shown. td: transduced, reis: reisolate.

To determine the mechanism of escape, the processing and presentation machinery of the escaped tumors were examined. Reisolates were stained for H-2<sup>k</sup> and analyzed by flow cytometry, which showed there was no downregulation of MHC I molecules on their surface (Figure 18A). To exclude any transient mechanism leading to the absence of the mp53 ligand on Ag104A tumor cell variants, four reisolates (M2/3-reis #1-4) were kept in culture and passaged for a total duration of four months (total of 48 passages). A co-culture with M2/3-engineered T cells was performed every month. Even when T cell pressure was absent for several weeks, recognition of mp53 could not be restored (Figure 18B). To check for deficiencies in antigen presentation, reisolated Ag104A tumor cell variants were pulsed with TMG-7, the tandem minigene containing mp53, or loaded with the mp53 peptide. In both cases, recognition by the M2/3 TCR was recapitulated suggesting no defects in processing and presentation (Figure 18C). This finding was further supported by treating reisolated tumor cells with IFN- $\gamma$  to enhance the function of the entire presentation machinery. IFN- $\gamma$  treatment did not restore T cell recognition (Figure 18D). Another explanation for tumor escape could be epigenetic changes in tumor cells targeted by a mutation-specific TCR. Promoter methylation

under T cell pressure could alter the expression profile of mp53. 5-Azacytidine (5-AZA) is an agent that unspecifically inhibits all methylation processes in a cell. As it is a highly cytotoxic agent, a tolerated concentration was determined by treating Ag104A tumor cells with several concentrations and monitoring their survival and proliferation rate. Subsequently, reisolates were treated with 5-AZA and co-cultured with M2/3-engineered T cells. Nevertheless, the T cells failed to recognize even the 5-AZA pre-treated reisolates (Figure 18E).

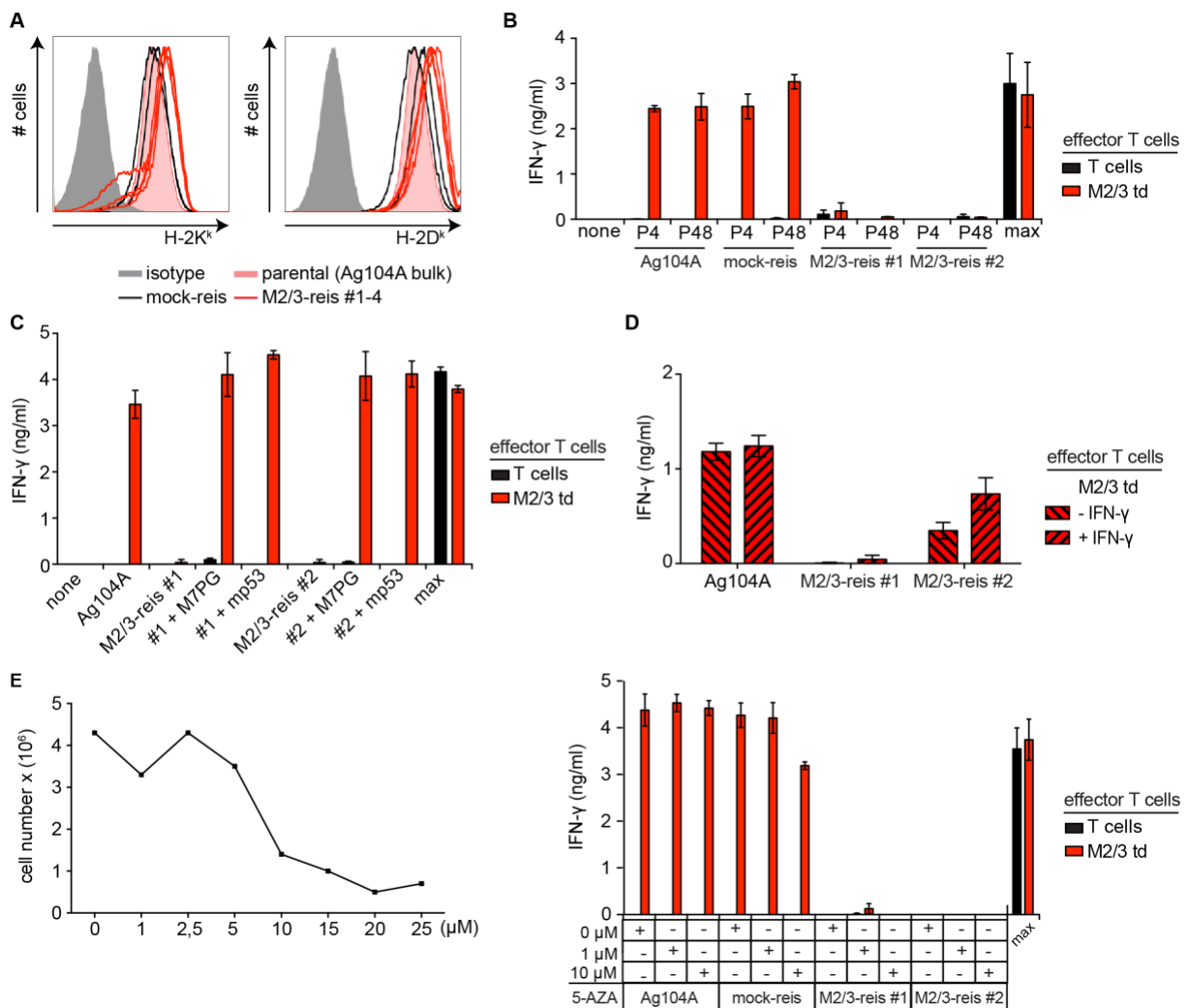


**Figure 18: The processing and presentation machinery of Ag104A variants that escaped mp53-specific ATT is intact**

(A) Ag104A reisolates were stained for H-2K<sup>k</sup> or H-2D<sup>k</sup> and analyzed by flow cytometry. Isotype controls and Ag104A bulk were included. (B) Ag104A bulk and Ag104A reisolates were cultured and passaged for 4 months. P4: Passage 4, P48: Passage 48 representing a 4-month culture. All reisolates from all passages were co-cultured with M2/3-engineered T cells. (C) Ag104A reisolates were electroporated with TMG-7 or peptide-loaded with mp53 ( $10^{-6}$ M) and co-cultured with M2/3-engineered T cells. (D) Ag104A reisolates were treated with 100 ng IFN- $\gamma$  for 48 hours. (E) A tolerance dose for 5-AZA was determined with Ag104A bulk tumor cells (left panel). Cells were treated with the indicated concentration

---

every 24 hours for 4 days and were counted. Ag104A bulk and reisolates were treated without (10  $\mu$ M) or with 1 or 10  $\mu$ M 5-AZA (right panel). 5-AZA: 5-Azacytidine. All treated cells in all panels were incubated with M2/3-transduced T cells. Representative reisolates are shown. The experimental setup was the same for every co-culture ( $5 \times 10^4$  cells, 1:1 ratio). Recognition was assessed by IFN- $\gamma$  secretion in ELISA assays. A representative example of two independent experiments is shown for all panels. td: transduced, reis: reisolate.

### **3.7 The level of mp53 gene copies in Ag104A variants that escaped T cell therapy is decreased**

As known by whole exome sequencing, both wt and mutant alleles of p53 are present in Ag104A at about 1:1 ratio (19 and 14 copies of wtp53 and mp53 respectively). The same holds true for mRNA levels as shown by RNA sequencing (131 and 100 copies of wtp53 and mp53 respectively, Table 16). To confirm this observation, genomic DNA (gDNA) and mRNA were isolated from Ag104A tumor cells. mRNA was used to synthesize cDNA. A primer pair that amplifies a part of the p53 gene where the mutation is found was designed and subsequently used in standard PCR reactions with gDNA or cDNA as templates. The expected product sizes for cDNA and gDNA were 327 and 1.130 bp respectively. This difference is explained by the fact that on genomic level, intron 6 is located between the sequence of the mp53 neoepitope (Figure 19A). DNA of PCR products was isolated and Sanger sequencing was performed. As expected, the wt and the mutant allele were detected as both C (wt) and G (mut) nucleotides peaks appeared in the electropherogram (Figure 19B, upper panels). To further investigate mp53 presence in reisolates, the same procedure was done in all Ag104A tumor cell variants that escaped therapy. Sanger sequencing revealed that the mutant allele was significantly less present in relapsed tumors, as the respective nucleotide peak was lower or not detected in gDNA and cDNA (Figure 19B, lower panels). These findings suggest that the mutant allele of p53 was less present in Ag104A variants that escaped mp53-specific T cell therapy, resulting in a subsequent absence of the mp53 ligand that is required for the activation of M2/3-engineered T cells.

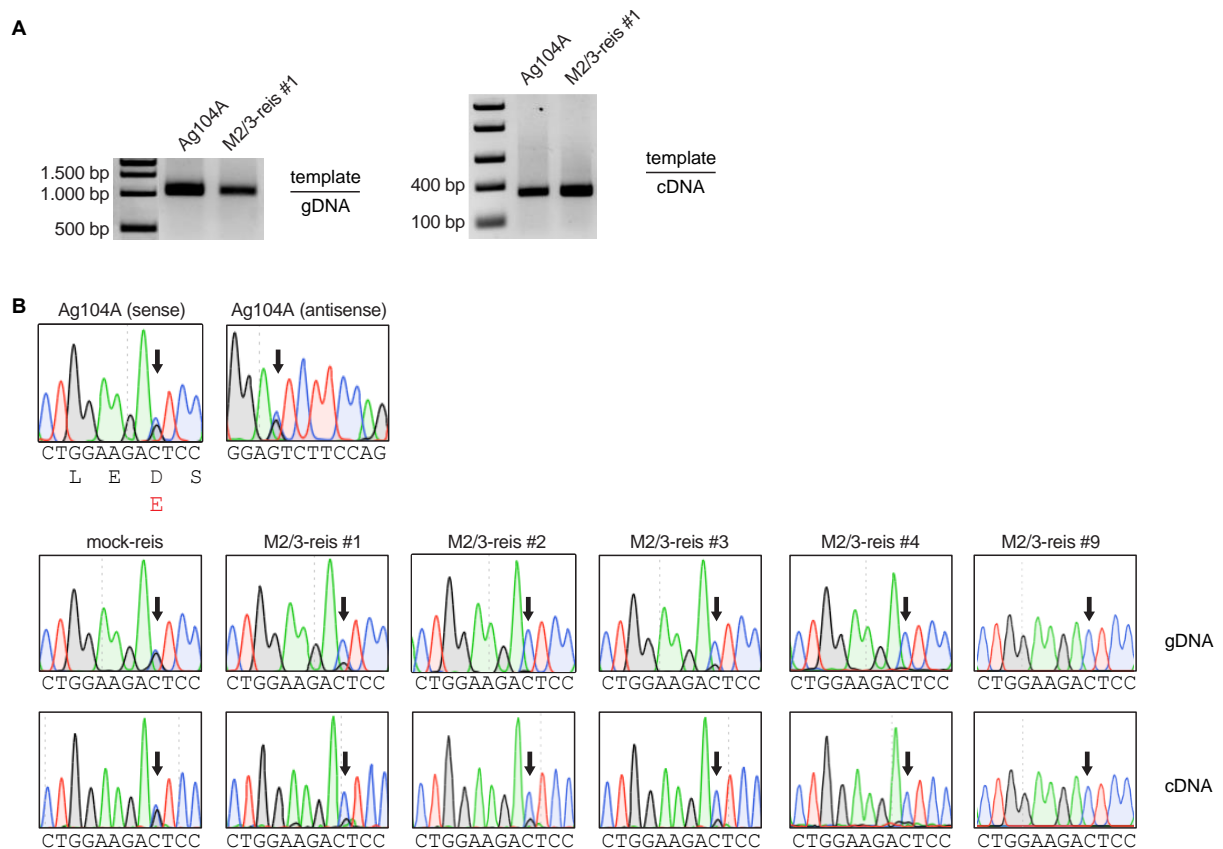


**Figure 19: Level of mp53 is lower in Ag104A variants that escaped T cell therapy**

(A) Genomic DNA (gDNA) and mRNA were isolated from Ag104A bulk and reisolates. mRNA was used to synthesize cDNA. Standard PCR reactions were performed with the same primer pair amplifying a part of p53 where the point mutation is located and with 50 ng gDNA or 100 ng cDNA as templates (expected product sizes: 1.130 bp for gDNA, 327 bp for cDNA). Band sizes of the DNA ladder are indicated. (B) Isolated DNA from PCR fragments was sequenced by standard Sanger sequencing. Electropherograms are shown. Arrows indicate the nucleotide where the mutation is located. Wild-type peptide amino acid sequence is shown in black and the mutation in red. For reisolates, the sense chain is shown. C: blue peak – wt, G: black peak – mut.

### 3.8 Genomic alterations affecting *Trp53* cannot explain escape of Ag104A variants from T cell therapy

One option that would explain loss of mp53 in Ag104A escape variants would be genomic alterations that result in loss of the mp53 gene while retaining the wt p53 allele. Such alterations might be second allele loss, chromosomal deletion or loss of heterozygosity [268]. All these alterations could be detected by changes of the copy number of both p53 alleles. Therefore, copy number analysis was performed in Ag104A bulk and selected reisolates. Real-time PCR was performed to detect any copy number variations. For this purpose, a set of primers that could distinguish between the wt and the mutant allele was designed. Tert

(telomerase reverse transcriptase) was used for normalization as a reference gene. The analysis was performed by Kazuma Kiyotani at the Cancer Precision Medicine Center in Japan. Spleen cells from immunocompetent C3H mice were used to normalize amplification. Spleen cells had two copies of the wt *Trp53* gene. Ag104A bulk showed both copies, the wtp53 and the mp53 allele (Figure 20A). This result was supported by whole exome sequencing as a similar amount of sequencing reads was observed for either the wt or the mutant allele (Figure 20B). In Ag104A variants that escaped mp53-specific T cell therapy, the frequency of the mutant copy was significantly lower or not detected (Figure 20B). However, two copies of p53 were observed in all Ag104A variants (Figure 20A), thus escape from adoptive T cell transfer could not be explained by a loss of the mp53 allele. These results rather suggest the presence of low-frequency occurring antigen-negative variants in the uncloned Ag104A population that was used to induce tumor growth in mice.

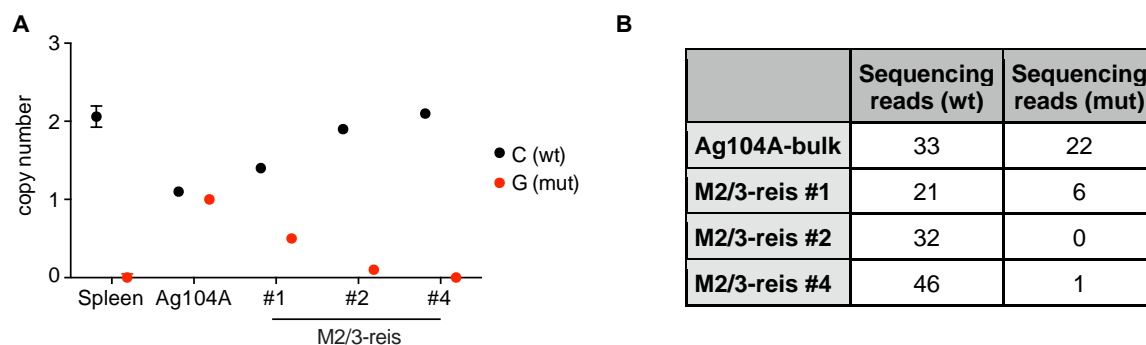


**Figure 20: Copy number analysis and whole exome sequencing of Ag104A variants reveals no genomic alterations in the p53 gene**

(A) Copy number analysis was performed with real-time PCR on genomic DNA of Ag104A bulk and selected reisolates. Spleen cells were used to normalize amplification. Tert was used as a reference gene that has 2 copies. (B) Whole exome sequencing was performed. The sequencing reads for Ag104A bulk or reisolates are given.

### 3.9 Clonotypes lacking the mp53 gene dominate the population of Ag104A variants that escaped mp53-specific T cell therapy

Previous analysis showed that M2/3-engineered T cells expanded in response to mp53 *in vivo* and also proved to be functional when reisolated from the tumor tissue. This suggests that mp53-positive Ag104A tumor cells are constantly eliminated during the approximate one-month period of stable disease. The selection of rare mp53-negative clonotypes, present in the uncloned Ag104A tumor cell population used to induce cancer in the mice, leads to transient tumor regression. To prove this hypothesis, Ag104A variants (reis #1, #3, #9) were single-cell cloned. For each of the 3 reisolates, 50-60 clones were obtained. All clones were

co-cultured with M2/3-engineered T cells and recognition was assessed by IFN- $\gamma$  secretion. For two variants (reis #1, #3), one clone was found to be recognized by M2/3-engineered T cells (Figure 21A). Variant #9 contained no clones that were recognized by the M2/3 TCR (Figure 21A). Genomic DNA was isolated from selected clones and subjected to Sanger sequencing. The results confirmed that the clones that retain recognition carry the mp53 allele, while the ones not recognized are only wtp53-positive (Figure 21B). These observations suggest that Ag104A variants are either rather homogeneous p53<sup>+/+</sup> populations or retain p53<sup>D253E/+</sup> clonotypes at such a low frequency that prohibits recognition by the M2/3 TCR.

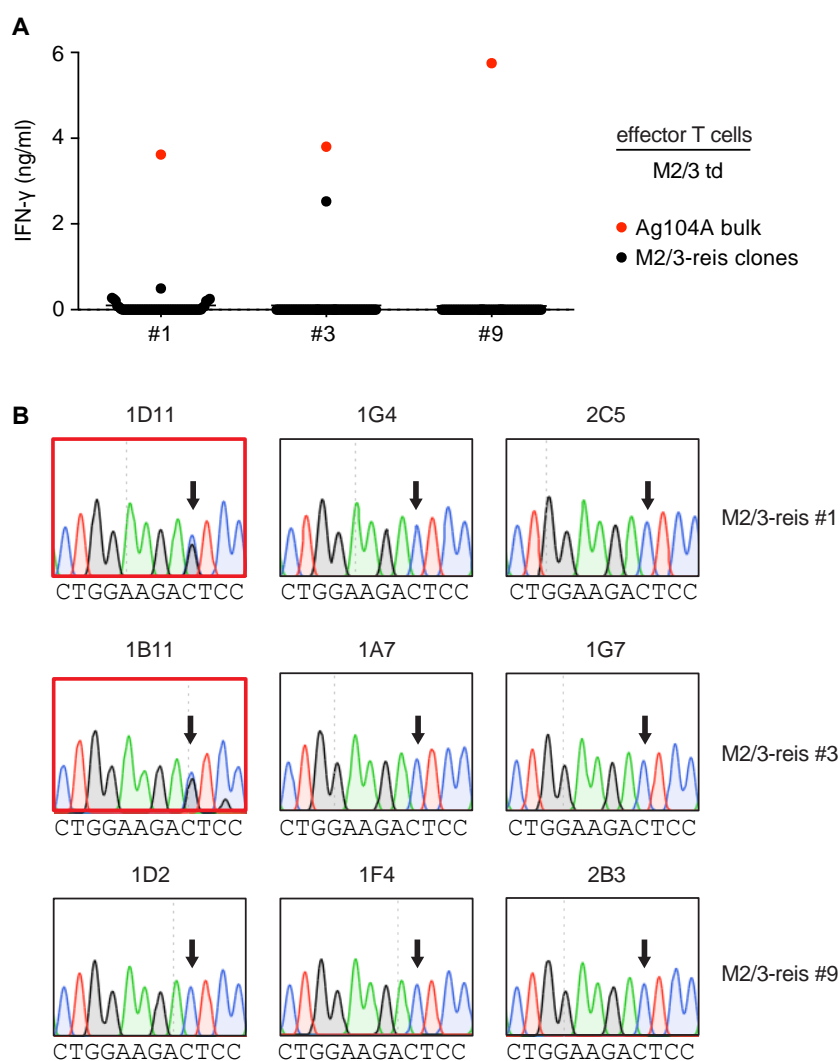


**Figure 21: Single-cell clones of Ag104A variants are rather homogeneous p53<sup>+/+</sup> populations**

(A) Three Ag104A reisolates (#1, #3, #9) were single-cell cloned and 50-60 clones were passaged 3 times and incubated with M2/3-transduced T cells *in vitro* ( $5 \times 10^4$  cells, 1:1 ratio). Recognition was assessed by IFN- $\gamma$  secretion in an ELISA assay. Ag104A bulk tumor cells were used as control and are indicated with red circles. (B) gDNA was isolated from selected clones. Standard PCRs were performed with the same primer pair amplifying a part of p53 where the point mutation is located and with 50 ng template gDNA. Isolated DNA from PCR fragments was sequenced by standard Sanger sequencing.



Electropherograms are shown. Arrows indicate the nucleotide where the mutation is located. The clones that were recognized by M2/3-engineered T cells are shown with red rectangles. C: blue peak – wt, G: black peak – mut, td: transduced.

### 3.10 Ag104A tumors expressing high and homogeneous levels of mp53 are rejected by ATT using M2/3-engineered T cells

To analyze whether higher and more homogeneous expression of mp53 in Ag104A could have prevented relapse from M2/3-TCR gene therapy, Ag104A tumor cells that stably expressed mp53 peptides were generated. GFP expression that was coupled to mp53 expression allowed to monitor antigen presence in 95% of the transduced Ag104A tumor cells (Figure 22A, 22B). The generated Ag104A-mp53-3x tumor cell line was recognized by the M2/3 TCR *in vitro* (Figure 22C). Tumor cells were injected into C3HxRag2<sup>-/-</sup> mice. ATT of M2/3-engineered T cells followed 14 days post tumor inoculation and all tumors were eradicated 20-40 days after T cell transfer. All mice were observed for a total duration of 100 days post ATT (Figure 22D). This experiment, comparable to a previous study, proved that a TCR targeting a single neoantigen can eradicate tumors with high and homogeneous antigen expression [223].

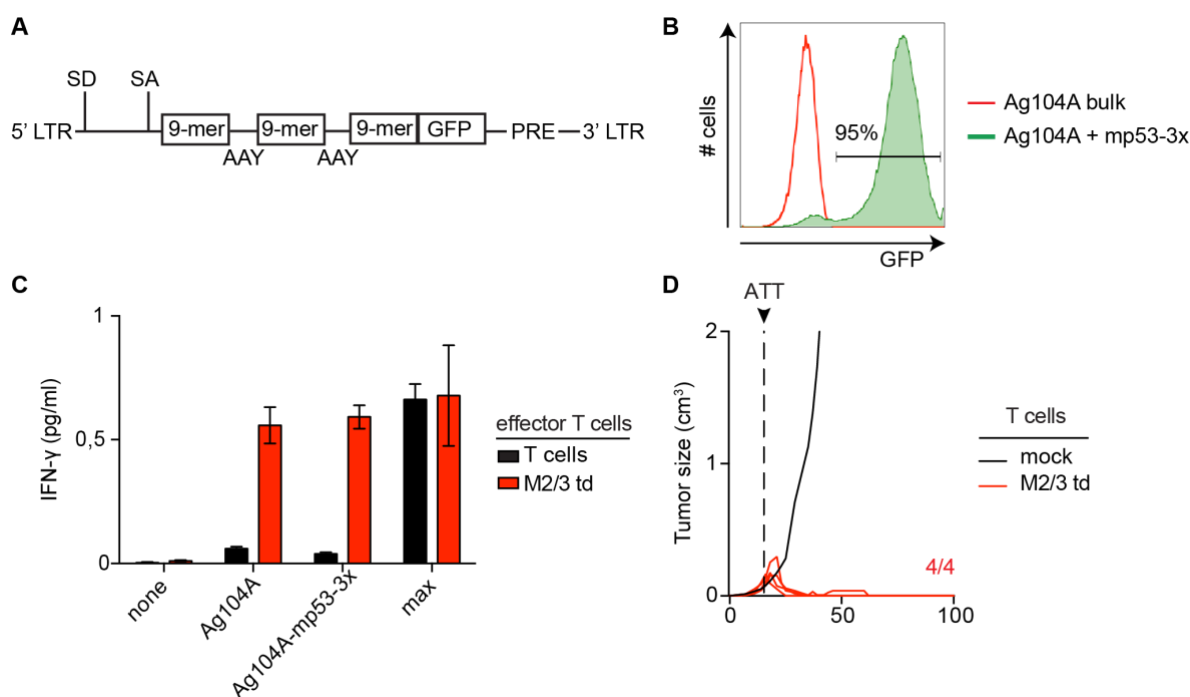


**Figure 22: mp53-specific T cell therapy can reject cancer with high and homogeneous antigen expression**

(A) Graphic illustration of the pMP71 vector encoding for a triple mp53 peptide repeat coupled to GFP. Each peptide is separated from the next one with an AAY cleavage site. (B) Ag104A bulk tumor cells were retrovirally transduced to stably express mp53 in high levels. (C) Ag104A-mp53-3x tumor cells were co-cultured with M2/3-engineered T cells *in vitro* ( $5 \times 10^4$  cells, 1:1 ratio). Recognition was assessed by IFN- $\gamma$  secretion in an ELISA assay. Ag104A tumor cells were used as control. A representative

---

example of two independent experiments is shown. (D) C3HxRag2<sup>-/-</sup> mice were injected with 5x10<sup>6</sup> Ag104A-mp53 tumor cells. After 14 days, 1x10<sup>6</sup> antigen-specific T cells were adoptively transferred to the mice. The number of mice treated and rejected the tumors (red lines) is indicated in red. One mock-treated animal that received non-engineered T cells is shown as control (black line). td: transduced.

### **3.11 The mutation D253E in p53 provides a growth advantage and higher tumorigenicity to Ag104A cancer cells**

The importance of the D253E mutation in p53 on cancer cell biology is not yet understood. Although not yet described for murine cancer, the presence of the same amino acid exchange in the human p53 homolog in human cancers suggests that the mutation provides an advantage to the cancer cells [265-267]. However, it remains unclear whether p53<sup>D253E</sup> in comparison to other known and well-described p53 mutations provides a growth advantage or higher tumorigenicity to cancer cells. The Ag104A variants that escaped T cell therapy and lack expression of mp53 can serve as a tool to study the p53<sup>D253E</sup> function. To obtain homogeneous p53<sup>+/+</sup> variants as comparison, Ag104A tumor cells of the parental uncloned population were modified by CRISPR/Cas9 (see Materials and methods). Modified Ag104A tumor cells were cloned and tested for M2/3 recognition assessed by IFN- $\gamma$  release in a screening assay (Figure 22A). Genomic DNA of clones that were not recognized by the M2/3 TCR was isolated and Sanger sequencing confirmed the repair of mp53 (Figure 22B). Less than 1% of all tested clones were successfully repaired as in the vast majority of them several other deletions and/or insertions were detected. Two clones repaired with the antisense template were found p53<sup>+/+</sup> (1D2, 3F7) and one of them was selected for subsequent experiments (1D2).

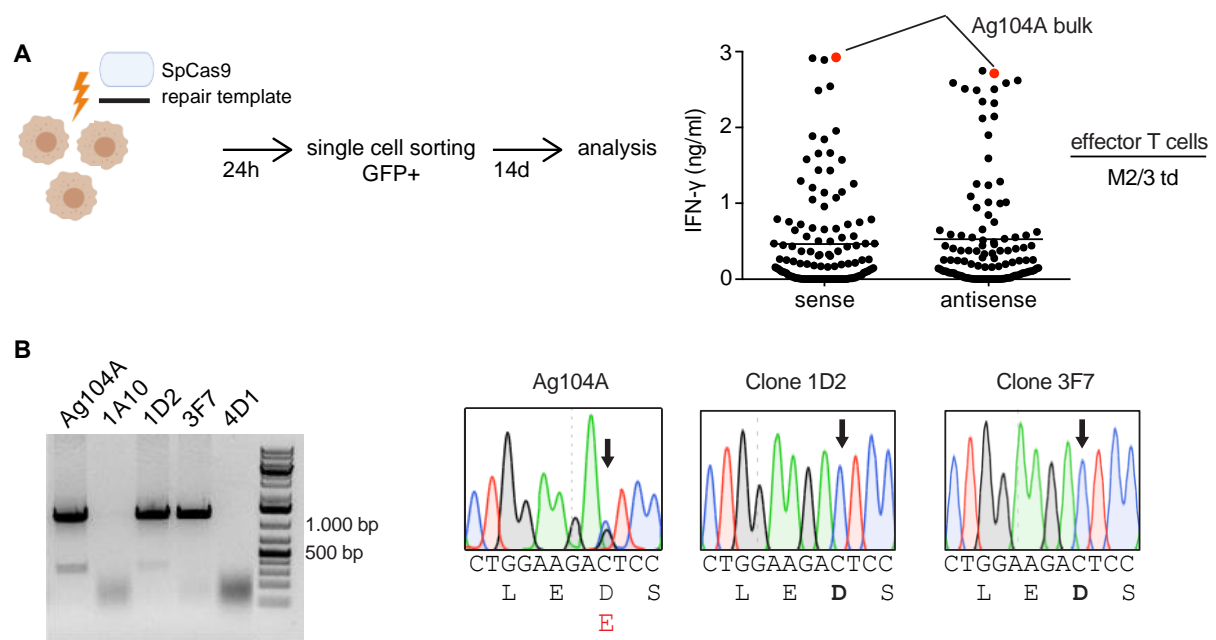


**Figure 23: The CRISPR/Cas9-mediated homology-directed-repair can correct mp53 in Ag104A tumor cells**

(A) The gRNA-Cas9 vector and the repair template were pulsed into Ag104A tumor cells. One repair template against the sense or the antisense chain was used in two independent reactions. GFP<sup>+</sup> cells were single-cell sorted 24h later and grew for 14 days. Each clone was incubated with M2/3-transduced T cells *in vitro* (5x10<sup>4</sup> cells, 1:1 ratio). Recognition was assessed by IFN- $\gamma$  secretion in an ELISA assay. Ag104A bulk tumor cells were used as control. (B) gDNA from non-recognized clones was isolated to perform a p53-specific PCR. DNA from PCR products was sequenced. The mutation in Ag104A cells is shown in red and the repair in CRISPR-derived clones in bold. td: transduced.

The growth rate of Ag104A variants (reis #1 - #11) and the Ag104A p53<sup>+/+</sup> clone (1D2) was investigated *in vitro*. Ag104A tumor cells were used as control. It was found that all reisolates as well as the p53<sup>+/+</sup> cell line grew slower than Ag104A bulk tumor cells (Figure 24A, 24B). The only exception was the reisolate where mp53 expression was partly retained (M2/3-reis #3). In these cells, growth was slower than in Ag104A but the difference was not significant as for the other variants. Reisolates originating from mock-treated mice grew similarly to Ag104A (Figure 24A, 24B). To test the impact of the p53<sup>D253E</sup> mutation on tumorigenicity, three reisolates and the p53<sup>+/+</sup> variant were inoculated in C3HxRag2<sup>-/-</sup> mice to observe their growth rate *in vivo*. In detail, one flank of each mouse was subcutaneously injected with Ag104A bulk tumor cells and the other flank with one of the reisolates or the p53<sup>+/+</sup> variant. Tumor sizes were measured every 2-3 days and the mice were sacrificed when at least one of the tumors was about to exceed 1.000 mm<sup>3</sup> in volume. It was again found that the Ag104A variants as well as the p53<sup>+/+</sup> cell line grew slower than Ag104A bulk (Figure 24C). The same exception

for the recognized reisolate (M2/3-reis #3) was confirmed *in vivo*. In this setting, no difference in tumor growth kinetics in comparison to Ag104A was observed (Figure 24C). These findings suggest an important role of the D253E mutation in p53 for tumor cell proliferation and progression.

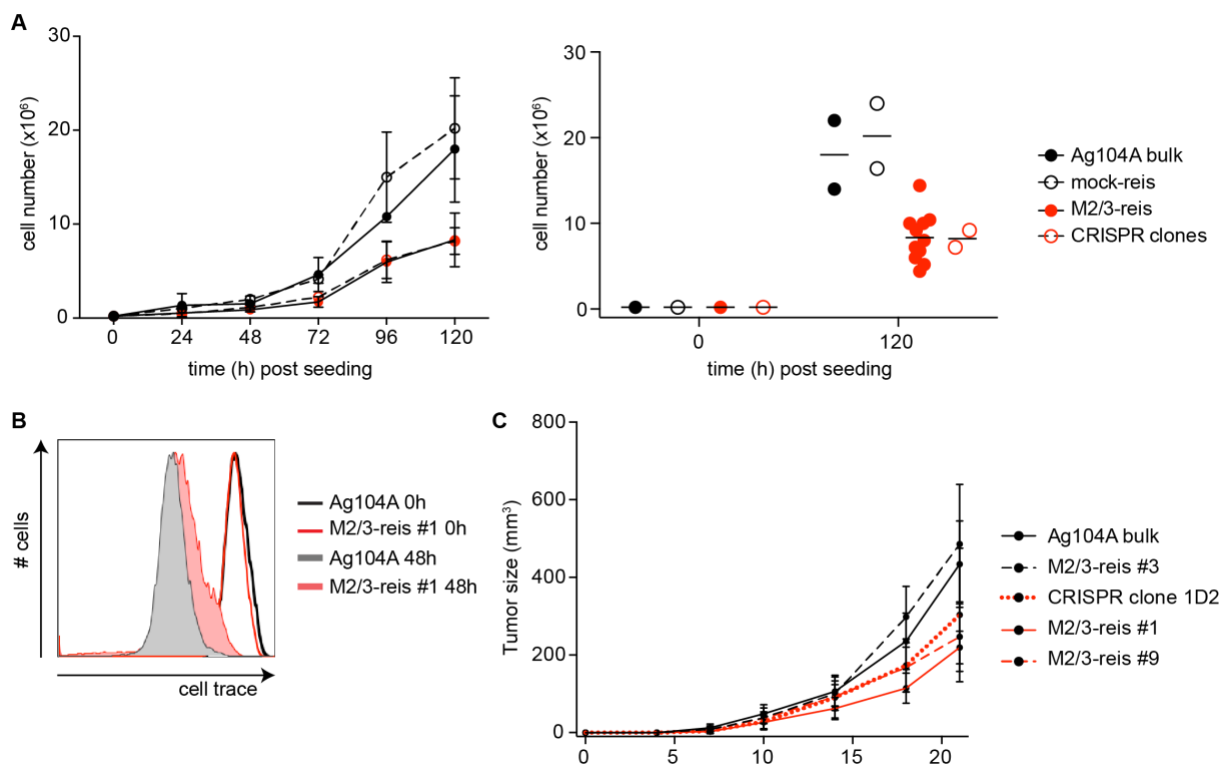


**Figure 24: Loss of the p53<sup>D253E</sup> mutation in Ag104A cancer cells leads to slower tumor cell growth *in vitro* and *in vivo***

(A) Growth of Ag104A reisolates and the CRISPR-derived p53<sup>+/+</sup> cell line was observed *in vitro* for 5 days. The same number of cells was seeded on day 0. Absolute cell numbers are given. (B) Cells were stained with a proliferation dye for flow cytometry analysis. A representative histogram comparing dye dilution at 48 hours post seeding is shown. (C) Growth of Ag104A reisolates and the CRISPR-derived p53<sup>+/+</sup> cell line was observed *in vivo*. Ag104A bulk was injected in the left flank of each mouse and a reisolate or the p53<sup>+/+</sup> cell line in the right flank. reis: reisolate.

## 4. Discussion

Cancer immunotherapy is an emerging field which includes several different forms ranging from off-the-shelf immunomodulatory agents to highly individualized cell therapies. Despite the rapid progress, to date there is a limited number of patients that faces an actual clinical benefit due to the undisputable diversity among each cancer entity and each patient, the lack of established common clinical protocols and the abundance of trial-and-error approaches.

T cell based therapies aim to provide new specificities to peripheral blood T cells via engineering with new receptors, so that they can be directed against cancer antigens. They hold the potential to circumvent central tolerance and inhibitory mechanisms, thus they do not rely on a cancer patient's already compromised immune system, where possible endogenous tumor-reactive T cell populations have failed. However, numerous questions remain to be answered in order to acquire a selection of standardized clinical protocols that could be applied upon a cancer diagnosis and especially in patients refractory to other common treatments. Experience with critical issues, like autoimmunity and severe post-therapy side effects, indicate the necessity for intensive research before any therapeutic attempt.

This doctoral thesis focused on parameters of mutation-specific TCR gene therapy in a model where the TCR, the targeted mutation as well as the T cells to be engineered are syngeneic to the tumor-bearing host being treated. This model should be able to provide insights on future individualized autologous T cell based therapies using autologous TCRs. The spontaneous tumor Ag104A was used as a preclinical model. A tumor-specific TCR (M2/3) was isolated from the spleens of immunized mice. Further analysis showed that the response was directed against a single point mutation in p53 (D253E), which was identified as a suitable T cell target for mutation-specific TCR gene therapy. Treatment of Ag104A tumors expressing natural antigen levels induced stable disease, delayed tumor outgrowth and improved the survival outcome of all treated mice. Tumor recurrence was a result of antigen-negative variants. There was no evidence that genetic alterations in the p53 gene occurred upon treatment. Therefore, tumor escape could be explained by the presence of low-frequency occurring antigen-negative variants, pointing out tumor heterogeneity as one of the main challenges of such therapeutic approach. Moreover, it was shown that p53<sup>D253E</sup> mutation provides Ag104A tumor cells with a growth advantage, thus promoting tumor growth. The overall analysis shows that neoantigen-specific TCR gene therapy can be effective against a single target and prioritizes the steps that would be needed to make this approach therapeutic in the clinic.

#### 4.1 Ag104A as a preclinical model for mutation-specific TCR gene therapy

One of the major challenges in cancer research is establishing preclinical mouse models that can mirror the human clinical situation and provide rapid answers to questions concerning immunotherapeutic protocols. An ideal system is an immune-competent model that can mimic tumor development and progression. However, given the lifespan and the different tumor kinetics in mice, it is unexpected to concentrate all characteristics in one model. Regarding tumor initiation and development, processes that can last for years in humans, there is a variety of genetically engineered models that allow for autochthonous tumor formation in mice, which is inducible under alterations in common driver genes holding a significant role, like *Trp53* and *Kras* [245, 269]. However, these models often develop precipitously within weeks with usually far fewer mutations than tumors developing spontaneously in mice or humans usually late in life. This thesis focuses on the study of T cell therapy that could be against such a tumor that spontaneously arose in an old mouse.

The scope of this thesis was the investigation of T cell based therapies in an attempt to establish a common strategy against solid tumors. Therefore, the mouse model Ag104A was chosen as it gathers a set of unique characteristics. First, Ag104A is a spontaneous tumor that developed in a mouse 2 years and one month of age (760 days). The median life span of C3H mice is 777 days (695 – 818 days, 95% CI) [270]. Aging is the most important risk factor for human cancer (mean peak incidence at 66 years of age). Second, most mouse tumors utilized in cancer research are induced by carcinogens, like UV light or MCA, and thus harbor an unnaturally high number of mutations. Such numbers are usually met in specific human cancers, like melanoma and lung adenocarcinoma, which are also associated with exposure to high doses of environmental carcinogens, virtually all of them being mutagens. Most human cancers exhibit a low number of mutations at the time of diagnosis, and specifically less than 100 mutations on average [31, 70]. Ag104A, as a spontaneous tumor, has a low mutational burden (77 expressed mutations), as commonly found in human cancers. It was proven that such tumors contain immunogenic epitopes, which can be selected as targets for mutation-specific TCR gene therapy. Also, the Ag104A cancer cell line does not originate from a tumor line that was serially transplanted in mice, another common practice that results in tumors that have undergone selection in immunocompetent mice. Such tumors are altered in comparison to the original ones often giving false impressions about the genomic landscape and tumor complexity. Therefore, Ag104A tumors closely resemble the original primary tumor. Third, Ag104A tumors were established at the time treatment was initiated. Tumors in preclinical models are often treated early at remarkably small sizes, which do not resemble actual tumor tissue but they are rather a mix of living and necrotic cancer cells due to the inflammation caused by the injection [271]. Moreover, for Ag104A, the microenvironment and all cellular

components involved in tumor establishment and therapy were of syngeneic mouse origin and there was therefore no risk of mismatches or cross-reactions between mouse and human cells. Fourth, the target that was selected for neoantigen-specific TCR gene therapy (mp53) was expressed in natural unmanipulated levels. Previous works have shown that ATT targeting neoantigens can be effective, when the target was expressed in high levels after induction of transduction [223, 224]. The natural expression levels of mp53 in Ag104A tumors allowed the study of the role of antigen abundance in mutation-specific TCR gene therapy and underlined tumor heterogeneity as a main challenge of such approach. Based on these properties, Ag104A represents a relevant preclinical model that mirrors the human clinical situation. At the time of diagnosis, patients bear established tumors with mutations expressed at natural levels. The steps from target selection to ATT can be modeled in a system like Ag104A, in order to determine crucial parameters of neoantigen-specific TCR gene therapy.

#### **4.2 Protocols to identify mutant neoantigens as T cell targets are essential for designing mutation-specific TCR gene therapy**

The most critical parameter to design mutation-specific TCR gene therapy is the selection of the targeted neoantigen. It has been shown that reactive T cells against neoepitopes do exist in the tumor microenvironment or circulate in the periphery but are often not reactive due to several reasons, like inhibition or poor tumor infiltration. To identify such endogenous responses, a TCR-antigen identification protocol was established in the scope of this work. All mutations of the spontaneous tumor Ag104A were determined by whole exome and RNA sequencing. Tumor-reactive T cells and their respective TCR (M2/3) were isolated upon immunization of immunocompetent hosts with lethally irradiated Ag104A tumor cells. This experimental setup also proved the ability of neoantigens to initiate specific T cell responses. The entire Ag104A mutanome was expressed in artificial antigen-presenting cells, engineered to constitutively express the MHCI molecules of the C3H mouse strain (H-2<sup>k</sup>), since the specific response was attributed to CD8<sup>+</sup> T cells. The interaction between M2/3-engineered T cells and these tumor substitutes revealed the neoantigen recognized encoded by a single point mutation in *Trp53* (mp53). The main idea behind the described antigen identification approach was the establishment of a protocol that can be broadly applied in different cancer entities. One of the main advantages of the method is that there is no need of primary tumor material for antigen presentation, as established cell lines of choice can be manipulated to stably express the restriction elements of interest. However, the respective human HLA system is more complex than the mouse one, as there are six HLA class I molecules, in contrast with two MHCI molecules that most mice bear. Additionally, the complexity of class II alleles is even higher, when CD4<sup>+</sup> neoantigen responses are in question. To circumvent this challenge and

still be independent of tumor material, lymphoblastoid cell lines (LCL) can be used in the antigen identification protocol. LCL are typically established from a patient's own peripheral blood and specifically own B cells with the prerequisite that they are infected with the Epstein-Barr virus (EBV) [272, 273]. EBV infection is thought to give B cells the ability to proliferate autonomously, although it has been shown that these cell lines are not truly immortal and they have a limited survival potential [274]. However, the strongest advantage of LCL is that they endogenously express all HLA class I and II molecules of a patient, as they are essentially autologous antigen-presenting cells. Equivalent alternatives are currently under investigation to circumvent the issue of limited lifespan and the necessity of an EBV infection. CD40-stimulated B cell cultures (CD40B) free of EBV have been shown to have an extended proliferation capacity [275]. Stimulation via the CD40 receptor with CD40L-expressing feeder cells or soluble recombinant CD40L promotes a strongly activated phenotype in both mice and humans [276, 277]. Furthermore, CD40B cells upregulate MHC and co-stimulatory molecules and are also able to induce CD4<sup>+</sup> and CD8<sup>+</sup> immune responses in an MHC-dependent manner, thus acting as professional APCs [278]. Therefore, established CD40B cell lines qualify as an immortalized autologous surrogate cancer cell line, as they can be engineered to express the TMG constructs described in this work. Importantly, tumor material is only required at the very first step of analysis in order to perform sequencing analysis and identify all mutations. This might be a limiting factor only in some patients. On the contrary, the supply of tumor material for further experimental procedures is a limiting factor for the majority of patients. Another advantage of using TMGs in the antigen identification protocol is that all mutations of a given tumor can be analyzed at the same time without the application of prediction algorithms or other forms of pre-selection. Such algorithms are often used to predict epitope binding to MHC molecules. However, they can be misleading in some cases, as they remain underdeveloped or even do not exist for certain MHC or HLA molecules, like H-2D<sup>k</sup> in the C3H mouse strain. Moreover, the endogenous processing and presentation of potential neoantigens is ensured due to TMG construct design, which therefore allows the examination of naturally occurring epitopes.

The TMG construct design established is not only valuable for the described antigen identification protocol but can be used in a number of other approaches. Neoantigen vaccines make use of such constructs but they often lack proof of sufficient processing and presentation of every neoepitope. Here, the subsequent analysis revealed that all positions in a TMG are equally processed and presented. Additionally, these constructs can be used in immunization assays to generate mutation-specific T cell responses by using TMG-expressing surrogate cancer cells for vaccination. TMGs can be brought into cells of interest either as DNA or RNA molecules. The use of peptides instead of lengthier constructs is frequently preferred. This might lead to false conclusions, as it can be later proved that the full-length protein cannot be



processed or presented *in vitro* or *in vivo*. Therefore, TMG constructs could be preferentially used to avoid such obstacles. Furthermore, construct design leaves room for certain flexibility. Specifically in Ag104A, analysis of spleens from immunized mice provided evidence that mp53 is an immunodominant antigen, as the M2/3 TCR $\alpha$  and TCR $\beta$  chain sequences were found in all analyzed cultures. This might have obstructed the induction of further T cell responses against other subdominant antigens. Using TMG constructs without mp53 but with all other mutations of Ag104A for vaccination might help to obtain further mutation-specific TCRs. Likewise, this strategy can be applied in other systems. These examples underline the importance of carefully controlled TMG constructs in subsequent experiments.

#### **4.3 Adoptive T cell therapy targeting mp53 in established Ag104A tumors leads to escape of antigen-negative variants**

In this work, the low number of mutations and the nature of Ag104A as a non-manipulated and heterogeneous cancer serve as important characteristics to evaluate neoantigen-specific TCR gene therapy. Immunization of immunocompetent C3H mice with Ag104A tumor cells resulted in a specific T cell response that was primarily directed against a mutation in *Trp53*. The experiments showed that a single mutation-specific TCR (M2/3) targeting mp53 induced stable disease and delayed tumor progression in mice bearing established solid Ag104A tumors expressing natural levels of the mutant neoantigen. Affinity of the mp53 peptide to H-2K<sup>k</sup> has a predicted value of approximately 25nM, which is in the range of pMHC affinities ( $IC_{50} < 186nM$ ) thought to be sufficient for tumor destruction [234, 235]. Endogenous antigen processing and presentation were also confirmed prior to therapy. Antigen abundance was also evaluated by investigating its presence in single-cell clones derived from the primary minimally passaged Ag104A cancer cell line. The analysis showed that mp53 was broadly expressed. These observations prove that spontaneous cancers with a low mutational load, like most human solid cancers, are immunogenic, an issue that is often debated. Despite the properties of the selected neoantigen, tumor relapse could not be avoided. It was shown Ag104A reisolates were mp53-negative variants that were no longer recognized by the M2/3 TCR.

Many mechanisms of tumor escape have been described that affect either T cells or the cancer cells to avoid immune destruction. First, it was investigated whether the transferred M2/3-engineered T cells could no longer recognize Ag104A *in vivo*, thus allowing tumor outgrowth. Tumor-specific T cells are often found dysfunctional in the tumor microenvironment. Due to persistent exposure to antigens and immunosuppressive signals transmitted directly by the cancer cells or through the tumor microenvironment, T cells upregulate inhibitory receptors, like PD-1, LAG-3 and 2B4, and exhibit alterations in several signaling pathways. Such T cells

are commonly described as exhausted [279, 280]. They display defects in direct antigen recognition, downregulate the production of cytokines, like IL-2 and IFN- $\gamma$ , thus becoming unable to fulfill their effector functions and show a lower proliferation capacity [281, 282]. For these reasons, checkpoint blockade therapy able to reverse these effects in some cases has gained interest. It has been shown that the dysfunctional state of CD8<sup>+</sup> T cells is acquired early during tumorigenesis and is antigen driven [179]. It has also been suggested that such T cells can be rescued from the epigenetic changes that program their anergic state, depending on their chromatin states [180]. However, it is possible that *ex vivo* engineered T cells transferred to tumor-bearing recipients can reach an exhaustion state. In the case of Ag104A, M2/3-engineered T cells transferred to tumor-bearing mice were not found to be exhausted. They persisted in the tumor environment during relapse and tumor outgrowth and were also shown to recognize Ag104A tumor cells *in vitro* after TIL isolation.

Next, alterations in the Ag104A cancer cells were analyzed. (i) Changes in antigen processing and presentation, such as TAP-1 loss, have been described as a tumor escape mechanism in some cancers, such as lung cancer [283]. It was proven that the processing and presentation of mp53 was not affected. Treatment of escape variants with IFN- $\gamma$  to upregulate presentation did not restore recognition by M2/3-engineered T cells. Escape variants were also exogenously loaded with the mp53 peptide or the TMG that contained the 25-mer construct and were subsequently recognized by M2/3-engineered T cells. Therefore, defects in the antigen processing and presentation machinery in tumor cells that escaped mutation-specific TCR gene therapy were experimentally excluded as mechanisms of tumor escape. (ii) Downregulation of MHCI molecules on the tumor cell surface has been described as a mechanism of tumor escape. Many human cancers consist of mixed populations of HLA class I positive and negative lesions and some are found to be entirely HLA-I negative at advanced stages [284]. Lack of HLA molecules allows the cancer cells to avoid immune destruction as it obstructs the presentation of antigens and thus the recognition by T cells. However, relapsing Ag104A tumors showed prominent expression of MHCI molecules on their surface. (iii) Tumor escape could have been attributed to downregulation of the targeted antigen. Mechanisms in Ag104A escape variants could lead to an active downregulation of mp53 due to promoter methylation or other epigenetic changes on genomic level. Dynamic and active mechanisms, like methylation, regulate gene expression. Differential changes in their patterns are often linked to cancers [285-287]. It has also been described that these changes can be reversible and not heritable once the pressure is taken away from the system, e.g. a drug that causes drug resistance through epigenetic changes [288]. However, such observations were not experimentally supported in Ag104A as shown by the analysis of Ag104A escape variants. Relapse variants were treated with 5-Azacytidine, which inhibits all methylation processes in a cell. The treatment did not restore recognition by M2/3-engineered T cells. Moreover,

selected variants were cultured for a long period without any T cell pressure. These late passage cell lines were also not recognized by the mp53-specific TCR, thus tumor escape did not take place due to therapeutic pressure. Finally, (iv) genomic changes could explain tumor escape. One possibility would be the acquirement of further mutations to prevent TCR recognition of the epitope or even antigenic loss on the genomic level [289]. Alternatively, changes in *Trp53* copy numbers could also explain the therapeutic outcome, as it has been described for other cancers [290]. None of the aforementioned genetic alterations were observed in Ag104A escape variants. The genomic locus surrounding the mp53 neoepitope was sequenced and no changes, such as insertions or deletions that could affect TCR recognition were observed. Additionally, copy number analysis showed that both Ag104A bulk and relapsing variants retained two copies of *Trp53*, indicating that genomic loss of mp53 could not explain tumor escape. However, the sequencing revealed that the escape variants were dominated by mp53-negative clonotypes. As a consequence, tumor escape was attributed to the presence of low-frequency occurring antigen-negative variants pre-existing in the inoculated tumor cell population. Before testing the potency of the M2/3 TCR *in vivo*, 133 single-cell clones originating from Ag104A bulk were examined for mp53 presence and none of them was mp53-negative. Therefore, the frequency of antigen-negative variants is less than 1%. Importantly, M2/3-engineered T cells were able to eradicate all p53<sup>D253/+</sup> cells *in vivo*. After this elimination, mp53-negative variants had the chance to grow further and dominate the relapsing cancer cell population, as the T cells could not act further against the tumor. This observation underlines the role of tumor heterogeneity in cancer immunotherapy. Cancers are multi-factor entities. Here, it was shown that a single mutation may not concentrate all essential characteristics required for tumor development and progression. Even if mutations occur in essential genes like p53, which are thought to drive tumor growth, a combination of events that a cancer cell acquires over time results in tumor formation and maintenance [28, 291]. Therefore, intratumor heterogeneity as a frequently described mechanism of tumor escape is a critical parameter [292]. However, it was shown that a single mutation-specific CD8<sup>+</sup> TCR is effective against its target and sufficient to eliminate antigen-positive variants.

#### 4.4 Nature of the p53<sup>D253E</sup> mutation in Ag104A

Mutations in the tumor suppressor gene *TP53* are found in the vast majority of all human cancer types and they are often considered to be driver mutations [24]. The p53 protein acts as a transcription factor and regulates a number of cellular processes such as G1 cycle arrest or apoptosis after DNA damage. In a steady state, p53 is rapidly degraded through its interaction with the protein Mdm2 that initiates a ubiquitin-mediated degradation of p53 [16]. In response to DNA damage e.g. radiation, p53 is subsequently subjected to post-translational

modifications, e.g. phosphorylation, which inhibit the interaction of p53 with Mdm2 and stabilize it [293]. After its stabilization, p53 assembles in tetramers, which bind to target genes in a sequence-specific manner and regulates their transcription [294]. The up- or downregulation of target genes leads to cell cycle control as well as to the activation of DNA repair mechanisms. A well-described process is the transactivation of p21<sup>Waf1/Cip1</sup>, which induces G1 arrest and inhibits cyclin-dependent kinases so that the cell cycle cannot be completed [295, 296]. Another major involvement of p53 in cell cycle control is the activation of GADD45, a protein mediating DNA repair and inhibition of entry into the S phase [297]. However, it is generally accepted that each mutation in p53 can lead to a distinct phenotype affecting many different cellular processes.

The human p53 protein consists of distinct domains, the N-terminal transactivation domain (TD) followed by a proline-rich region, a DNA-binding domain (DBD), a tetramerization domain and a C-terminal regulatory domain [298]. The mouse p53 protein is highly similar in structure and more than 91% are identical to the human one. According to the International Agency for Research on Cancer (IARC) TP53 database, the vast majority of human cancer-associated p53 mutations are found in the DBD domain, while more than 70% of them are missense mutations that lead to single amino acid substitutions. *TP53* mutations are classified in several distinct subcategories that refer to either their function or their structure. Structural mutations are divided into contact mutations that abrogate the binding of p53 to target genes and conformational mutations that reduce p53 stability [299, 300]. Regarding function, p53 mutations can be further divided to loss-of-function mutations that result in the disruption of classical p53 pathways and gain-of-function (GOF) mutations, which are thought to promote invasion, metastasis and angiogenesis [301-303]. Separation-of-function mutations are also described, as in the case of p53<sup>R175P</sup>, where p53 retains some of its functions, while other functions are abrogated [304]. Loss of heterozygosity (LOH) describes cases where either both alleles are affected by a mutation or the second wt allele is lost, both resulting in complete p53 deficiency. This is observed in the majority of p53 missense mutations and it is suggested that loss of the wt allele stabilizes mutant p53 and is a prerequisite for the presence of GOF mutations [305]. However, when only one allele carries a mutation and the wt one is retained, wt and mutant p53 proteins co-exist. This fact has resulted in a debate concerning the assembly of p53 tetramers. In some cases, one or two mutant p53 monomers in a tetramer are sufficient to abolish p53 function and are described as dominant-negative mutations [306, 307]. Other studies suggest that at least three monomers in a tetramer have to be mutated in order to inactivate p53 functional properties, as it is described in the case of the p53<sup>R273H</sup> and p53<sup>R249S</sup> mutations [308]. Furthermore, it has become evident that the outcome of a mutation might depend on the structure of the residue that replaces the wt one. For instance, the R175H

mutation, which is one of the most frequent ones in human cancer, leads to a severe loss of p53 function, whereas the R175C has a mild effect on p53 transcriptional activity [309].

Taken into consideration the important role of p53 in cell cycle regulation, the nature of the p53<sup>D253E</sup> mutation in Ag104A was investigated. Since this specific mutation has not been described before in mice, little is known about its function. The mutation is located in the DBD domain. In Ag104A, no LOH was observed since the wt allele was found in both Ag104A bulk tumor cells and tumor escape variants. Ag104A tumor cells were modified by CRISPR/Cas9 to obtain a p53<sup>+/+</sup> variant, which was used as a tool to study the p53<sup>D253E</sup> function along with Ag104A variants that escaped T cell therapy. It was shown that both the escape variants that lack mp53 and the p53<sup>+/+</sup> variant grew slower than Ag104A bulk both *in vitro* and *in vivo*, suggesting that the D253E mutation provided the tumor cells with a growth advantage that might have impacted tumor cell proliferation and progression of the autochthonous Ag104A cancer. However, the mutation was not indispensable for cancer cell survival and maintenance. These first observations in this work suggest that mp53 in Ag104A might have gained some functions. However, since LOH was not observed, the characterization of the D253E mutation as a GOF mutation requires further investigation. Furthermore, the p53<sup>D253E</sup> mutation reflects the exchange of aspartic acid against glutamic acid. Both residues are negatively charged and have similar side chains as glutamic acid bears only an extra methylene group. Therefore, it is unknown how the residue exchange has affected the DNA-binding properties of p53 and a biochemical analysis is needed to examine this. It can be assumed that the p53<sup>D253E</sup> mutation in Ag104A is a passenger mutation, assuming that it does not result in complete p53 deficiency due to the similarities of the two residues. Passenger p53 mutations are also described in human cancer [310]. Moreover, the effect of the p53<sup>D253E</sup> mutation on the formation of p53 tetramers has to be studied. Based on RNA sequencing data, wt and mutant p53 are equally expressed in Ag104A. Therefore, an equal presence of wt and mutant proteins can be assumed. However, it is unknown which form dominates the other and whether mutant p53 in Ag104A is able to form tetramers with wt p53 and lead to differential p53 downstream functions. It has been suggested that the preferential formation of wt p53 tetramers together with the simultaneous accumulation of mutant p53 suppresses the effects of GOF mutations [311]. It is also possible that the D253E mutation was acquired later during tumor cell development and clonal evolution, thus providing Ag104A tumor cells with higher tumorigenic properties. Last but not least, it has been shown that although human and mouse p53 are highly conserved, they exhibit major differences in their gene regulatory networks [312, 313]. As a result, each mutation has to be investigated separately, as it is apparent that mutant p53 effects highly depend on the cellular context and tumor type.

The DBD of p53 is considered a “hotspot” for mutations as most tumor-associated genetic alterations are located in this region, while about 25% of them are recurrent [314]. The D253E

mutation described in Ag104A has only been described in three isolated cases of human cancers (in position 259) according to the COSMIC database [265-267]. Therefore, it cannot be characterized as a recurrent one. However, plenty of p53 mutations in human cancers, especially those found in hotspots, are frequently shared among patients. The analysis in this work showed that mutations frequently affecting essential genes like *TP53* can be successfully targeted and are an option for neoantigen-specific TCR gene therapy. Indeed, TCRs against recurrent human p53 mutations have been isolated from patient material and their evaluation in preclinical models or clinical trials is currently pending [228].

#### **4.5 Combinatorial T cell therapy to overcome relapse caused by antigen-negative variants**

Targeting neoantigens by T cell therapy in solid cancers is a promising strategy. Several approaches can be explored to overcome the challenge of intratumor heterogeneity, which can lead to tumor escape due to the presence of antigen-negative variants. As shown in this work, these variants can occur at a low frequency, thus lowering the chances of determining them with conventional techniques.

##### **Simultaneous targeting of multiple neoantigens**

One option to tackle relapse due to intratumor heterogeneity is simultaneous targeting of multiple independent neoantigens in the same cancer. Multiple targets can be identified by analyzing tumor-specific T cell responses after immunizations or in TIL populations. However, it is not trivial to dissect clonal differences in antigen expression. In mice and in the case of Ag104A specifically, a whole exome and RNA sequencing analysis on variants that escape T cell therapy can highlight differences between the genomic landscape of the bulk tumor and these variants. The next step is to identify T cell responses directed against escape variants. Such T cells can be located in T cell cultures originating from spleens of immunized mice. Importantly, these T cell cultures should recognize both the bulk tumor and the escape variants to ensure that possible targets are not mutant neoantigens that were acquired during therapy. The tandem minigene approach could be again employed to identify the genetic origin of T cell responses and thus select further targets for immunotherapy. Cancer cell clones can be used as a tool to determine antigen abundance and the distribution of selected targets in the parental tumor cell population. Therefore, the combination of different TCR-engineered populations adoptively transferred simultaneously to tumor-bearing hosts could successfully target phenotypically distinct parts of a tumor. In humans, primary tumor material is frequently a limiting factor and the genomic heterogeneity of a tumor can be underestimated. Therefore, simultaneous targeting of different neoepitopes could be exploited against cancers with

confirmed spatial differences.

### **The importance of CD4<sup>+</sup> T cells and their combination with CD8<sup>+</sup> T cells in tumor eradication**

Cancer cells of solid tumors express MHC I molecules as all nucleated cells. As they are not professional APCs, they usually lack MHC II molecules on the cell surface. Therefore, cancer cells are directly recognized by CD8<sup>+</sup> T cells. As previously described, tumor stroma is an essential part of every cancer. It bears tumor-promoting properties and sustains tumor growth [315]. Stromal cells often form an immunosuppressive microenvironment that results in poor T cell infiltration and provide inhibitory signals that obstruct T cell function [316]. Destruction of the tumor stroma is thought to be a critical process for tumor eradication [317]. CD8<sup>+</sup> T cells are thought to recognize and kill stromal cells that cross-present antigens [102]. CD4<sup>+</sup> T cells are essential to provide help and activate them. However, they are also shown to recognize the tumor stroma and act synergistically with CD8<sup>+</sup> T cells to achieve tumor elimination [318]. In the aforementioned study, Ag104A tumor cells were transduced to stably express two described epitopes recognized by CD8<sup>+</sup> or CD4<sup>+</sup> T cells respectively only when cross-presented by stromal cells due to the experimental setup. Tumors were eradicated upon simultaneous administration of CD8<sup>+</sup> or CD4<sup>+</sup> engineered T cells. In a native situation, CD4<sup>+</sup> T cells can be directed against mutant neoantigens cross-presented by stromal cells, which include macrophages and dendritic cells that express MHC II molecules and are professional APCs. To elicit CD4<sup>+</sup> T cell responses against Ag104A or other murine cancers, tumor cells can be used for immunization injected into the hind feet of immunocompetent mice. Cells from draining lymph nodes can be re-stimulated *ex vivo* with tumor cells similar to the steps followed with spleens of immunized mice for this work. This method was adapted and used to characterize one of the first cancer-specific mutations to be described [59]. The CD4<sup>+</sup> T cell response was directed against a mutation caused by a single amino acid substitution in the ribosomal protein L9 (mRPL9) in a UV-induced tumor model. Later, it was shown that adoptively transferred CD4<sup>+</sup> T cells against mRPL9 cross-presented by stromal cells could destroy tumors *in vivo* even in the absence of CD8<sup>+</sup> T cells. It was also shown that IFN- $\gamma$  released by the CD4<sup>+</sup> T cells acted on stromal and not on tumor cells [319]. Alternatively, lymph node cells of immunized mice can be cultured *ex vivo* with autologous TMG-loaded dendritic cells in order to detect mutation-specific CD4<sup>+</sup> T cell responses. Prominent specific CD4<sup>+</sup> T cell responses have been also detected in TILs from human cancers [183, 320]. In some patients, they are more frequent than mutation-specific CD8<sup>+</sup> T cell responses [321]. The therapeutic potential of neoantigen-specific CD4<sup>+</sup> T cells has been shown in several case studies of human cancers, where durable complete responses were achieved [221, 259, 322]. These patients

received TIL populations expanded *ex vivo* prior to adoptive transfer, which were dominated by mutation-specific CD4<sup>+</sup> T cells. The use of CD4<sup>+</sup> T cells in neoantigen-specific T cell therapy could offer certain advantages. First, antigen-negative variants cannot be selected to overgrow the cancer cell population, because CD4<sup>+</sup> T cells recognize only stromal cells directly. Therefore, the surrounding stroma can be constantly loaded with antigens of the adjacent tumor tissue, which are cross-presented to CD4<sup>+</sup> T cells. Second, the production of the effector cytokines IFN- $\gamma$  and TNF- $\alpha$  by CD4<sup>+</sup> T cells can aid the destruction of tumor stroma, which is thought to be necessary for tumor eradication as the growth of cancer cells is no longer supported and the tumor architecture collapses. Third, there is evidence that CD4<sup>+</sup> T cells can achieve direct tumor cell killing through the activation of the Fas-FasL pathway and the secretion of perforin and granzyme B [323]. As a consequence, the combination of neoantigen-specific CD4<sup>+</sup> and CD8<sup>+</sup> TCR-engineered T cells with known specificities *in vivo* could lead to tumor eradication and the prevention of relapse. Such a combination would exploit the beneficial properties of both T cell subpopulations and act simultaneously against cancer and stromal cells to achieve tumor eradication.

### **Combining TCR- and CAR-engineered T cells in vivo**

Another strategy to prevent tumor escape due to intratumor heterogeneity would be the combination of TCR- and CAR-engineered T cell populations. CAR-T cell therapy has been proven successful against certain hematological malignancies. However, the use of CARs against solid tumors remains a challenge. Most CARs being researched nowadays are designed against TAAs in order to be broadly applied to a variety of cancer types and patients expressing those antigens. The main limitation of this approach, as with TCR-engineered T cells targeting TAAs, is correlated with severe side effects due to the presence of these antigens in healthy tissues. A class of antigens that can be classified as cancer-specific are the Tn antigens, caused by aberrant glycosylation patterns affecting mostly the O-linked glycosylation process on Serine/Threonine residues [324]. Such changes are a result of recurrent mutations in the *Cosmc* gene, which encodes for a chaperone essential for the function of the enzyme T-synthase [325]. Any alterations of the COSMC chaperone obstruct the transfer of O-linked glycol groups by T-synthase, resulting in partially synthesized and uncompleted glycosylation trees, which are often associated with cancer [326, 327]. Such differential glycol moieties, the so-called Tn and STn (sialyl Tn) antigens, are present exclusively on the tumor cell surface and can be targeted by antibodies, as they are surface antigens. Ag104A bears a mutation in *Cosmc*, which leads to the deletion of 26 amino acids (nucleotides 509 to 587). The 237 monoclonal antibody isolated from a hybridoma cell line containing spleen cells of mice immunized with Ag104A tumor cells binds Tn antigens on



Podoplanin (PDPN) and has been used to design the respective 237CAR [252, 328]. It has been shown that the 237CAR has a broader specificity and 237CAR-T cells can eradicate leukemia induced by Jurkat cells in an NSG model [329]. The efficacy of 237CAR-T cell therapy against a solid tumor like Ag104A has not been shown. In ongoing work from our group, it is shown that 237CAR-modified T cells recognize both Ag104A bulk cancer cells and variants that escaped mp53-specific TCR gene therapy *in vitro*. Therefore, mp53-negative variants retain Tn antigens, which can be targeted by 237CAR-T cells. As a consequence, the combination of TCR- and CAR-engineered T cells *in vivo* could overcome intratumor heterogeneity. Moreover, the use of CAR-modified T cells could also engage the beneficial actions of CD4<sup>+</sup> T cells. CAR construct design allows for some flexibility in order to determine which configuration leads to the optimal activation of both CD8<sup>+</sup> and CD4<sup>+</sup>-engineered T cells. The use of different signaling domains confers different antitumor effects. CD28 as a co-stimulatory domain seems to induce a rapid cytotoxic response [192, 330], whereas 4-1BB supports the longer persistence of CAR-T cells by promoting a T cell memory phenotype [331, 332]. The combination of both co-stimulatory domains in order to make use of different downstream signaling pathways can also enhance the antitumor response, as it has been suggested in the case of a CAR targeting the multiple myeloma-associated CD38 antigen [333]. Sufficient activation of CAR-T cells is essential, otherwise they may not be able to overcome the immunosuppressive tumor microenvironment and rapidly become anergic or inhibited.

A CAR with clinical relevance against human cancers is the 5E5CAR, which recognizes a Tn glycoform on the cell membrane protein MUC1 overexpressed in many adenocarcinomas [334, 335]. The Tn-MUC1 epitope is frequently found in ovarian cancer and myeloma. The therapeutic potential of the 5E5CAR has been evaluated in two models of leukemia and pancreatic cancer [336]. Targeting Tn antigens in human cancers with CARs can be broadly applied to a number of patients as an “off-the-shelf” therapy. The combination of Tn-specific CAR-T cell therapy with mutation-specific TCR-engineered T cells can be a promising strategy to overcome intratumor heterogeneity. Furthermore, CAR-engineered T cells recognize their targets in an MHC-independent manner. Cancer cells frequently exhibit defects in antigen processing and presentation as a way to avoid T cell recognition and destruction. Such changes are also introduced due to therapeutic pressure. However, CAR-modified T cells would still be able to function under such conditions, as their ligands do not depend on MHC molecules and related proteins.

#### **4.6 The prospect of patient-individualized mutation-specific T cell therapy as a powerful cancer treatment**

The work in this thesis showed that a single mutation-specific TCR is sufficient to eradicate cancer cells that bear the mutation. Neoantigen-specific TCR gene therapy is directed against truly cancer-specific antigens that are not expressed in healthy tissues. Therefore, the risk of severe autoimmune effects is significantly reduced. Given interpatient heterogeneity and the nature of cancers as diverse entities, such T cell therapy is a highly personalized approach. To manufacture a final cellular therapeutic product that is tailored to each patient, a pre-arranged set of protocols is required. Preclinical models, like Ag104A established in this thesis, serve as tools to investigate critical parameters of neoantigen-specific TCR gene therapy.

The realization of personalized T cell therapy consists of distinct steps upon diagnosis. The first step is the identification of all somatic mutations in a cancer, which can be achieved with DNA and RNA sequencing. The tumor tissue subjected to sequencing can be obtained from biopsy material or surgical resections and compared with normal tissue as a reference e.g. a blood sample. The emerging technology of NGS has made the determination of cancer mutations a rapid and reliable process [337]. It is a cost-effective procedure that identifies all genomic alterations in a cancer, like single amino acid substitutions, insertions, deletions, gene fusions and copy number variations. Obtaining a library with all somatic mutations facilitates optimal target selection. Moreover, it allows the generation of surrogate cancer cell lines as previously described to circumvent the further need for primary tumor material.

The second step of this approach requires the isolation of relevant neoantigen-specific T cells from a patient's own system. Such T cells might exist in the tumor microenvironment, where they are often found anergic or in insufficient numbers, thus unable to act against cancer cells. TCR repertoire and single-cell analysis with the aid of NGS reveal TCR $\alpha$  and TCR $\beta$  chain combinations that can be used to reconstruct a TCR for further investigation [338, 339]. The starting material for sequencing can be TILs found in the tumor microenvironment or other sources, like ascites that often co-exists in several cancer types and serves as a diagnostic tool [340]. However, the frequency of neoantigen-specific T cells is frequently too low, thus making their identification challenging. To overcome this obstacle, TILs can be re-stimulated *ex vivo* with surrogate cancer cell lines expressing all mutations and MHC molecules of the given cancer. Tumor-reactive T cells will preferentially expand in the presence of their ligands, thus their isolation will be distinguishable from clinically irrelevant T cells. An alternative strategy is the immunization of a patient with nonmalignant neoantigen-expressing cells used as vaccines in order to enrich cancer-specific T cell responses, which can be later identified in the peripheral blood of the patient. In both approaches, the necessity for neoantigen prioritization or pre-selection can be circumvented with the use of TMGs, so that the search

for optimal targets is unbiased. Neoantigen-specific TCRs can also be obtained from other sources. A patient's own peripheral blood lymphocytes or allogeneic T cells can be primed *in vitro* with MHC molecules loaded with antigens, e.g. on the surface of dendritic cells [341-343]. Another source is the generation of neoantigen-specific T cells in MHC transgenic mice that bear a human TCR repertoire [344]. However, these approaches usually require some level of antigen pre-selection thought to be able to elicit a T cell response. They also often do not examine antigen processing and presentation. Therefore, the identification of autologous T cells responses in an unbiased manner can indicate the antigens that are truly able to initiate an antitumor response, as they have already generated specific T cell responses in a native tumor environment. Candidate TCRs can be re-expressed in T cells to identify their targets. Once the neoantigen has been determined, its suitability as a target for mutation-specific TCR gene therapy can be evaluated. Examining parameters such as antigen abundance and expression levels, pMHC binding affinity or possible cross-reactivity with other epitopes are essential.

The last step is the adoptive transfer of TCR-engineered T cells into the patient. TCR delivery into T cells prior to their *ex vivo* expansion is often debated. Nowadays, it is widely accepted that TCR $\beta$  chain sequence is encoded at the 5' end of the cassette and connected to the  $\alpha$  chain at the 3' end via a 2A element [210, 211]. The constructs are usually codon optimized, which is thought to enhance translation of the transgene [345]. However, the level of chain murinization varies significantly between different TCRs used in the clinic or for research purposes. The constant regions of  $\alpha$  and  $\beta$  chains can be entirely murinized or utilize the so-called minimal murinization, where 9 amino acids of the human constant regions are exchanged against the mouse ones with an additional disulfite bond [346-349]. Additional modifications are frequently met, like the exchange to certain amino acids which are thought to stabilize TCR expression and cell surface prominence [350-352]. In general, minimally murinized TCRs are well accepted in clinical trials, as the risk for immune reactivity against the mouse regions is minimized. What is important is to evaluate TCR surface expression as well as mispairing with endogenous chains in order to find a balance with the least possible compromise as different TCRs might call for different construct design. Regarding transgene delivery systems, lentiviral and retroviral vectors are usually employed. Lentiviral vectors are often preferred as they integrate into the genome in a random fashion, whereas retroviral vectors integrate into dividing cells [353, 354]. However, there are concerns about their safety as they are thought to be able to cause mutagenesis in the genes they are integrating. As a consequence, TCR copy number upon transduction of T cells needs to be considered as it depends on the transfection system and thus the virus titer that has been used. In connection with T cell engineering, different T cell subsets seem to play a vital role in T cell persistence. TCR-engineered T cells are transferred to the patient after long culturing periods, which have

affected their phenotype. They are mostly late effector T cells and thus bear limited proliferation capacity and potential for persistence [355, 356]. On the contrary, early effector CD8<sup>+</sup> T cells elicit more potent antitumor responses, they have an increased proliferation and survival potential and they have been found to home better in the tumor microenvironment and secrete cytokines necessary for cytotoxicity. Consequently, less-differentiated T cell subsets are considered ideal for ATT [357, 358]. Retroviral vectors might compromise this parameter as they integrate into dividing cells and therefore promote T cell differentiation. An approach that is gaining interest is the genomic editing of T cells mediated by the CRISPR/Cas9 system in order to increase safety and limit T cell exhaustion. It has been shown that TCR engineering via CRISPR/Cas9 and homology-directed repair results in antitumor responses *in vitro* and *in vivo* [359]. The disruption of endogenous TCR chains and genes that promote immunosuppression and T cell inhibition, like PD-1, is also possible via genome editing [360]. This approach has been utilized in a clinical trial together with NY-ESO-1-specific T cells in patients with refractory cancer [361]. These strategies can lead to the rapid generation of specific and potent TCR-engineered populations, but require further research and optimization.

Overall, the common goal of all research approaches concerning neoantigen-specific T cell therapy is to modify a patient's own PBLs with neoantigen-specific TCRs. TCR-engineered T cells are then expanded *ex vivo* to sufficient numbers in order to be transferred into the cancer patient to eradicate tumor cells with the least possible toxicity. As this is an ambitious, forward-looking approach, there are certain aspects that are not yet implemented in a meaningful and practical manner. One aspect concerns the procedures required to generate a final T cell product under good manufacturing practice (GMP) conditions. GMP-scale production is still a time-consuming method, which is additionally prolonged by the time required to acquire permission by the respective authorities. Moreover, treating different patients by neoantigen-specific TCR gene therapy at the same time would require simultaneous GMP production of multiple T cell products, which is logistically challenging. The time periods calculated nowadays to obtain a final therapeutic product could be detrimental to a patient as cancer might progress before the T cell product is ready for therapy. Another aspect are the high costs; a concern that arises due to the nature of mutation-specific TCR gene therapy as a highly individualized approach. In the light of these challenges, the goal from the research point of view should be to resolve remaining questions about neoantigen-specific TCR gene therapy in order to gradually facilitate its clinical implementation. This includes not only elaborating on basic principles of this therapeutic approach, as is the subject of this work, but also the further development of protocols and procedures, which simplify the production of cellular products on the one hand and make it more cost-effective on the other.

---

## 5. References

1. Berenblum, I. and P. Shubik, *A new, quantitative, approach to the study of the stages of chemical carcinogenesis in the mouse's skin*. Br J Cancer, 1947. 1(4): p. 383-91.
2. Shubik, P., *Current status of chemical carcinogenesis*. Proc Natl Acad Sci U S A, 1972. 69(4): p. 1052-5.
3. Land, H., L.F. Parada, and R.A. Weinberg, *Cellular oncogenes and multistep carcinogenesis*. Science, 1983. 222(4625): p. 771-8.
4. Norquist, B.M., et al., *Inherited Mutations in Women With Ovarian Carcinoma*. JAMA Oncol, 2016. 2(4): p. 482-90.
5. Roberts, N.J., et al., *ATM mutations in patients with hereditary pancreatic cancer*. Cancer Discov, 2012. 2(1): p. 41-6.
6. Scott, R.E., J.J. Wille, Jr., and M.L. Wier, *Mechanisms for the initiation and promotion of carcinogenesis: a review and a new concept*. Mayo Clin Proc, 1984. 59(2): p. 107-17.
7. Foulds, L., *The experimental study of tumor progression: a review*. Cancer Res, 1954. 14(5): p. 327-39.
8. Rous, P. and J.W. Beard, *The Progression to Carcinoma of Virus-Induced Rabbit Papillomas (Shope)*. J Exp Med, 1935. 62(4): p. 523-48.
9. Yokota, J., *Tumor progression and metastasis*. Carcinogenesis, 2000. 21(3): p. 497-503.
10. Bodmer, W., *The somatic evolution of cancer. The Harveian Oration of 1996*. J R Coll Physicians Lond, 1997. 31(1): p. 82-9.
11. Fearon, E.R. and B. Vogelstein, *A genetic model for colorectal tumorigenesis*. Cell, 1990. 61(5): p. 759-67.
12. Strasser, A., et al., *Novel primitive lymphoid tumours induced in transgenic mice by cooperation between myc and bcl-2*. Nature, 1990. 348(6299): p. 331-3.
13. Finlay, C.A., P.W. Hinds, and A.J. Levine, *The p53 proto-oncogene can act as a suppressor of transformation*. Cell, 1989. 57(7): p. 1083-93.
14. Donehower, L.A., et al., *Mice deficient for p53 are developmentally normal but susceptible to spontaneous tumours*. Nature, 1992. 356(6366): p. 215-21.
15. Lane, D.P., *Cancer. p53, guardian of the genome*. Nature, 1992. 358(6381): p. 15-6.
16. Haupt, Y., et al., *Mdm2 promotes the rapid degradation of p53*. Nature, 1997. 387(6630): p. 296-9.
17. Shieh, S.Y., et al., *DNA damage-induced phosphorylation of p53 alleviates inhibition by MDM2*. Cell, 1997. 91(3): p. 325-34.
18. Honda, R. and H. Yasuda, *Association of p19(ARF) with Mdm2 inhibits ubiquitin ligase activity of Mdm2 for tumor suppressor p53*. EMBO J, 1999. 18(1): p. 22-7.

19. Riley, T., et al., *Transcriptional control of human p53-regulated genes*. Nat Rev Mol Cell Biol, 2008. 9(5): p. 402-12.
20. Giono, L.E. and J.J. Manfredi, *The p53 tumor suppressor participates in multiple cell cycle checkpoints*. J Cell Physiol, 2006. 209(1): p. 13-20.
21. Hildesheim, J., et al., *Gadd45a protects against UV irradiation-induced skin tumors, and promotes apoptosis and stress signaling via MAPK and p53*. Cancer Res, 2002. 62(24): p. 7305-15.
22. Jeffers, J.R., et al., *Puma is an essential mediator of p53-dependent and -independent apoptotic pathways*. Cancer Cell, 2003. 4(4): p. 321-8.
23. Bates, S., et al., *p14ARF links the tumour suppressors RB and p53*. Nature, 1998. 395(6698): p. 124-5.
24. Hollstein, M., et al., *p53 mutations in human cancers*. Science, 1991. 253(5015): p. 49-53.
25. Olivier, M., M. Hollstein, and P. Hainaut, *TP53 mutations in human cancers: origins, consequences, and clinical use*. Cold Spring Harb Perspect Biol, 2010. 2(1): p. a001008.
26. Bouaoun, L., et al., *TP53 Variations in Human Cancers: New Lessons from the IARC TP53 Database and Genomics Data*. Hum Mutat, 2016. 37(9): p. 865-76.
27. Hainaut, P. and G.P. Pfeifer, *Somatic TP53 Mutations in the Era of Genome Sequencing*. Cold Spring Harb Perspect Med, 2016. 6(11).
28. Nowell, P.C., *The clonal evolution of tumor cell populations*. Science, 1976. 194(4260): p. 23-8.
29. Merlo, L.M., et al., *Cancer as an evolutionary and ecological process*. Nat Rev Cancer, 2006. 6(12): p. 924-35.
30. Gerlinger, M., et al., *Intratumor heterogeneity and branched evolution revealed by multiregion sequencing*. N Engl J Med, 2012. 366(10): p. 883-892.
31. Vogelstein, B., et al., *Cancer genome landscapes*. Science, 2013. 339(6127): p. 1546-58.
32. Blankenstein, T., *The role of tumor stroma in the interaction between tumor and immune system*. Curr Opin Immunol, 2005. 17(2): p. 180-6.
33. Quail, D.F. and J.A. Joyce, *Microenvironmental regulation of tumor progression and metastasis*. Nat Med, 2013. 19(11): p. 1423-37.
34. Elenbaas, B. and R.A. Weinberg, *Heterotypic signaling between epithelial tumor cells and fibroblasts in carcinoma formation*. Exp Cell Res, 2001. 264(1): p. 169-84.
35. Tlsty, T.D. and P.W. Hein, *Know thy neighbor: stromal cells can contribute oncogenic signals*. Curr Opin Genet Dev, 2001. 11(1): p. 54-9.
36. Silzle, T., et al., *The fibroblast: sentinel cell and local immune modulator in tumor tissue*. Int J Cancer, 2004. 108(2): p. 173-80.

- 
37. Kalluri, R., *The biology and function of fibroblasts in cancer*. Nat Rev Cancer, 2016. 16(9): p. 582-98.
  38. Mantovani, A., et al., *Macrophage polarization: tumor-associated macrophages as a paradigm for polarized M2 mononuclear phagocytes*. Trends Immunol, 2002. 23(11): p. 549-55.
  39. Joyce, J.A. and J.W. Pollard, *Microenvironmental regulation of metastasis*. Nat Rev Cancer, 2009. 9(4): p. 239-52.
  40. Bussard, K.M., et al., *Tumor-associated stromal cells as key contributors to the tumor microenvironment*. Breast Cancer Res, 2016. 18(1): p. 84.
  41. Pamer, E. and P. Cresswell, *Mechanisms of MHC class I--restricted antigen processing*. Annu Rev Immunol, 1998. 16: p. 323-58.
  42. Bouvier, M. and D.C. Wiley, *Importance of peptide amino and carboxyl termini to the stability of MHC class I molecules*. Science, 1994. 265(5170): p. 398-402.
  43. Busch, R., et al., *Accessory molecules for MHC class II peptide loading*. Curr Opin Immunol, 2000. 12(1): p. 99-106.
  44. Busch, R. and E.D. Mellins, *Developing and shedding inhibitions: how MHC class II molecules reach maturity*. Curr Opin Immunol, 1996. 8(1): p. 51-8.
  45. Rudensky, Y., et al., *Sequence analysis of peptides bound to MHC class II molecules*. Nature, 1991. 353(6345): p. 622-7.
  46. Sercarz, E.E. and E. Maverakis, *Mhc-guided processing: binding of large antigen fragments*. Nat Rev Immunol, 2003. 3(8): p. 621-9.
  47. *Complete sequence and gene map of a human major histocompatibility complex. The MHC sequencing consortium*. Nature, 1999. 401(6756): p. 921-3.
  48. Kumanovics, A., T. Takada, and K.F. Lindahl, *Genomic organization of the mammalian MHC*. Annu Rev Immunol, 2003. 21: p. 629-57.
  49. Schreiber, H., *Cancer Immunology*, in *Fundamental Immunology*. 2008, Lippincott Williams & Wilkins.
  50. van der Bruggen, P., et al., *A gene encoding an antigen recognized by cytolytic T lymphocytes on a human melanoma*. Science, 1991. 254(5038): p. 1643-7.
  51. Chen, Y.T., et al., *A testicular antigen aberrantly expressed in human cancers detected by autologous antibody screening*. Proc Natl Acad Sci U S A, 1997. 94(5): p. 1914-8.
  52. Thompson, J.A., *Molecular cloning and expression of carcinoembryonic antigen gene family members*. Tumour Biol, 1995. 16(1): p. 10-6.
  53. Gold, P. and S.O. Freedman, *Specific carcinoembryonic antigens of the human digestive system*. J Exp Med, 1965. 122(3): p. 467-81.
-

- 
54. Hammarstrom, S., *The carcinoembryonic antigen (CEA) family: structures, suggested functions and expression in normal and malignant tissues*. Semin Cancer Biol, 1999. 9(2): p. 67-81.
  55. Kawakami, Y., et al., *Cloning of the gene coding for a shared human melanoma antigen recognized by autologous T cells infiltrating into tumor*. Proc Natl Acad Sci U S A, 1994. 91(9): p. 3515-9.
  56. Scheuermann, R.H. and E. Racila, *CD19 antigen in leukemia and lymphoma diagnosis and immunotherapy*. Leuk Lymphoma, 1995. 18(5-6): p. 385-97.
  57. Gross, L., *Intradermal Immunization of C3H Mice against a Sarcoma That Originated in an Animal of the Same Line*. Cancer Research, 1943. 3(5): p. 326-333.
  58. Prehn, R.T. and J.M. Main, *Immunity to methylcholanthrene-induced sarcomas*. J Natl Cancer Inst, 1957. 18(6): p. 769-78.
  59. Monach, P.A., et al., *A unique tumor antigen produced by a single amino acid substitution*. Immunity, 1995. 2(1): p. 45-59.
  60. Stratton, M.R., P.J. Campbell, and P.A. Futreal, *The cancer genome*. Nature, 2009. 458(7239): p. 719-24.
  61. Stratton, M.R., *Exploring the genomes of cancer cells: progress and promise*. Science, 2011. 331(6024): p. 1553-8.
  62. Lalloo, F. and D.G. Evans, *Familial breast cancer*. Clin Genet, 2012. 82(2): p. 105-14.
  63. Greenman, C., et al., *Patterns of somatic mutation in human cancer genomes*. Nature, 2007. 446(7132): p. 153-8.
  64. Venkitaraman, A.R., *Cancer susceptibility and the functions of BRCA1 and BRCA2*. Cell, 2002. 108(2): p. 171-82.
  65. Ebstein, F., et al., *Proteasomes generate spliced epitopes by two different mechanisms and as efficiently as non-spliced epitopes*. Sci Rep, 2016. 6: p. 24032.
  66. Golub, T.R., et al., *Fusion of the TEL gene on 12p13 to the AML1 gene on 21q22 in acute lymphoblastic leukemia*. Proc Natl Acad Sci U S A, 1995. 92(11): p. 4917-21.
  67. Romana, S.P., et al., *The t(12;21) of acute lymphoblastic leukemia results in a tel-AML1 gene fusion*. Blood, 1995. 85(12): p. 3662-70.
  68. Rowley, J.D., *Letter: A new consistent chromosomal abnormality in chronic myelogenous leukaemia identified by quinacrine fluorescence and Giemsa staining*. Nature, 1973. 243(5405): p. 290-3.
  69. Freed-Pastor, W.A. and C. Prives, *Mutant p53: one name, many proteins*. Genes Dev, 2012. 26(12): p. 1268-86.
  70. Alexandrov, L.B., et al., *Signatures of mutational processes in human cancer*. Nature, 2013. 500(7463): p. 415-21.
-



71. Anderson, G., et al., *Cellular interactions in thymocyte development*. Annu Rev Immunol, 1996. 14: p. 73-99.
72. Wilson, I.A. and K.C. Garcia, *T-cell receptor structure and TCR complexes*. Curr Opin Struct Biol, 1997. 7(6): p. 839-48.
73. Al-Lazikani, B., A.M. Lesk, and C. Chothia, *Canonical structures for the hypervariable regions of T cell alphabeta receptors*. J Mol Biol, 2000. 295(4): p. 979-95.
74. Davis, M.M. and P.J. Bjorkman, *T-cell antigen receptor genes and T-cell recognition*. Nature, 1988. 334(6181): p. 395-402.
75. Chien, Y.H., et al., *Somatic recombination in a murine T-cell receptor gene*. Nature, 1984. 309(5966): p. 322-6.
76. Raulat, D.H., et al., *Developmental regulation of T-cell receptor gene expression*. Nature, 1985. 314(6006): p. 103-7.
77. Call, M.E., et al., *The organizing principle in the formation of the T cell receptor-CD3 complex*. Cell, 2002. 111(7): p. 967-79.
78. Huang, C.Y., B.P. Sleckman, and O. Kanagawa, *Revision of T cell receptor {alpha} chain genes is required for normal T lymphocyte development*. Proc Natl Acad Sci U S A, 2005. 102(40): p. 14356-61.
79. Garcia, K.C., L. Teyton, and I.A. Wilson, *Structural basis of T cell recognition*. Annu Rev Immunol, 1999. 17: p. 369-97.
80. McDuffie, M., et al., *The role of the T-cell receptor in thymocyte maturation: effects in vivo of anti-receptor antibody*. Proc Natl Acad Sci U S A, 1986. 83(22): p. 8728-32.
81. Kappler, J.W., N. Roehm, and P. Marrack, *T cell tolerance by clonal elimination in the thymus*. Cell, 1987. 49(2): p. 273-80.
82. Rowley, D.A. and F.W. Fitch, *The road to the discovery of dendritic cells, a tribute to Ralph Steinman*. Cell Immunol, 2012. 273(2): p. 95-8.
83. Friedl, P. and E.B. Brocker, *TCR triggering on the move: diversity of T-cell interactions with antigen-presenting cells*. Immunol Rev, 2002. 186: p. 83-9.
84. Bour-Jordan, H. and J.A. Blueston, *CD28 function: a balance of costimulatory and regulatory signals*. J Clin Immunol, 2002. 22(1): p. 1-7.
85. Russell, J.H. and T.J. Ley, *Lymphocyte-mediated cytotoxicity*. Annu Rev Immunol, 2002. 20: p. 323-70.
86. Weninger, W., N. Manjunath, and U.H. von Andrian, *Migration and differentiation of CD8+ T cells*. Immunol Rev, 2002. 186: p. 221-33.
87. O'Shea, J.J. and W.E. Paul, *Mechanisms underlying lineage commitment and plasticity of helper CD4+ T cells*. Science, 2010. 327(5969): p. 1098-102.
88. Schoenberger, S.P., et al., *T-cell help for cytotoxic T lymphocytes is mediated by CD40-CD40L interactions*. Nature, 1998. 393(6684): p. 480-3.

- 
89. Fazilleau, N., et al., *Follicular helper T cells: lineage and location*. *Immunity*, 2009. 30(3): p. 324-35.
  90. Bevan, M.J., *Cross-priming for a secondary cytotoxic response to minor H antigens with H-2 congenic cells which do not cross-react in the cytotoxic assay*. *J Exp Med*, 1976. 143(5): p. 1283-8.
  91. Steinman, R.M. and M.D. Witmer, *Lymphoid dendritic cells are potent stimulators of the primary mixed leukocyte reaction in mice*. *Proc Natl Acad Sci U S A*, 1978. 75(10): p. 5132-6.
  92. Huang, A.Y., et al., *Role of bone marrow-derived cells in presenting MHC class I-restricted tumor antigens*. *Science*, 1994. 264(5161): p. 961-5.
  93. Wolkers, M.C., et al., *Redundancy of direct priming and cross-priming in tumor-specific CD8+ T cell responses*. *J Immunol*, 2001. 167(7): p. 3577-84.
  94. van den Broek, M.F. and H. Hengartner, *The role of perforin in infections and tumour surveillance*. *Exp Physiol*, 2000. 85(6): p. 681-5.
  95. Barth, R.J., Jr., et al., *Interferon gamma and tumor necrosis factor have a role in tumor regressions mediated by murine CD8+ tumor-infiltrating lymphocytes*. *J Exp Med*, 1991. 173(3): p. 647-58.
  96. Zhang, B., et al., *IFN-gamma- and TNF-dependent bystander eradication of antigen-loss variants in established mouse cancers*. *J Clin Invest*, 2008. 118(4): p. 1398-404.
  97. Schuler, T. and T. Blankenstein, *Cutting edge: CD8+ effector T cells reject tumors by direct antigen recognition but indirect action on host cells*. *J Immunol*, 2003. 170(9): p. 4427-31.
  98. Kammertoens, T., et al., *Tumour ischaemia by interferon-gamma resembles physiological blood vessel regression*. *Nature*, 2017. 545(7652): p. 98-102.
  99. Qin, Z., et al., *A critical requirement of interferon gamma-mediated angiostasis for tumor rejection by CD8+ T cells*. *Cancer Res*, 2003. 63(14): p. 4095-100.
  100. Stoelcker, B., et al., *Tumor necrosis factor induces tumor necrosis via tumor necrosis factor receptor type 1-expressing endothelial cells of the tumor vasculature*. *Am J Pathol*, 2000. 156(4): p. 1171-6.
  101. Wu, T.H., et al., *Long-term suppression of tumor growth by TNF requires a Stat1- and IFN regulatory factor 1-dependent IFN-gamma pathway but not IL-12 or IL-18*. *J Immunol*, 2004. 172(5): p. 3243-51.
  102. Spiotto, M.T. and H. Schreiber, *Rapid destruction of the tumor microenvironment by CTLs recognizing cancer-specific antigens cross-presented by stromal cells*. *Cancer Immun*, 2005. 5: p. 8.
-

103. Cella, M., et al., *Ligation of CD40 on dendritic cells triggers production of high levels of interleukin-12 and enhances T cell stimulatory capacity: T-T help via APC activation*. J Exp Med, 1996. 184(2): p. 747-52.
104. Qin, Z. and T. Blankenstein, *CD4+ T cell--mediated tumor rejection involves inhibition of angiogenesis that is dependent on IFN gamma receptor expression by nonhematopoietic cells*. Immunity, 2000. 12(6): p. 677-86.
105. Schuler, T., S. Kornig, and T. Blankenstein, *Tumor rejection by modulation of tumor stromal fibroblasts*. J Exp Med, 2003. 198(10): p. 1487-93.
106. Volpert, O.V., et al., *Inhibition of angiogenesis by interleukin 4*. J Exp Med, 1998. 188(6): p. 1039-46.
107. Cohen, M.C. and S. Cohen, *Cytokine function: a study in biologic diversity*. Am J Clin Pathol, 1996. 105(5): p. 589-98.
108. Ardolino, M., J. Hsu, and D.H. Raulet, *Cytokine treatment in cancer immunotherapy*. Oncotarget, 2015. 6(23): p. 19346-7.
109. Goldstein, D. and J. Laszlo, *The role of interferon in cancer therapy: a current perspective*. CA Cancer J Clin, 1988. 38(5): p. 258-77.
110. Lee, S. and K. Margolin, *Cytokines in cancer immunotherapy*. Cancers (Basel), 2011. 3(4): p. 3856-93.
111. Rosenberg, S.A., et al., *Regression of established pulmonary metastases and subcutaneous tumor mediated by the systemic administration of high-dose recombinant interleukin 2*. J Exp Med, 1985. 161(5): p. 1169-88.
112. Lotze, M.T., et al., *High-dose recombinant interleukin 2 in the treatment of patients with disseminated cancer. Responses, treatment-related morbidity, and histologic findings*. JAMA, 1986. 256(22): p. 3117-24.
113. Rosenberg, S.A., *IL-2: the first effective immunotherapy for human cancer*. J Immunol, 2014. 192(12): p. 5451-8.
114. Atkins, M.B., et al., *High-dose recombinant interleukin 2 therapy for patients with metastatic melanoma: analysis of 270 patients treated between 1985 and 1993*. J Clin Oncol, 1999. 17(7): p. 2105-16.
115. Dutcher, J.P., et al., *High dose interleukin-2 (Aldesleukin) - expert consensus on best management practices-2014*. J Immunother Cancer, 2014. 2(1): p. 26.
116. Waldmann, T.A., *The biology of interleukin-2 and interleukin-15: implications for cancer therapy and vaccine design*. Nat Rev Immunol, 2006. 6(8): p. 595-601.
117. Klebanoff, C.A., et al., *IL-15 enhances the in vivo antitumor activity of tumor-reactive CD8+ T cells*. Proc Natl Acad Sci U S A, 2004. 101(7): p. 1969-74.

- 
118. Liu, R.B., et al., *IL-15 in tumor microenvironment causes rejection of large established tumors by T cells in a noncognate T cell receptor-dependent manner*. Proc Natl Acad Sci U S A, 2013. 110(20): p. 8158-63.
  119. Conlon, K.C., et al., *Redistribution, hyperproliferation, activation of natural killer cells and CD8 T cells, and cytokine production during first-in-human clinical trial of recombinant human interleukin-15 in patients with cancer*. J Clin Oncol, 2015. 33(1): p. 74-82.
  120. Miller, J.S., et al., *A First-in-Human Phase I Study of Subcutaneous Outpatient Recombinant Human IL15 (rhIL15) in Adults with Advanced Solid Tumors*. Clin Cancer Res, 2018. 24(7): p. 1525-1535.
  121. Lasek, W., R. Zagozdzon, and M. Jakobisiak, *Interleukin 12: still a promising candidate for tumor immunotherapy?* Cancer Immunol Immunother, 2014. 63(5): p. 419-35.
  122. Schmidt, H., et al., *Safety and clinical effect of subcutaneous human interleukin-21 in patients with metastatic melanoma or renal cell carcinoma: a phase I trial*. Clin Cancer Res, 2010. 16(21): p. 5312-9.
  123. Sportes, C., et al., *Phase I study of recombinant human interleukin-7 administration in subjects with refractory malignancy*. Clin Cancer Res, 2010. 16(2): p. 727-35.
  124. Aulitzky, W.E., et al., *Recombinant tumour necrosis factor alpha administered subcutaneously or intramuscularly for treatment of advanced malignant disease: a phase I trial*. Eur J Cancer, 1991. 27(4): p. 462-7.
  125. Fraker, D.L., et al., *Treatment of patients with melanoma of the extremity using hyperthermic isolated limb perfusion with melphalan, tumor necrosis factor, and interferon gamma: results of a tumor necrosis factor dose-escalation study*. J Clin Oncol, 1996. 14(2): p. 479-89.
  126. Roberts, N.J., et al., *Systemic use of tumor necrosis factor alpha as an anticancer agent*. Oncotarget, 2011. 2(10): p. 739-51.
  127. Huyghe, L., et al., *Safe eradication of large established tumors using neovasculature-targeted tumor necrosis factor-based therapies*. EMBO Mol Med, 2020. 12(2): p. e11223.
  128. Johansson, A., et al., *Tumor-targeted TNFalpha stabilizes tumor vessels and enhances active immunotherapy*. Proc Natl Acad Sci U S A, 2012. 109(20): p. 7841-6.
  129. Zou, W. and L. Chen, *Inhibitory B7-family molecules in the tumour microenvironment*. Nat Rev Immunol, 2008. 8(6): p. 467-77.
  130. Linsley, P.S., et al., *Human B7-1 (CD80) and B7-2 (CD86) bind with similar avidities but distinct kinetics to CD28 and CTLA-4 receptors*. Immunity, 1994. 1(9): p. 793-801.
  131. Riley, J.L., et al., *Modulation of TCR-induced transcriptional profiles by ligation of CD28, ICOS, and CTLA-4 receptors*. Proc Natl Acad Sci U S A, 2002. 99(18): p. 11790-5.
  132. Schneider, H., et al., *Reversal of the TCR stop signal by CTLA-4*. Science, 2006. 313(5795): p. 1972-5.
-

133. Wing, K., et al., *CTLA-4 control over Foxp3+ regulatory T cell function*. *Science*, 2008. 322(5899): p. 271-5.
134. Curiel, T.J., et al., *Specific recruitment of regulatory T cells in ovarian carcinoma fosters immune privilege and predicts reduced survival*. *Nat Med*, 2004. 10(9): p. 942-9.
135. Leach, D.R., M.F. Krummel, and J.P. Allison, *Enhancement of antitumor immunity by CTLA-4 blockade*. *Science*, 1996. 271(5256): p. 1734-6.
136. Beck, K.E., et al., *Enterocolitis in patients with cancer after antibody blockade of cytotoxic T-lymphocyte-associated antigen 4*. *J Clin Oncol*, 2006. 24(15): p. 2283-9.
137. Phan, G.Q., et al., *Cancer regression and autoimmunity induced by cytotoxic T lymphocyte-associated antigen 4 blockade in patients with metastatic melanoma*. *Proc Natl Acad Sci U S A*, 2003. 100(14): p. 8372-7.
138. Ribas, A., et al., *Antitumor activity in melanoma and anti-self responses in a phase I trial with the anti-cytotoxic T lymphocyte-associated antigen 4 monoclonal antibody CP-675,206*. *J Clin Oncol*, 2005. 23(35): p. 8968-77.
139. Bennett, F., et al., *Program death-1 engagement upon TCR activation has distinct effects on costimulation and cytokine-driven proliferation: attenuation of ICOS, IL-4, and IL-21, but not CD28, IL-7, and IL-15 responses*. *J Immunol*, 2003. 170(2): p. 711-8.
140. Brown, J.A., et al., *Blockade of programmed death-1 ligands on dendritic cells enhances T cell activation and cytokine production*. *J Immunol*, 2003. 170(3): p. 1257-66.
141. Keir, M.E., et al., *PD-1 and its ligands in tolerance and immunity*. *Annu Rev Immunol*, 2008. 26: p. 677-704.
142. Ahmadzadeh, M., et al., *Tumor antigen-specific CD8 T cells infiltrating the tumor express high levels of PD-1 and are functionally impaired*. *Blood*, 2009. 114(8): p. 1537-44.
143. Dong, H., et al., *Tumor-associated B7-H1 promotes T-cell apoptosis: a potential mechanism of immune evasion*. *Nat Med*, 2002. 8(8): p. 793-800.
144. Blank, C., et al., *PD-L1/B7H-1 inhibits the effector phase of tumor rejection by T cell receptor (TCR) transgenic CD8+ T cells*. *Cancer Res*, 2004. 64(3): p. 1140-5.
145. Iwai, Y., et al., *Involvement of PD-L1 on tumor cells in the escape from host immune system and tumor immunotherapy by PD-L1 blockade*. *Proc Natl Acad Sci U S A*, 2002. 99(19): p. 12293-7.
146. Larkin, J., F.S. Hodi, and J.D. Wolchok, *Combined Nivolumab and Ipilimumab or Monotherapy in Untreated Melanoma*. *N Engl J Med*, 2015. 373(13): p. 1270-1.
147. Ribas, A., et al., *Association of Pembrolizumab With Tumor Response and Survival Among Patients With Advanced Melanoma*. *JAMA*, 2016. 315(15): p. 1600-9.
148. Rizvi, N.A., et al., *Cancer immunology. Mutational landscape determines sensitivity to PD-1 blockade in non-small cell lung cancer*. *Science*, 2015. 348(6230): p. 124-8.

149. Snyder, A., et al., *Genetic basis for clinical response to CTLA-4 blockade in melanoma*. N Engl J Med, 2014. 371(23): p. 2189-2199.
150. Koyama, S., et al., *Adaptive resistance to therapeutic PD-1 blockade is associated with upregulation of alternative immune checkpoints*. Nat Commun, 2016. 7: p. 10501.
151. Maynard, J.E., *Passive immunization against hepatitis B: a review of recent studies and comment on current aspects of control*. Am J Epidemiol, 1978. 107(2): p. 77-86.
152. Yu, A.S., R.C. Cheung, and E.B. Keeffe, *Hepatitis B vaccines*. Infect Dis Clin North Am, 2006. 20(1): p. 27-45.
153. Frazer, I.H., *Prevention of cervical cancer through papillomavirus vaccination*. Nat Rev Immunol, 2004. 4(1): p. 46-54.
154. Harper, D.M., et al., *Sustained efficacy up to 4.5 years of a bivalent L1 virus-like particle vaccine against human papillomavirus types 16 and 18: follow-up from a randomised control trial*. Lancet, 2006. 367(9518): p. 1247-55.
155. Kirnbauer, R., et al., *Papillomavirus L1 major capsid protein self-assembles into virus-like particles that are highly immunogenic*. Proc Natl Acad Sci U S A, 1992. 89(24): p. 12180-4.
156. van Zyl, D.G., J. Mautner, and H.J. Delecluse, *Progress in EBV Vaccines*. Front Oncol, 2019. 9: p. 104.
157. Rosenberg, S.A., J.C. Yang, and N.P. Restifo, *Cancer immunotherapy: moving beyond current vaccines*. Nat Med, 2004. 10(9): p. 909-15.
158. Melero, I., et al., *Therapeutic vaccines for cancer: an overview of clinical trials*. Nat Rev Clin Oncol, 2014. 11(9): p. 509-24.
159. Tarhini, A.A., et al., *Safety and immunogenicity of vaccination with MART-1 (26-35, 27L), gp100 (209-217, 210M), and tyrosinase (368-376, 370D) in adjuvant with PF-3512676 and GM-CSF in metastatic melanoma*. J Immunother, 2012. 35(4): p. 359-66.
160. Kantoff, P.W., et al., *Sipuleucel-T immunotherapy for castration-resistant prostate cancer*. N Engl J Med, 2010. 363(5): p. 411-22.
161. Kreiter, S., et al., *Mutant MHC class II epitopes drive therapeutic immune responses to cancer*. Nature, 2015. 520(7549): p. 692-6.
162. Hundal, J., et al., *pVAC-Seq: A genome-guided in silico approach to identifying tumor neoantigens*. Genome Med, 2016. 8(1): p. 11.
163. Lundegaard, C., et al., *NetMHC-3.0: accurate web accessible predictions of human, mouse and monkey MHC class I affinities for peptides of length 8-11*. Nucleic Acids Res, 2008. 36(Web Server issue): p. W509-12.
164. Carreno, B.M., et al., *Cancer immunotherapy. A dendritic cell vaccine increases the breadth and diversity of melanoma neoantigen-specific T cells*. Science, 2015. 348(6236): p. 803-8.

- 
165. Cafri, G., et al., *mRNA vaccine-induced neoantigen-specific T cell immunity in patients with gastrointestinal cancer*. J Clin Invest, 2020. 130(11): p. 5976-5988.
  166. Ott, P.A., et al., *An immunogenic personal neoantigen vaccine for patients with melanoma*. Nature, 2017. 547(7662): p. 217-221.
  167. Sahin, U., et al., *Personalized RNA mutanome vaccines mobilize poly-specific therapeutic immunity against cancer*. Nature, 2017. 547(7662): p. 222-226.
  168. Fefer, A., *Immunotherapy and chemotherapy of Moloney sarcoma virus-induced tumors in mice*. Cancer Res, 1969. 29(12): p. 2177-83.
  169. Dudley, M.E., et al., *Generation of tumor-infiltrating lymphocyte cultures for use in adoptive transfer therapy for melanoma patients*. J Immunother, 2003. 26(4): p. 332-42.
  170. Rosenberg, S.A., P. Spiess, and R. Lafreniere, *A new approach to the adoptive immunotherapy of cancer with tumor-infiltrating lymphocytes*. Science, 1986. 233(4770): p. 1318-21.
  171. Dudley, M.E., et al., *Adoptive cell therapy for patients with metastatic melanoma: evaluation of intensive myeloablative chemoradiation preparative regimens*. J Clin Oncol, 2008. 26(32): p. 5233-9.
  172. Rosenberg, S.A., et al., *Durable complete responses in heavily pretreated patients with metastatic melanoma using T-cell transfer immunotherapy*. Clin Cancer Res, 2011. 17(13): p. 4550-7.
  173. Klebanoff, C.A., et al., *Sinks, suppressors and antigen presenters: how lymphodepletion enhances T cell-mediated tumor immunotherapy*. Trends Immunol, 2005. 26(2): p. 111-7.
  174. Goff, S.L., et al., *Tumor infiltrating lymphocyte therapy for metastatic melanoma: analysis of tumors resected for TIL*. J Immunother, 2010. 33(8): p. 840-7.
  175. Rohaan, M.W., et al., *Adoptive transfer of tumor-infiltrating lymphocytes in melanoma: a viable treatment option*. J Immunother Cancer, 2018. 6(1): p. 102.
  176. Yang, J.C., *Toxicities Associated With Adoptive T-Cell Transfer for Cancer*. Cancer J, 2015. 21(6): p. 506-9.
  177. Hall, M., et al., *Expansion of tumor-infiltrating lymphocytes (TIL) from human pancreatic tumors*. J Immunother Cancer, 2016. 4: p. 61.
  178. Nielsen, M., et al., *In vitro 4-1BB stimulation promotes expansion of CD8(+) tumor-infiltrating lymphocytes from various sarcoma subtypes*. Cancer Immunol Immunother, 2020. 69(11): p. 2179-2191.
  179. Schietinger, A., et al., *Tumor-Specific T Cell Dysfunction Is a Dynamic Antigen-Driven Differentiation Program Initiated Early during Tumorigenesis*. Immunity, 2016. 45(2): p. 389-401.
-

- 
180. Philip, M., et al., *Chromatin states define tumour-specific T cell dysfunction and reprogramming*. Nature, 2017. 545(7655): p. 452-456.
  181. Andersen, R.S., et al., *Dissection of T-cell antigen specificity in human melanoma*. Cancer Res, 2012. 72(7): p. 1642-50.
  182. Frosig, T.M., et al., *Broadening the repertoire of melanoma-associated T-cell epitopes*. Cancer Immunol Immunother, 2015. 64(5): p. 609-20.
  183. Linnemann, C., et al., *High-throughput epitope discovery reveals frequent recognition of neo-antigens by CD4+ T cells in human melanoma*. Nat Med, 2015. 21(1): p. 81-5.
  184. Robbins, P.F., et al., *Mining exomic sequencing data to identify mutated antigens recognized by adoptively transferred tumor-reactive T cells*. Nat Med, 2013. 19(6): p. 747-52.
  185. van Rooij, N., et al., *Tumor exome analysis reveals neoantigen-specific T-cell reactivity in an ipilimumab-responsive melanoma*. J Clin Oncol, 2013. 31(32): p. e439-42.
  186. Gross, G., T. Waks, and Z. Eshhar, *Expression of immunoglobulin-T-cell receptor chimeric molecules as functional receptors with antibody-type specificity*. Proc Natl Acad Sci U S A, 1989. 86(24): p. 10024-8.
  187. June, C.H., et al., *CAR T cell immunotherapy for human cancer*. Science, 2018. 359(6382): p. 1361-1365.
  188. Kuwana, Y., et al., *Expression of chimeric receptor composed of immunoglobulin-derived V regions and T-cell receptor-derived C regions*. Biochem Biophys Res Commun, 1987. 149(3): p. 960-8.
  189. Eshhar, Z., et al., *Specific activation and targeting of cytotoxic lymphocytes through chimeric single chains consisting of antibody-binding domains and the gamma or zeta subunits of the immunoglobulin and T-cell receptors*. Proc Natl Acad Sci U S A, 1993. 90(2): p. 720-4.
  190. Hombach, A., et al., *Tumor-specific T cell activation by recombinant immunoreceptors: CD3 zeta signaling and CD28 costimulation are simultaneously required for efficient IL-2 secretion and can be integrated into one combined CD28/CD3 zeta signaling receptor molecule*. J Immunol, 2001. 167(11): p. 6123-31.
  191. Imai, C., et al., *Chimeric receptors with 4-1BB signaling capacity provoke potent cytotoxicity against acute lymphoblastic leukemia*. Leukemia, 2004. 18(4): p. 676-84.
  192. Maher, J., et al., *Human T-lymphocyte cytotoxicity and proliferation directed by a single chimeric TCRzeta /CD28 receptor*. Nat Biotechnol, 2002. 20(1): p. 70-5.
  193. Avanzi, M.P., et al., *Engineered Tumor-Targeted T Cells Mediate Enhanced Anti-Tumor Efficacy Both Directly and through Activation of the Endogenous Immune System*. Cell Rep, 2018. 23(7): p. 2130-2141.
-



- 
194. Chmielewski, M. and H. Abken, *TRUCKs: the fourth generation of CARs*. *Expert Opin Biol Ther*, 2015. 15(8): p. 1145-54.
  195. Hu, B., et al., *Augmentation of Antitumor Immunity by Human and Mouse CAR T Cells Secreting IL-18*. *Cell Rep*, 2017. 20(13): p. 3025-3033.
  196. Chavez, J.C., C. Bachmeier, and M.A. Kharfan-Dabaja, *CAR T-cell therapy for B-cell lymphomas: clinical trial results of available products*. *Ther Adv Hematol*, 2019. 10: p. 2040620719841581.
  197. Lee, D.W., et al., *T cells expressing CD19 chimeric antigen receptors for acute lymphoblastic leukaemia in children and young adults: a phase 1 dose-escalation trial*. *Lancet*, 2015. 385(9967): p. 517-528.
  198. Maude, S.L., et al., *Tisagenlecleucel in Children and Young Adults with B-Cell Lymphoblastic Leukemia*. *N Engl J Med*, 2018. 378(5): p. 439-448.
  199. Cho, S.F., K.C. Anderson, and Y.T. Tai, *Targeting B Cell Maturation Antigen (BCMA) in Multiple Myeloma: Potential Uses of BCMA-Based Immunotherapy*. *Front Immunol*, 2018. 9: p. 1821.
  200. Friedman, K.M., et al., *Effective Targeting of Multiple B-Cell Maturation Antigen-Expressing Hematological Malignancies by Anti-B-Cell Maturation Antigen Chimeric Antigen Receptor T Cells*. *Hum Gene Ther*, 2018. 29(5): p. 585-601.
  201. Fry, T.J., et al., *CD22-targeted CAR T cells induce remission in B-ALL that is naive or resistant to CD19-targeted CAR immunotherapy*. *Nat Med*, 2018. 24(1): p. 20-28.
  202. Ahmed, N., et al., *Human Epidermal Growth Factor Receptor 2 (HER2) -Specific Chimeric Antigen Receptor-Modified T Cells for the Immunotherapy of HER2-Positive Sarcoma*. *J Clin Oncol*, 2015. 33(15): p. 1688-96.
  203. Caruso, H.G., et al., *Tuning Sensitivity of CAR to EGFR Density Limits Recognition of Normal Tissue While Maintaining Potent Antitumor Activity*. *Cancer Res*, 2015. 75(17): p. 3505-18.
  204. Lamers, C.H., et al., *Treatment of metastatic renal cell carcinoma with CAIX CAR-engineered T cells: clinical evaluation and management of on-target toxicity*. *Mol Ther*, 2013. 21(4): p. 904-12.
  205. Textor, A., et al., *Efficacy of CAR T-cell therapy in large tumors relies upon stromal targeting by IFN $\gamma$* . *Cancer Res*, 2014. 74(23): p. 6796-805.
  206. Baum, C., et al., *Retrovirus vectors: toward the lentivirus?* *Mol Ther*, 2006. 13(6): p. 1050-63.
  207. Schambach, A. and C. Baum, *Clinical application of lentiviral vectors - concepts and practice*. *Curr Gene Ther*, 2008. 8(6): p. 474-82.
-

- 
208. Mizuguchi, H., et al., *IRES-dependent second gene expression is significantly lower than cap-dependent first gene expression in a bicistronic vector*. Mol Ther, 2000. 1(4): p. 376-82.
209. de Felipe, P., et al., *Use of the 2A sequence from foot-and-mouth disease virus in the generation of retroviral vectors for gene therapy*. Gene Ther, 1999. 6(2): p. 198-208.
210. Leisegang, M., et al., *Enhanced functionality of T cell receptor-redirectioned T cells is defined by the transgene cassette*. J Mol Med (Berl), 2008. 86(5): p. 573-83.
211. Szymczak, A.L., et al., *Correction of multi-gene deficiency in vivo using a single 'self-cleaving' 2A peptide-based retroviral vector*. Nat Biotechnol, 2004. 22(5): p. 589-94.
212. Morgan, R.A., et al., *Cancer regression in patients after transfer of genetically engineered lymphocytes*. Science, 2006. 314(5796): p. 126-9.
213. Robbins, P.F., et al., *A pilot trial using lymphocytes genetically engineered with an NY-ESO-1-reactive T-cell receptor: long-term follow-up and correlates with response*. Clin Cancer Res, 2015. 21(5): p. 1019-27.
214. Robbins, P.F., et al., *Tumor regression in patients with metastatic synovial cell sarcoma and melanoma using genetically engineered lymphocytes reactive with NY-ESO-1*. J Clin Oncol, 2011. 29(7): p. 917-24.
215. Johnson, L.A., et al., *Gene therapy with human and mouse T-cell receptors mediates cancer regression and targets normal tissues expressing cognate antigen*. Blood, 2009. 114(3): p. 535-46.
216. Parkhurst, M.R., et al., *T cells targeting carcinoembryonic antigen can mediate regression of metastatic colorectal cancer but induce severe transient colitis*. Mol Ther, 2011. 19(3): p. 620-6.
217. Hinrichs, C.S. and N.P. Restifo, *Reassessing target antigens for adoptive T-cell therapy*. Nat Biotechnol, 2013. 31(11): p. 999-1008.
218. Coulie, P.G., et al., *A mutated intron sequence codes for an antigenic peptide recognized by cytolytic T lymphocytes on a human melanoma*. Proc Natl Acad Sci U S A, 1995. 92(17): p. 7976-80.
219. Robbins, P.F., et al., *A mutated beta-catenin gene encodes a melanoma-specific antigen recognized by tumor infiltrating lymphocytes*. J Exp Med, 1996. 183(3): p. 1185-92.
220. Wolfel, T., et al., *A p16INK4a-insensitive CDK4 mutant targeted by cytolytic T lymphocytes in a human melanoma*. Science, 1995. 269(5228): p. 1281-4.
221. Zacharakis, N., et al., *Immune recognition of somatic mutations leading to complete durable regression in metastatic breast cancer*. Nat Med, 2018. 24(6): p. 724-730.
222. Tran, E., P.F. Robbins, and S.A. Rosenberg, *'Final common pathway' of human cancer immunotherapy: targeting random somatic mutations*. Nat Immunol, 2017. 18(3): p. 255-262.
-

- 
223. Leisegang, M., et al., *Eradication of Large Solid Tumors by Gene Therapy with a T-Cell Receptor Targeting a Single Cancer-Specific Point Mutation*. Clin Cancer Res, 2016. 22(11): p. 2734-43.
224. Leisegang, M., et al., *Targeting human melanoma neoantigens by T cell receptor gene therapy*. J Clin Invest, 2016. 126(3): p. 854-8.
225. Turtle, C.J. and S.R. Riddell, *Artificial antigen-presenting cells for use in adoptive immunotherapy*. Cancer J, 2010. 16(4): p. 374-81.
226. Popovic, J., et al., *The only proposed T-cell epitope derived from the TEL-AML1 translocation is not naturally processed*. Blood, 2011. 118(4): p. 946-54.
227. Cao, K., et al., *Analysis of the frequencies of HLA-A, B, and C alleles and haplotypes in the five major ethnic groups of the United States reveals high levels of diversity in these loci and contrasting distribution patterns in these populations*. Hum Immunol, 2001. 62(9): p. 1009-30.
228. Malekzadeh, P., et al., *Antigen Experienced T Cells from Peripheral Blood Recognize p53 Neoantigens*. Clin Cancer Res, 2020. 26(6): p. 1267-1276.
229. Tran, E., et al., *T-Cell Transfer Therapy Targeting Mutant KRAS in Cancer*. N Engl J Med, 2016. 375(23): p. 2255-2262.
230. Sette, A., et al., *Peptide binding to the most frequent HLA-A class I alleles measured by quantitative molecular binding assays*. Mol Immunol, 1994. 31(11): p. 813-22.
231. Kyewski, B. and L. Klein, *A central role for central tolerance*. Annu Rev Immunol, 2006. 24: p. 571-606.
232. Andreatta, M. and M. Nielsen, *Gapped sequence alignment using artificial neural networks: application to the MHC class I system*. Bioinformatics, 2016. 32(4): p. 511-7.
233. Nielsen, M., et al., *Reliable prediction of T-cell epitopes using neural networks with novel sequence representations*. Protein Sci, 2003. 12(5): p. 1007-17.
234. Engels, B., et al., *Relapse or eradication of cancer is predicted by peptide-major histocompatibility complex affinity*. Cancer Cell, 2013. 23(4): p. 516-26.
235. Kammertoens, T. and T. Blankenstein, *It's the peptide-MHC affinity, stupid*. Cancer Cell, 2013. 23(4): p. 429-31.
236. Shultz, L.D., F. Ishikawa, and D.L. Greiner, *Humanized mice in translational biomedical research*. Nat Rev Immunol, 2007. 7(2): p. 118-30.
237. Zah, E., et al., *T Cells Expressing CD19/CD20 Bispecific Chimeric Antigen Receptors Prevent Antigen Escape by Malignant B Cells*. Cancer Immunol Res, 2016. 4(6): p. 498-508.
238. Cassidy, J.W., C. Caldas, and A. Bruna, *Maintaining Tumor Heterogeneity in Patient-Derived Tumor Xenografts*. Cancer Res, 2015. 75(15): p. 2963-8.
-

- 
239. Tentler, J.J., et al., *Patient-derived tumour xenografts as models for oncology drug development*. Nat Rev Clin Oncol, 2012. 9(6): p. 338-50.
240. Lai, Y., et al., *Current status and perspectives of patient-derived xenograft models in cancer research*. J Hematol Oncol, 2017. 10(1): p. 106.
241. Byrne, A.T., et al., *Interrogating open issues in cancer precision medicine with patient-derived xenografts*. Nat Rev Cancer, 2017. 17(4): p. 254-268.
242. Ngiow, S.F., et al., *Mouse Models of Tumor Immunotherapy*. Adv Immunol, 2016. 130: p. 1-24.
243. DuPage, M. and T. Jacks, *Genetically engineered mouse models of cancer reveal new insights about the antitumor immune response*. Curr Opin Immunol, 2013. 25(2): p. 192-9.
244. Fisher, G.H., et al., *Induction and apoptotic regression of lung adenocarcinomas by regulation of a K-Ras transgene in the presence and absence of tumor suppressor genes*. Genes Dev, 2001. 15(24): p. 3249-62.
245. Greenberg, N.M., et al., *Prostate cancer in a transgenic mouse*. Proc Natl Acad Sci U S A, 1995. 92(8): p. 3439-43.
246. Johnson, L., et al., *Somatic activation of the K-ras oncogene causes early onset lung cancer in mice*. Nature, 2001. 410(6832): p. 1111-6.
247. Pascolo, S., et al., *HLA-A2.1-restricted education and cytolytic activity of CD8(+) T lymphocytes from beta2 microglobulin (beta2m) HLA-A2.1 monochain transgenic H-2Db beta2m double knockout mice*. J Exp Med, 1997. 185(12): p. 2043-51.
248. Alexander, J., et al., *Derivation of HLA-B\*0702 transgenic mice: functional CTL repertoire and recognition of human B\*0702-restricted CTL epitopes*. Hum Immunol, 2003. 64(2): p. 211-23.
249. Yatsuda, J., et al., *Establishment of HLA-DR4 transgenic mice for the identification of CD4+ T cell epitopes of tumor-associated antigens*. PLoS One, 2013. 8(12): p. e84908.
250. Obenaus, M., et al., *Identification of human T-cell receptors with optimal affinity to cancer antigens using antigen-negative humanized mice*. Nat Biotechnol, 2015. 33(4): p. 402-7.
251. Briles, E.B. and S. Kornfeld, *Isolation and metastatic properties of detachment variants of B16 melanoma cells*. J Natl Cancer Inst, 1978. 60(6): p. 1217-22.
252. Ward, P.L., et al., *Tumor antigens defined by cloned immunological probes are highly polymorphic and are not detected on autologous normal cells*. J Exp Med, 1989. 170(1): p. 217-32.
253. Brochet, X., M.P. Lefranc, and V. Giudicelli, *IMGT/V-QUEST: the highly customized and integrated system for IG and TR standardized V-J and V-D-J sequence analysis*. Nucleic Acids Res, 2008. 36(Web Server issue): p. W503-8.
-

- 
254. Giudicelli, V., X. Brochet, and M.P. Lefranc, *IMGT/V-QUEST: IMGT standardized analysis of the immunoglobulin (IG) and T cell receptor (TR) nucleotide sequences*. Cold Spring Harb Protoc, 2011. 2011(6): p. 695-715.
  255. Ran, F.A., et al., *Genome engineering using the CRISPR-Cas9 system*. Nat Protoc, 2013. 8(11): p. 2281-2308.
  256. Paquet, D., et al., *Efficient introduction of specific homozygous and heterozygous mutations using CRISPR/Cas9*. Nature, 2016. 533(7601): p. 125-9.
  257. Christman, J.K., *5-Azacytidine and 5-aza-2'-deoxycytidine as inhibitors of DNA methylation: mechanistic studies and their implications for cancer therapy*. Oncogene, 2002. 21(35): p. 5483-95.
  258. Tran, E., et al., *Immunogenicity of somatic mutations in human gastrointestinal cancers*. Science, 2015. 350(6266): p. 1387-90.
  259. Tran, E., et al., *Cancer immunotherapy based on mutation-specific CD4+ T cells in a patient with epithelial cancer*. Science, 2014. 344(6184): p. 641-5.
  260. Velders, M.P., et al., *Defined flanking spacers and enhanced proteolysis is essential for eradication of established tumors by an epitope string DNA vaccine*. J Immunol, 2001. 166(9): p. 5366-73.
  261. Textor, A., et al., *Preventing tumor escape by targeting a post-proteasomal trimming independent epitope*. J Exp Med, 2016. 213(11): p. 2333-2348.
  262. Pircher, H., et al., *Viral escape by selection of cytotoxic T cell-resistant virus variants in vivo*. Nature, 1990. 346(6285): p. 629-33.
  263. Clarke, S.R., et al., *Characterization of the ovalbumin-specific TCR transgenic line OT-I: MHC elements for positive and negative selection*. Immunol Cell Biol, 2000. 78(2): p. 110-7.
  264. Ralph, P., *Retention of lymphocyte characteristics by myelomas and theta + - lymphomas: sensitivity to cortisol and phytohemagglutinin*. J Immunol, 1973. 110(6): p. 1470-5.
  265. Bosga-Bouwer, A.G., et al., *Molecular, cytogenetic, and immunophenotypic characterization of follicular lymphoma grade 3B; a separate entity or part of the spectrum of diffuse large B-cell lymphoma or follicular lymphoma?* Hum Pathol, 2006. 37(5): p. 528-33.
  266. Chomchai, J.S., et al., *Prognostic significance of p53 gene mutations in laryngeal cancer*. Laryngoscope, 1999. 109(3): p. 455-9.
  267. Sarkar, F.H., et al., *Tumor suppressor p53 gene mutation in squamous cell carcinoma of the larynx*. Diagn Mol Pathol, 1996. 5(3): p. 201-5.
  268. Donehower, L.A., et al., *Integrated Analysis of TP53 Gene and Pathway Alterations in The Cancer Genome Atlas*. Cell Rep, 2019. 28(5): p. 1370-1384 e5.
-

- 
269. McFadden, D.G., et al., *Mutational landscape of EGFR-, MYC-, and Kras-driven genetically engineered mouse models of lung adenocarcinoma*. Proc Natl Acad Sci U S A, 2016. 113(42): p. E6409-E6417.
270. Yuan, R., et al., *Aging in inbred strains of mice: study design and interim report on median lifespans and circulating IGF1 levels*. Aging Cell, 2009. 8(3): p. 277-87.
271. Schreiber, K., et al., *Cancer immunotherapy and preclinical studies: why we are not wasting our time with animal experiments*. Hematol Oncol Clin North Am, 2006. 20(3): p. 567-84.
272. Pope, J.H., M.K. Horne, and W. Scott, *Transformation of foetal human leukocytes in vitro by filtrates of a human leukaemic cell line containing herpes-like virus*. Int J Cancer, 1968. 3(6): p. 857-66.
273. Sugimoto, M., et al., *Steps involved in immortalization and tumorigenesis in human B-lymphoblastoid cell lines transformed by Epstein-Barr virus*. Cancer Res, 2004. 64(10): p. 3361-4.
274. Counter, C.M., et al., *Stabilization of short telomeres and telomerase activity accompany immortalization of Epstein-Barr virus-transformed human B lymphocytes*. J Virol, 1994. 68(5): p. 3410-4.
275. Wiesner, M., et al., *Conditional immortalization of human B cells by CD40 ligation*. PLoS One, 2008. 3(1): p. e1464.
276. Garcia-Marquez, M.A., et al., *A multimerized form of recombinant human CD40 ligand supports long-term activation and proliferation of B cells*. Cytotherapy, 2014. 16(11): p. 1537-1544.
277. Wennhold, K., et al., *CD40-activated B cells induce anti-tumor immunity in vivo*. Oncotarget, 2017. 8(17): p. 27740-27753.
278. Lapointe, R., et al., *CD40-stimulated B lymphocytes pulsed with tumor antigens are effective antigen-presenting cells that can generate specific T cells*. Cancer Res, 2003. 63(11): p. 2836-43.
279. Philip, M. and A. Schietinger, *Heterogeneity and fate choice: T cell exhaustion in cancer and chronic infections*. Curr Opin Immunol, 2019. 58: p. 98-103.
280. Schietinger, A. and P.D. Greenberg, *Tolerance and exhaustion: defining mechanisms of T cell dysfunction*. Trends Immunol, 2014. 35(2): p. 51-60.
281. Wang, C., M. Singer, and A.C. Anderson, *Molecular Dissection of CD8(+) T-Cell Dysfunction*. Trends Immunol, 2017. 38(8): p. 567-576.
282. Zhang, Z., et al., *T Cell Dysfunction and Exhaustion in Cancer*. Front Cell Dev Biol, 2020. 8: p. 17.
283. Korkolopoulou, P., et al., *Loss of antigen-presenting molecules (MHC class I and TAP-1) in lung cancer*. Br J Cancer, 1996. 73(2): p. 148-53.
-

- 
284. Aptsiauri, N., F. Ruiz-Cabello, and F. Garrido, *The transition from HLA-I positive to HLA-I negative primary tumors: the road to escape from T-cell responses*. *Curr Opin Immunol*, 2018. 51: p. 123-132.
  285. Kondo, Y. and J.P. Issa, *Epigenetic changes in colorectal cancer*. *Cancer Metastasis Rev*, 2004. 23(1-2): p. 29-39.
  286. Lipkin, G., *Plasticity of the cancer cell: implications for epigenetic control of melanoma and other malignancies*. *J Invest Dermatol*, 2008. 128(9): p. 2152-5.
  287. Walker, B.A., et al., *Aberrant global methylation patterns affect the molecular pathogenesis and prognosis of multiple myeloma*. *Blood*, 2011. 117(2): p. 553-62.
  288. Sun, C., et al., *Reversible and adaptive resistance to BRAF(V600E) inhibition in melanoma*. *Nature*, 2014. 508(7494): p. 118-22.
  289. Bai, X.F., et al., *Different lineages of P1A-expressing cancer cells use divergent modes of immune evasion for T-cell adoptive therapy*. *Cancer Res*, 2006. 66(16): p. 8241-9.
  290. Davoli, T., et al., *Tumor aneuploidy correlates with markers of immune evasion and with reduced response to immunotherapy*. *Science*, 2017. 355(6322).
  291. Greaves, M. and C.C. Maley, *Clonal evolution in cancer*. *Nature*, 2012. 481(7381): p. 306-13.
  292. Swanton, C., *Intratumor heterogeneity: evolution through space and time*. *Cancer Res*, 2012. 72(19): p. 4875-82.
  293. Appella, E. and C.W. Anderson, *Post-translational modifications and activation of p53 by genotoxic stresses*. *Eur J Biochem*, 2001. 268(10): p. 2764-72.
  294. el-Deiry, W.S., et al., *Definition of a consensus binding site for p53*. *Nat Genet*, 1992. 1(1): p. 45-9.
  295. Brugarolas, J., et al., *Radiation-induced cell cycle arrest compromised by p21 deficiency*. *Nature*, 1995. 377(6549): p. 552-7.
  296. Harper, J.W., et al., *The p21 Cdk-interacting protein Cip1 is a potent inhibitor of G1 cyclin-dependent kinases*. *Cell*, 1993. 75(4): p. 805-16.
  297. Kastan, M.B., et al., *A mammalian cell cycle checkpoint pathway utilizing p53 and GADD45 is defective in ataxia-telangiectasia*. *Cell*, 1992. 71(4): p. 587-97.
  298. Joerger, A.C. and A.R. Fersht, *Structural biology of the tumor suppressor p53*. *Annu Rev Biochem*, 2008. 77: p. 557-82.
  299. Bullock, A.N., J. Henckel, and A.R. Fersht, *Quantitative analysis of residual folding and DNA binding in mutant p53 core domain: definition of mutant states for rescue in cancer therapy*. *Oncogene*, 2000. 19(10): p. 1245-56.
  300. Joerger, A.C. and A.R. Fersht, *Structure-function-rescue: the diverse nature of common p53 cancer mutants*. *Oncogene*, 2007. 26(15): p. 2226-42.
-

- 
301. Muller, P.A., et al., *Mutant p53 enhances MET trafficking and signalling to drive cell scattering and invasion*. *Oncogene*, 2013. 32(10): p. 1252-65.
  302. Pfister, N.T., et al., *Mutant p53 cooperates with the SWI/SNF chromatin remodeling complex to regulate VEGFR2 in breast cancer cells*. *Genes Dev*, 2015. 29(12): p. 1298-315.
  303. Weissmueller, S., et al., *Mutant p53 drives pancreatic cancer metastasis through cell-autonomous PDGF receptor beta signaling*. *Cell*, 2014. 157(2): p. 382-394.
  304. Liu, G., et al., *Chromosome stability, in the absence of apoptosis, is critical for suppression of tumorigenesis in Trp53 mutant mice*. *Nat Genet*, 2004. 36(1): p. 63-8.
  305. Alexandrova, E.M., et al., *p53 loss-of-heterozygosity is a necessary prerequisite for mutant p53 stabilization and gain-of-function in vivo*. *Cell Death Dis*, 2017. 8(3): p. e2661.
  306. Boettcher, S., et al., *A dominant-negative effect drives selection of TP53 missense mutations in myeloid malignancies*. *Science*, 2019. 365(6453): p. 599-604.
  307. Willis, A., et al., *Mutant p53 exerts a dominant negative effect by preventing wild-type p53 from binding to the promoter of its target genes*. *Oncogene*, 2004. 23(13): p. 2330-8.
  308. Chan, W.M., et al., *How many mutant p53 molecules are needed to inactivate a tetramer?* *Mol Cell Biol*, 2004. 24(8): p. 3536-51.
  309. Ryan, K.M. and K.H. Vousden, *Characterization of structural p53 mutants which show selective defects in apoptosis but not cell cycle arrest*. *Mol Cell Biol*, 1998. 18(7): p. 3692-8.
  310. Leroy, B., et al., *Analysis of TP53 mutation status in human cancer cell lines: a reassessment*. *Hum Mutat*, 2014. 35(6): p. 756-65.
  311. Walerych, D., et al., *Wild-type p53 oligomerizes more efficiently than p53 hot-spot mutants and overcomes mutant p53 gain-of-function via a "dominant-positive" mechanism*. *Oncotarget*, 2018. 9(62): p. 32063-32080.
  312. Fischer, M., *Mice Are Not Humans: The Case of p53*. *Trends Cancer*, 2021. 7(1): p. 12-14.
  313. Fischer, M., *Conservation and divergence of the p53 gene regulatory network between mice and humans*. *Oncogene*, 2019. 38(21): p. 4095-4109.
  314. Hainaut, P. and M. Hollstein, *p53 and human cancer: the first ten thousand mutations*. *Adv Cancer Res*, 2000. 77: p. 81-137.
  315. Seung, L.P., et al., *Synergy between T-cell immunity and inhibition of paracrine stimulation causes tumor rejection*. *Proc Natl Acad Sci U S A*, 1995. 92(14): p. 6254-8.
  316. Binnewies, M., et al., *Understanding the tumor immune microenvironment (TIME) for effective therapy*. *Nat Med*, 2018. 24(5): p. 541-550.
-



- 
317. Kammertoens, T., T. Schuler, and T. Blankenstein, *Immunotherapy: target the stroma to hit the tumor*. Trends Mol Med, 2005. 11(5): p. 225-31.
318. Schietinger, A., et al., *Bystander killing of cancer requires the cooperation of CD4(+) and CD8(+) T cells during the effector phase*. J Exp Med, 2010. 207(11): p. 2469-77.
319. Mumberg, D., et al., *CD4(+) T cells eliminate MHC class II-negative cancer cells in vivo by indirect effects of IFN-gamma*. Proc Natl Acad Sci U S A, 1999. 96(15): p. 8633-8.
320. Yossef, R., et al., *Enhanced detection of neoantigen-reactive T cells targeting unique and shared oncogenes for personalized cancer immunotherapy*. JCI Insight, 2018. 3(19).
321. Leko, V., et al., *Identification of Neoantigen-Reactive Tumor-Infiltrating Lymphocytes in Primary Bladder Cancer*. J Immunol, 2019. 202(12): p. 3458-3467.
322. Veatch, J.R., et al., *Tumor-infiltrating BRAFV600E-specific CD4+ T cells correlated with complete clinical response in melanoma*. J Clin Invest, 2018. 128(4): p. 1563-1568.
323. Stalder, T., S. Hahn, and P. Erb, *Fas antigen is the major target molecule for CD4+ T cell-mediated cytotoxicity*. J Immunol, 1994. 152(3): p. 1127-33.
324. Bennett, E.P., et al., *Control of mucin-type O-glycosylation: a classification of the polypeptide GalNAc-transferase gene family*. Glycobiology, 2012. 22(6): p. 736-56.
325. Ju, T., R.D. Cummings, and W.M. Canfield, *Purification, characterization, and subunit structure of rat core 1 Beta1,3-galactosyltransferase*. J Biol Chem, 2002. 277(1): p. 169-77.
326. Ju, T., et al., *Human tumor antigens Tn and sialyl Tn arise from mutations in Cosmc*. Cancer Res, 2008. 68(6): p. 1636-46.
327. Springer, G.F., *T and Tn, general carcinoma autoantigens*. Science, 1984. 224(4654): p. 1198-206.
328. Schietinger, A., et al., *A mutant chaperone converts a wild-type protein into a tumor-specific antigen*. Science, 2006. 314(5797): p. 304-8.
329. He, Y., et al., *Multiple cancer-specific antigens are targeted by a chimeric antigen receptor on a single cancer cell*. JCI Insight, 2019. 4(21).
330. Chmielewski, M., A.A. Hombach, and H. Abken, *CD28 cosignaling does not affect the activation threshold in a chimeric antigen receptor-redirectioned T-cell attack*. Gene Ther, 2011. 18(1): p. 62-72.
331. Song, D.G., et al., *In vivo persistence, tumor localization, and antitumor activity of CAR-engineered T cells is enhanced by costimulatory signaling through CD137 (4-1BB)*. Cancer Res, 2011. 71(13): p. 4617-27.
332. Zhao, Z., et al., *Structural Design of Engineered Costimulation Determines Tumor Rejection Kinetics and Persistence of CAR T Cells*. Cancer Cell, 2015. 28(4): p. 415-428.
-

- 
333. Drent, E., et al., *Combined CD28 and 4-1BB Costimulation Potentiates Affinity-tuned Chimeric Antigen Receptor-engineered T Cells*. Clin Cancer Res, 2019. 25(13): p. 4014-4025.
334. Tarp, M.A., et al., *Identification of a novel cancer-specific immunodominant glycopeptide epitope in the MUC1 tandem repeat*. Glycobiology, 2007. 17(2): p. 197-209.
335. Sorensen, A.L., et al., *Chemoenzymatically synthesized multimeric Tn/STn MUC1 glycopeptides elicit cancer-specific anti-MUC1 antibody responses and override tolerance*. Glycobiology, 2006. 16(2): p. 96-107.
336. Posey, A.D., Jr., et al., *Engineered CAR T Cells Targeting the Cancer-Associated Tn-Glycoform of the Membrane Mucin MUC1 Control Adenocarcinoma*. Immunity, 2016. 44(6): p. 1444-54.
337. Morganti, S., et al., *Next Generation Sequencing (NGS): A Revolutionary Technology in Pharmacogenomics and Personalized Medicine in Cancer*. Adv Exp Med Biol, 2019. 1168: p. 9-30.
338. Newell, E.W. and M.M. Davis, *Beyond model antigens: high-dimensional methods for the analysis of antigen-specific T cells*. Nat Biotechnol, 2014. 32(2): p. 149-57.
339. Han, A., et al., *Linking T-cell receptor sequence to functional phenotype at the single-cell level*. Nat Biotechnol, 2014. 32(7): p. 684-92.
340. Jang, M., et al., *Characterization of T cell repertoire of blood, tumor, and ascites in ovarian cancer patients using next generation sequencing*. Oncoimmunology, 2015. 4(11): p. e1030561.
341. Battisto, J.R. and N.M. Ponzio, *Autologous and syngeneic mixed lymphocyte reactions and their immunological significance*. Prog Allergy, 1981. 28: p. 160-92.
342. Sadovnikova, E., et al., *Generation of human tumor-reactive cytotoxic T cells against peptides presented by non-self HLA class I molecules*. Eur J Immunol, 1998. 28(1): p. 193-200.
343. Wilde, S., et al., *Dendritic cells pulsed with RNA encoding allogeneic MHC and antigen induce T cells with superior antitumor activity and higher TCR functional avidity*. Blood, 2009. 114(10): p. 2131-9.
344. Li, L.P., et al., *Transgenic mice with a diverse human T cell antigen receptor repertoire*. Nat Med, 2010. 16(9): p. 1029-34.
345. Scholten, K.B., et al., *Codon modification of T cell receptors allows enhanced functional expression in transgenic human T cells*. Clin Immunol, 2006. 119(2): p. 135-45.
346. Cohen, C.J., et al., *Enhanced antitumor activity of T cells engineered to express T-cell receptors with a second disulfide bond*. Cancer Res, 2007. 67(8): p. 3898-903.
-

- 
347. Sebestyén, Z., et al., *Human TCR that incorporate CD3zeta induce highly preferred pairing between TCRalpha and beta chains following gene transfer*. J Immunol, 2008. 180(11): p. 7736-46.
348. Sommermeyer, D., et al., *Designer T cells by T cell receptor replacement*. Eur J Immunol, 2006. 36(11): p. 3052-9.
349. Sommermeyer, D. and W. Uckert, *Minimal amino acid exchange in human TCR constant regions fosters improved function of TCR gene-modified T cells*. J Immunol, 2010. 184(11): p. 6223-31.
350. Haga-Friedman, A., M. Horovitz-Fried, and C.J. Cohen, *Incorporation of transmembrane hydrophobic mutations in the TCR enhance its surface expression and T cell functional avidity*. J Immunol, 2012. 188(11): p. 5538-46.
351. Kuball, J., et al., *Facilitating matched pairing and expression of TCR chains introduced into human T cells*. Blood, 2007. 109(6): p. 2331-8.
352. Yang, S., et al., *Development of optimal bicistronic lentiviral vectors facilitates high-level TCR gene expression and robust tumor cell recognition*. Gene Ther, 2008. 15(21): p. 1411-23.
353. Oldham, R.A., E.M. Berinstein, and J.A. Medin, *Lentiviral vectors in cancer immunotherapy*. Immunotherapy, 2015. 7(3): p. 271-84.
354. Uckert, W., et al., *Efficient gene transfer into primary human CD8+ T lymphocytes by MuLV-10A1 retrovirus pseudotype*. Hum Gene Ther, 2000. 11(7): p. 1005-14.
355. Gattinoni, L., et al., *Acquisition of full effector function in vitro paradoxically impairs the in vivo antitumor efficacy of adoptively transferred CD8+ T cells*. J Clin Invest, 2005. 115(6): p. 1616-26.
356. Huang, J., et al., *Survival, persistence, and progressive differentiation of adoptively transferred tumor-reactive T cells associated with tumor regression*. J Immunother, 2005. 28(3): p. 258-67.
357. Kaech, S.M., et al., *Selective expression of the interleukin 7 receptor identifies effector CD8 T cells that give rise to long-lived memory cells*. Nat Immunol, 2003. 4(12): p. 1191-8.
358. Klebanoff, C.A., et al., *Central memory self/tumor-reactive CD8+ T cells confer superior antitumor immunity compared with effector memory T cells*. Proc Natl Acad Sci U S A, 2005. 102(27): p. 9571-6.
359. Roth, T.L., et al., *Reprogramming human T cell function and specificity with non-viral genome targeting*. Nature, 2018. 559(7714): p. 405-409.
360. Schober, K., et al., *Orthotopic replacement of T-cell receptor alpha- and beta-chains with preservation of near-physiological T-cell function*. Nat Biomed Eng, 2019. 3(12): p. 974-984.
-

361. Stadtmauer, E.A., et al., *CRISPR-engineered T cells in patients with refractory cancer*. *Science*, 2020. 367(6481).

---

## 6. Abbreviations

5-AZA	5-Azacytidine
aa	amino acid
ALL	acute lymphoblastic leukemia
APC	antigen-presenting cell
APC	antigen presenting cell
APC	allophycocyanine
ATT	adoptive T cell transfer
bFGF	basic fibroblast growth factor
bp	base pair
BV	brilliant violet
CAR	chimeric antigen receptor
CD	cluster of differentiation
cDNA	complementary DNA
CDR3	complementarity determining region 3
CLIP	class II-associated invariant chain peptide
CML	chronic myelogenous leukemia
COSMIC	Catalogue of somatic mutations in cancer
CRISPR	clustered regularly interspersed short palindromic repeat
CTL	cytotoxic T cell
CTLA-4	cytotoxic T-lymphocyte antigen 4
d	day(s)
D	diversity region
DBD	DNA-binding domain
DC	dendritic cell
DMSO	dimethyl sulfoxide
DNA	deoxyribonucleid acid
EBV	Epstein-Barr virus
ELISA	enzyme-linked-immunosorbent assay
FACS	fluorescence-activated cell sorting
FDA	U.S. food and drug administration
FITC	fluorescing isothiocyanate
gDNA	genomic DNA
GEMM	genetically engineered mouse model
GFP	green fluorescent protein

GM-CSF	granulocyte-macrophage colony stimulating factor
GMP	good manufacturing practice
GOF	gain-of-function
gp33	LCMV glycoprotein 33
gRNA	guide RNA
h	hour
HBV	hepatitis B virus
HEK 293T	Human Embryonic Kidney 293T
HLA	human leukocyte antigen
HLF	heart-and-lung fibroblasts
HPV	human papillomavirus
IC <sub>50</sub>	half maximal inhibitory concentration
IFN	interferon
IARC	International Agency for Research on Cancer
IL	interleukin
IRES	internal ribosomal entry site
ivtRNA	<i>in vitro</i> transcribed RNA
J	joining region
kb	kilobase
LCL	lymphoblastoid cell line
LOH	loss of heterozygosity
LTR	long terminal repeats
max	maximum stimulation
MCA	methylcholanthrene
μFD	microfarad
MFI	mean fluorescence intensity
MHC	major histocompatibility complex
min	minute
MLV	murine leukemia virus
MPSV	mouse proliferative sarcoma virus
MP71	MPSV-derived promoter variant
mRNA	messenger RNA
mut	mutant
NGS	next-generation sequencing
NK	natural killer cells
NOD	non-obese diabetic mouse

---

NSG	NOD-SCID-IL2 $\gamma^{\text{null}}$ mouse
OVA	ovalbumine
OT-I	OVA-specific TCR
P14	lymphocytic choriomeningitis virus-derived gp33-specific TCR
p2a	picorna virus-derived peptide element
PAM	protospacer adjacent motif
pI	peptide I of SV40 large T
pIV	peptide IV of SV40 large T
PBL	peripheral blood lymphocyte
PBS	phosphate-buffered saline
PCR	polymerase chain reaction
PD-1	programmed death protein 1
PD-L1	programmed death ligand 1
PD-L2	programmed death ligand 2
PDX	patient-derived xenograft
PE	phycoerythrine
pMHC	peptide-MHC complex
Plate-E	cell line Platinum E
PRE	post-transcriptional regulatory element
RACE	rapid amplification of cDNA ends
Rag	recombination-activating gene
reis	reisolated tumor
RNA	ribonucleic acid
RT	reverse transcriptase
SA	splice acceptor
SCID	severe combined immunodeficiency mouse
scFv	single chain variable fragment
SD	splice donor
SV40	simian virus 40
TAA	tumor associated antigen
TAF	tumor-associated fibroblast
TAM	tumor-associated macrophage
TAP	transporter associated with antigen processing
TCR	T cell receptor
TD	transactivation domain
T <sub>H</sub>	CD4 <sup>+</sup> helper T cells

TIL	tumor infiltrating lymphocyte
TMG	tandem minigene
TNF	tumor necrosis factor
T-reg	T regulatory cell
TSA	tumor specific antigen
UV	ultraviolet
vb	variable region of b chain
VEGF	vascular endothelial growth factor
V	variable region
V	Volt
wt	wild-type



## 7. List of tables and figures

### 7.1 Tables

- Table 1: Reaction mix and protocol of cDNA synthesis
- Table 2: Reaction mix of 5' RACE PCR
- Table 3: Reaction protocol of 5' RACE PCR
- Table 4: List of primers used in 5' RACE PCR
- Table 5: List of primers specific for H-2<sup>k</sup> MHCI sequences
- Table 6: Reaction mix and protocol of *in vitro* RNA transcription
- Table 7: Reaction mix and protocol of RNA tailing
- Table 8: List of mouse p53 specific primers
- Table 9: Standard PCR protocol
- Table 10: Standard PCR mix
- Table 11: List of TMG-specific primers
- Table 12: List of antibodies used for flow cytometry
- Table 13: TCR $\alpha$  and TCR $\beta$  chain frequencies isolated from Ag104A-specific CTLs
- Table 14: TCR $\alpha$  and TCR $\beta$  chain combinations
- Table 15: List of epitopes used to construct control TMGs
- Table 16: Expressed mutations in Ag104A

### 7.2 Figures

- Figure 1: Clonal evolution of cancer
- Figure 2: Schematic representation of adoptive T cell transfer
- Figure 3: CRISPR/Cas9 to target p53
- Figure 4: 5' RACE PCR on CTL cultures
- Figure 5: TCR transgene cassettes
- Figure 6: Expression of TCR transgene cassettes and recognition of Ag104A
- Figure 7: Design of tandem minigenes
- Figure 8: Each position of a TMG construct supports antigen expression and presentation
- Figure 9: Varying pMHC affinity and gene expression of potential Ag104A neoepitopes
- Figure 10: The antigen recognized by TCR M2/3 is presented by H-2K<sup>k</sup>
- Figure 11: TCR M2/3 recognizes a neoepitope resulting from a mutation in *Trp53*
- Figure 12: M2/3-engineered T cells recognized all Ag104A single-cell clones
- Figure 13: Targeting mp53 in Ag104A tumors prolongs survival

- Figure 14: Proliferation of CD8<sup>+</sup> M2/3-engineered T cells peaks 7 – 14 days after ATT and T cells persist over time
- Figure 15: M2/3-engineered T cells infiltrate the tumor microenvironment and are functional
- Figure 16: Expression of exhaustion markers in TILs isolated from M2/3- and mock-treated mice is similar
- Figure 17: Ag104A tumor cell variants that escaped mp53-specific TCR gene therapy are no longer recognized by M2/3-engineered T cells *in vitro*
- Figure 18: The processing and presentation machinery of Ag104A variants that escaped mp53-specific ATT is intact
- Figure 19: Level of mp53 is lower in Ag104A variants that escaped T cell therapy
- Figure 20: Copy number analysis and whole exome sequencing of Ag104A variants reveals no genomic alterations in the p53 gene
- Figure 21: Single-cell clones of Ag104A variants are rather homogeneous p53<sup>+/+</sup> populations
- Figure 22: mp53-specific T cell therapy can reject cancer with high and homogeneous antigen expression
- Figure 23: The CRISPR/Cas9-mediated homology-directed-repair can correct mp53 in Ag104A tumor cells
- Figure 24: Loss of the p53<sup>D253E</sup> mutation in Ag104A cancer cells leads to slower tumor cell growth *in vitro* and *in vivo*

## **Statement (Eidesstattliche Erklärung)**

Hiermit bestätige ich, dass ich die Arbeit selbständig und ohne fremde Hilfe verfasst und keine anderen als die angegebenen Hilfsmittel benutzt habe.

Außerdem versichere ich, dass die Arbeit noch nicht veröffentlicht oder in einem anderen Prüfungsverfahren als Prüfungsleistung vorgelegt worden ist.

Berlin, den 17.06.2021

Vasiliki Anastasopoulou